Investigation of Genetic Causes of Developmental Eye Disorders in Consanguineous Families

By

Kinza Arshad

Department of Biochemistry

Faculty of Biological Sciences

Quaid-I-Azam University

Islamabad, Pakistan

2023

Investigation of Genetic Causes of Developmental Eye Disorders in Consanguineous Families

A thesis submitted in partial fulfillment of requirements for the degree of

Master of Philosophy

In

Biochemistry/Molecular Biology

By

Kinza Arshad

Department of Biochemistry

Faculty of Biological Sciences

Quaid-I-Azam University

Islamabad, Pakistan

2023

Certificate

This thesis titled as "**Investigation of Genetic Causes of Developmental Eye Disorders in Consanguineous Families"** submitted by **Kinza Arshad** is accepted in its present form by the Department of Biochemistry, Quaid-I-Azam University Islamabad,Pakistan; as satisfying the thesis requirements for the degree of Master of Philosophy in Biochemistry/Molecular Biology.

Supervisor _____

Dr. Muhammad Ansar

Professor

External Examiner _____

Chairperson _____

Dr. Iram Murtaza

Professor

Dated _____

Declaration

I hereby declare that the work presented in the following thesis is my own effort and the thesis is composed by me. No part of this thesis has been previously presented elsewhere for any other degree or certificate.

Kinza Arshad

Dedication

Firstly, I would like to dedicate this little effort to Almighty Allah without whom my life has no meaning. His divine grace and mercy have illuminated the path of my academic pursuit, offering me strength and perseverance during moments of challenge and uncertainty. As Allah says in the Quran:

"And whoever fears Allah - He will make for him a way out. And will provide for him from where he does not expect. And whoever relies upon Allah - then He is sufficient for him. Indeed, Allah will accomplish His purpose . Allah has already set for everything a [decreed] extent." (Qur'an, 65: 2-3)

I wish to dedicate this thesis to my parents, especially my mother and my sibling Maria Arshad, who have always been my source of strength, encouragement, prayers, and unwavering support throughout this journey. Your sacrifices and belief in me have made this achievement possible.

Acknowledgments

In the Name of Allah, the Most Beneficent, the Most Merciful. All the praises and glories be to Almighty Allah the Lord of the universe for His infinite mercy and blessings upon us, whosoever He guides shall never goastray and whomsoever He allows to astray shall never find the guidance, may the peace and blessing of Allah be upon to His noble Prophet Muhammad S.A.W and his companions.

I feel highly privileged in expressing my gratitude to my supervisor **Dr. Muhammad Ansar**, Professor, Department of Biochemistry, Quaid-I-Azam University, Islamabad for his continuous support, scholarly guidance, and valuable suggestions. I would like to express my thanks to **Dr. Iram Murtaza**, Professor and Chairperson of Department of Biochemistry, Quaid- I-Azam University, Islamabad for providing the research facilities and constructive environment to accomplish this work.

I would like to thank all my respected teachers who taught me and made it possible for me to achieve this goal in my life. I would like to pay my gratitude to all those lab seniors who guided me, whenever I needed **Samra Akram, Ammara Saleem, Ayesha Ishtiaq, Dr. Saba Kiran** and **Itrat Fatima.** I feel great pleasure in expressing my sincerest thanks to my lab fellow **Alina Murtaza,** and my best friend **Pakeeza Arshad** for their friendly attitude, encouraging behavior and moral support.

My sincere appreciation does to all my fellows and friends especially **Fiza Ahmed Tariq**, **Laiba Asad**, **Sana Batool** and **Mirub Shaukut** who engaged in thought provoking discussions, provided valuable insights and emotional support. I would like to thank to my juniors **Khadeeja Ahsan** and **Kainat Qadeer** for their prayers and moral support.

Last but not the least, special thanks to my mother without whom I am nothing May she witness my success. May Allah grant her higher ranks in Jannah (Ameen). Finally, I would like to thank all the **participants** who donated their blood for this research. May Allah bless them with His blessings (Ameen).

Kinza Arshad

Table of Contents

List of Tables Page Number

List of Figures Page Number

List of Abbreviations	Description
WHO	World Health Organization
PDE6A	cGMA phosphodiesterase
LRAT	Lecithin Retinol Dehydrogenase
IOP	Intraocular Pressure
GPCR	G-Protein Coupled Receptor
RDH	Retinol Dehydrogenases
RPE	Retinal Pigment Epithelium
RBP3	Retinal Binding Protein 3
IRDs	Inherited Retinal Dystrophies
RGS	Retinal Ganglion Cells
TM	Trabecular Meshwork.
CORD	Cone and Rod Dystrophy
STGD	Stargardt Disease
FA	Fundus Albipunctatus
MIGS	Minimally Invasive Glaucoma Surgery
BEC	Bioethical Committee
EDTA	Ethylenediamine Tetra-acetic Acid
SDS	Sodium Dodecyl Sulphate

TE	Tris-EDTA
DMSO	Dimethyl sulfoxide
MgCl2	Magnesium Chloride
NaCl	Sodium Chloride
PDB	Protein Data Bank

Abstract

Inherited eye disorders constitute a diverse group of genetic conditions that affect the structure and function of the visual system during development. These disorders often leading to significant visual impairments or blindness and are classified into different types depending on clinical features presented by the patients. The present study is aimed to decipher the genetic basis of three common inherited eye disorders including cone and rod dystrophy (CORD), stargardt disease (STGD) and primary congenital glaucoma (PCG). For this purpose, four consanguineous Pakistani families were recruited, and genetic analysis was performed to identify disease-causing variants. Four genes (*ABCA4*, *CNGA3*, *CNGB3* and *RPGRIP1)* were sequenced in family A, B and D and a single gene *(CYP1B1)* was sequenced in family C with PCG. Sequence analysis identified two heterozygous variants c.1694C>T (p.T565M) and c. 1678A>T (p.R560W) in family A, a homozygous deletion c.1298_1298delT (p. L433Wfs*32) and two polymorphisms g.49583T>A and c.3288G>A in family B, two non-pathogenic homozygous variants c.142C>G (p.R48G) and c. 355G>T (p.A119S) in family C and one heterozygous variant c.6004A>T (p.S2002C) in family D. The p.T565M variant identified in family A is present in cGMP binding site and modeling of protein indicates the effect of variant on binding of cGMP with *CNGA3*. A homozygous deletion c.1298_1298delT in family B results in the pre-termination codon which results in the formation of truncated protein. It can be concluded that c.1298_1298delT (p. L433Wfs*32) is responsible for CORD in affected individual of family B. The c.6004A>T (p.S2002C) variant is present in NBD2 motif of *ABCA4* that is expected to affect its interaction with the respective substrate. The 3D structure analysis of *ABCA4* revealed that p.S2002C variant affects the proper folding of protein, which ultimately disrupts the structure. However, current data could not identify the disease-causing mutation in two families (Family C and D) and further research will be required to find the disease-causing variants in the respective families.

1.Introduction

Genetic disorders include a diverse group of conditions that result from alterations or mutations in an individual's DNA. These disorders can affect the quality of life, ranging from physical traits and organ function to intellectual and developmental capabilities. According to World Health Organization (WHO), more than 70 million people are living with genetic disorders worldwide (World Health Organization, 2021). Its prevalence is high in developing countries like Pakistan where rate of consanguineous marriages is high. According to Pakistan Genetic Mutation Database (PGMD), more than 1000 mutations have been reported in 130 different types of genetic disorders in Pakistan (http://www.pakmutation.com).

Inherited retinal dystrophies is one of the leading cause of blindness with the prevalence of 1 in 2000 individuals, affecting more than two million people worldwide (Hamel, 2006; Cremers et al., 2018). More than 20 different types of retinal dystrophies have been identified so far (Chaumet-Riffaud et al., 2017).

1.1. Anatomy and Physiology of Eye

Eyes, one of the most complex and important organ of vision that Allah has blessed us with to explore and comprehend the things around us. It is believed that the idea of scientific study of eye was initiated from the Greek physician Herophilus (Senior, 2010). The human eye consists of the eyeball within the socket termed as orbit along with the several supporting external structures i-e muscles, accessory glands, conjunctiva, tear film and eye lids. The eyeball comprises of three main layers. 1) The outer fibrous layer contains the sclera, white portion of eye and the transparent cornea. 2) The middle vascular layer is also termed as uvea, comprising of iris, ciliary body and choroid. 3) The innermost layer contains retina , lens and vitreous humor (Kolb et al., 2011; Pradeep et al., 2019). The dense connective tissues in sclera provides the structural protection whereas the cornea, iris, ciliary body, and lens help in image formation by focusing the light on the retina (Willoughby et al., 2010). The blood vessels within choroid along with lacrimal system, aqueous and vitreous humor, are involved in providing physiological balance, maintaining pressure, and nourishing the ocular tissues (Ludwig et al., 2022).

1.1.1. **Retina**

The retina is a neurosensory multilayered structure involved in vision formation (Masland, 2012). Six different types of cells (rod cells, cone cells, bipolar cells, ganglion cells, muller ganglion cells and horizontal cells), each with specific function within distinct layers of retina as shown in figure 1.1 (Mahabadi & Al Khalili, 2021). Visual signals captured by rods and cones are further passed on to bipolar and ganglion cells and finally reach to the brain via optic nerve (Grossniklaus et al., 2015). Horizontal and bipolar cells form synapses for transferring information within plexiform layer (Mahabadi & Al Khalili, 2021). Retinal pigment epithelium (RPE) supports the retina as it contains photopigments and perform many important functions (Silverman & Wong, 2018; Yang et al., 2021).

1.1.1.1. Cones

Rods and cones are two types of photoreceptors present within human retina. Approximately 96 million photoreceptors are present in human retina where cone makes up only 5% (6 million), and are responsible for photopic vision (Lamb, 2016; Ludwig et al., 2022). Four structural domains: outer part, inner part, cell bodies and synaptic terminals are present in rod and cone cells. Infoldings of cell membrane form the lamella like structures within cone cells (Mustafi et al., 2009).

The cone cells sensitivity to light is low. Their concentration is high in the middle region of the retina (macula) which further deepens to form a depression called fovea. The visual acuity is highest at this spot due to absence of rod cells (Lamb, 2016; Ludwig et al., 2022). Cone cells are further classified into S, M and L types on the basis of photopigments they contain and their response to different wavelength of light (de Nava et al., 2022).

1.1.1.2. Rods

Rods make 95% (90 million) of photoreceptors and contain the rhodopsin pigment which is responsible for scotopic vision (Lamb, 2016; Ludwig et al., 2022). Rods contain the disc membrane structures surrounded by plasma membrane forming stacks, present in the peripheral region. Their sensitivity to light is high and can respond to the single wavelength of light (Kawamura & Tachibanaki, 2008).

1.2. Molecular Basis of Vision

The event of conversion of photochemical signal into electrical signal is termed as visual cycle or retinoid cycle. The electrical signal is then perceived by brain in the form of image. These molecular processes take place in retina and are collectively termed as phototransduction cycle.

i. In the photoreceptor (PR), opsin, a G protein coupled receptor, is bounded to 11-cis-retinal forms rhodopsin. The absorption of light by opsin isomerises all 11- cis-retinal to all trans form.

ii. This photoisomerization alters the opsin conformation and results in the closure of cGMP-gated cation channels. The closure of channel creates the potential difference across the membranes of the cells, resulting in generation of nerve impulse. This nerve impulse is interpreted by brain in the form of image. One of the most important enzyme involved in this is cGMP-phosphodiesterase (PDE6A) (Senior, 2010; Grossniklaus et al., 2015; Tsin et al., 2018).

iii. After isomerization, all trans retinal are reduced to all trans retinol by an enzyme retinol dehydrogenase (RDH 8, 12, 14) and then release the opsins in the nearby RPE.

iv. 11 trans retinol is esterified into 11 cis retinyl ester which is further converted into 11 cis retinol and finally oxidized to 11 cis retinal by the action of enzymes lecithin-retinol acyltransferase (LRAT), isomerohydrolase, retinal pigment epithelium-specific protein 65 kDa (RPE65) and retinol dehydrogenase (RDH 5,11) respectively.

v. Now 11 cis retinal bound to opsin and forms rhodopsin to enter into a new cycle of phototransduction. The shuttling of these metabolites across PR and RPE is carried out by retinoid-binding protein 3 (RBP3) (Moiseyev et al., 2005; Muniz et al., 2007; Wang & Kefalov, 2011; Saari, 2016; Koster et al., 2021).

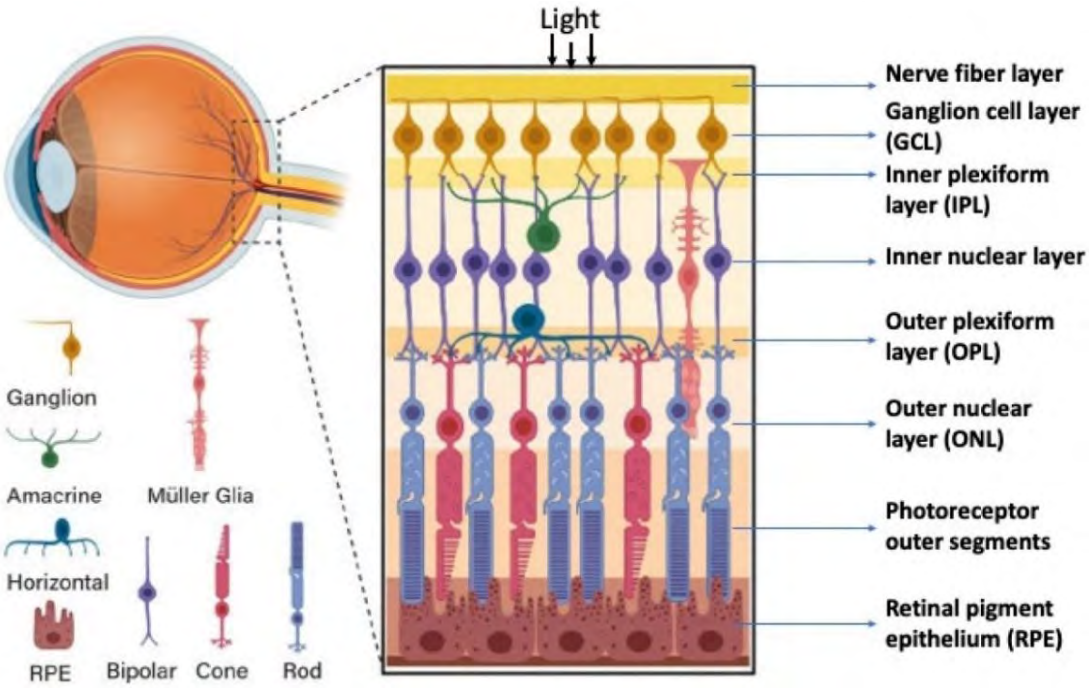

Figure 1.1: Anatomy of human retina showing different types of cells and layers (Grigoryan, 2022).

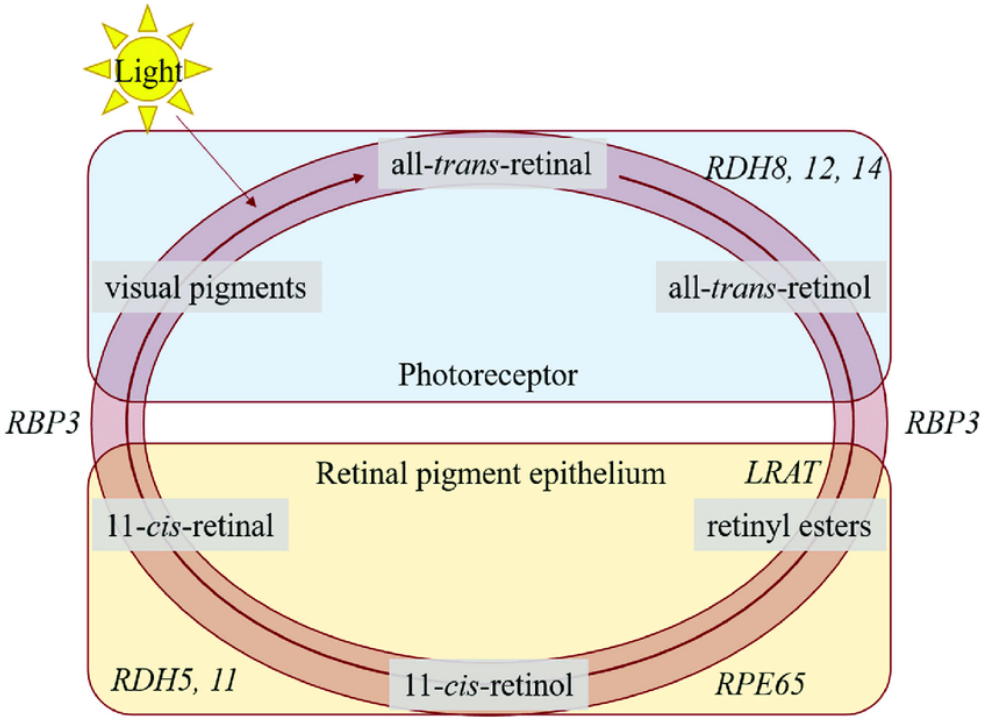

Figure 1.2: Schematic representation of molecular basis of visual cycle (Koster et al., 2021).

1.3. Inherited Retinal Dystrophies (IRDs)

Inherited retinal dystrophies (IRDs) fall under the category of degenerative disorders of the retina with heterogeneity in genetic and clinical presentations. It has been reported that different phenotypes of retinal dystrophies are known to be linked with over 270 genes (García Bohórquez et al., 2021; Chawla & Vohra, 2022). A single mutation in any of these genes is enough to disrupt either the structural or functional dynamics of eye. Like cone and rod dystrophy results from the disruptive function of cone cells followed by rod cells (Chawla & Vohra, 2022), whereas glaucoma falls under the spectrum of developmental disorders associated with elevated level of intraocular pressure (IOP).Due to overlapping clinical and genetic characteristics of retinal dystrophies (RDs), it is difficult to classify them but based on the type of photoreceptor cells, they can be categorized as mentioned below:

1.3.1. Rod Dominant

Rod cells are predominantly affected like in retinitis pigmentosa (RP) and congenital stationary night blindness (CSNB).

1.3.2. Cone Dominant

Cone photoreceptors are predominantly affected like juvenile macular dystrophy (JMD) and age-related macular dystrophy (AMD). Classification is shown in figure 1.3.

1.4. Cone and Rod Dystrophy (CORD)

Cone and rod dystrophy (CORD) is group of IRDs with a prevalence of 1/40,000 (Hamel et al., 2000). CORD affects the function of cone cells primarily and later on rod cells, leading to progressive vision loss. It belongs to the group of pigmentary retinopathies as deposition of retinal pigments, mainly localized to the macular region, is observed on fundus (Christian, 2007). Sometimes it overlaps with other cone dystrophies like achromatopsia and macular dystrophy as firstly central vision is affected (macular degeneration takes place) which is followed by progressive loss in peripheral vision (Michaelides et al., 2004; Aboshiha et al., 2016). In some cases, degeneration of both rod and cones photoreceptors occur simultaneously (Hamel et al., 2000).

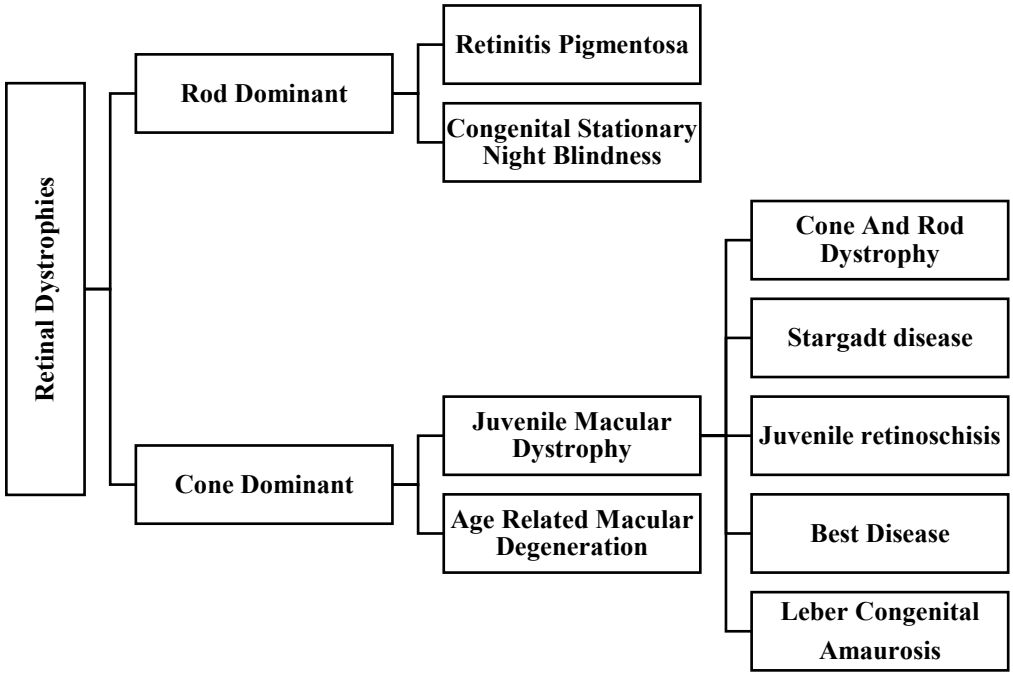

Figure 1.3: Classification of IRDs (Chawla & Vohra, 2022).

1.4.1. Clinical Features of CORD

Clinically, it is characterized by decreased visual acuity, abnormal color vision, photophobia, and appearance of scotoma at an early age. Nystagmus often occurs in some cases. Patchy loss of peripheral vision takes place which is later on followed by night blindness. Initially macular region is normal on fundus but later on macular lesions start to appear and in some case with attenuation of the retinal vessels and waxy polar of the optic disc with the progression of disease resulting in bull's eye maculopathy. Cone responses are severely affected as compared to rod responses in electroretinogram (Moore, 1992; Christian, 2007; Thiadens et al., 2012; Gill et al., 2019).

1.4.2. Genetic Causes of CORD

CORD is inherited as autosomal dominant, recessive and X-linked form. Approximately mutations within 32 genes have been linked with CORD and out of these 18 genes are reported in autosomal recessive CORD (Gill et al., 2019). Most of the cases are reported in autosomal recessive. Mutations in the ABCA4 are responsible for approximately 62% cases followed by *CNGA3, KCNV2, CERKL, CNGB3, CDHR1, PDE6C, TTLL5, C21ORF2, C8ORF37, ADAM9, RPGRIP1*, *POCIB, SEMA4A, RAB28, CACNA2D4* and

PDE6H (Gill et al., 2019).

1.4.3. Structure of CNG channels

CNG channels, member of voltage gated ion channels, are heterotetrameric complex of alpha (A) and beta subunits (B) (Peng et al., 2004). Four different types of A subunits (CNGA 1-4) and two different types of B subunits (CNGB1 & CNGB3) have been identified so far that increase the diversity in mammals. They are expressed in the ratio of 3 CNGA1 : 1 CNGB1a and 2 CNGA3 : 2 CNGB3 in cone and rod cells respectively (Podda & Grassi, 2014).

CNGA3 and CNGB3 gene encodes the alpha 3 and beta 3 subunits of cyclic nucleotide gated channel CNG, comprising of 757 and 809 amino acids respectively, primarily expressed in the outer segments of cone photoreceptors (Podda & Grassi, 2014). Even though they do not individually produce functional channels, the CNGB3, and CNGA4 subunits can alter the channel properties when coassembled with the other subunit types (Liu and Varnum 2005).

The topological model of A and B subunit comprise of hexa transmembrane segments (S1–S6), a loop between S5 and S6 segments forming the functional ion conducting pore, and intracellular N and C termini. C-terminus consists of further regions i.e. the cyclic nucleotide-binding domain (CNBD), the linker region connecting the CNBD to S6 in the pore region and the distal C-terminus. It also contains the the regulatory site for Ca2+ calmodulin (CaM). Mutation in any of the functional domain affects the function of CNGA3 (Long et al., 2005; Podda & Grassi, 2014).

1.4.4. Role of *CNGA3* & *CNGB3* in vision

CNGA3 plays an important role in phototransduction in retinal cells as it forms the pore region of CNG channel complex. It regulates the flow of ions, generating the nerve impulse and controlling the release of neurotransmitters in response to light dependent changes of cyclic guanosine monophosphate (cGMP) and cyclic adenosine monophosphate (cAMP) (Peng et al., 2004). Normally, when opsin absorbs light, it dissociates the transducin from its subunits and activates PDE6. Activated PDE6 reduces the level of cGMP via catalytic hydrolysis of cGMP into GMP. Reduced level of cGMP closes CNG channels and results

in the reduced influx of Ca within cell. This leads to hyperpolarization of cells and ceases neurotransmitter release. Guanylate cyclase-activating proteins (GCAPs) is in active form in case of low level of Ca, stimulates the guanylate cyclase (GC) to synthesize cGMP which ultimately leads to the opening of CNG channels again (Iribarne & Masai, 2017).

It has been observed that in case of mutant CNG channels, high level of cGMP causes the activation of stress response regulators which ultimately results in cell death (Iribarne & Masai, 2017). In a study, many morphological and molecular changes like cone outer membrane structures disruptions, downregulation and mislocalization of cone opsins and loss of cone mediated light response were observed in CNGA3$^{-/-}$ knock out mouse model (Biel et al., 1999; Michalakis et al., 2005).

Gootwine and his colleagues have demonstrated that an Awassi sheep model with a mutant CNGA3 channel carrying a missense variation (c.1618G>A/p.(Gly540Ser) was unable to see during daytime (Gootwine et al., 2017). In another study, mutant CNGB3 with frameshift mutation linked to achromatopsia (Kohl et al., 2000; Sundin et al., 2000) was unable to form the functional form of the subunit B3 that resulted in non-functionality of CNGA3 channels (Peng et al., 2003). Several studies have proved that mutations within CNGB3 subunits impact the functioning of heteromeric channels when co-expressed with CNGA3 subunits and vice versa (Peng et al., 2003; Okada e al., 2004).

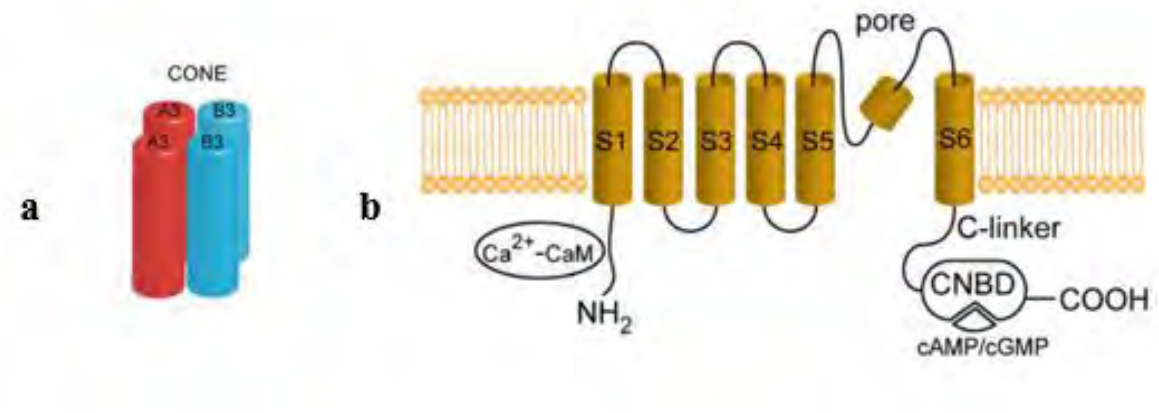

Figure 1.4: a) Tetrameric subunit assembly of CNG channels in cone cells **b)** topological model of CNG channel subunit structure (Podda & Grassi, 2014). CNG heterotetrameric complex is formed in rods and cones when 2 CNGA3 combines with 2 CNGB3.

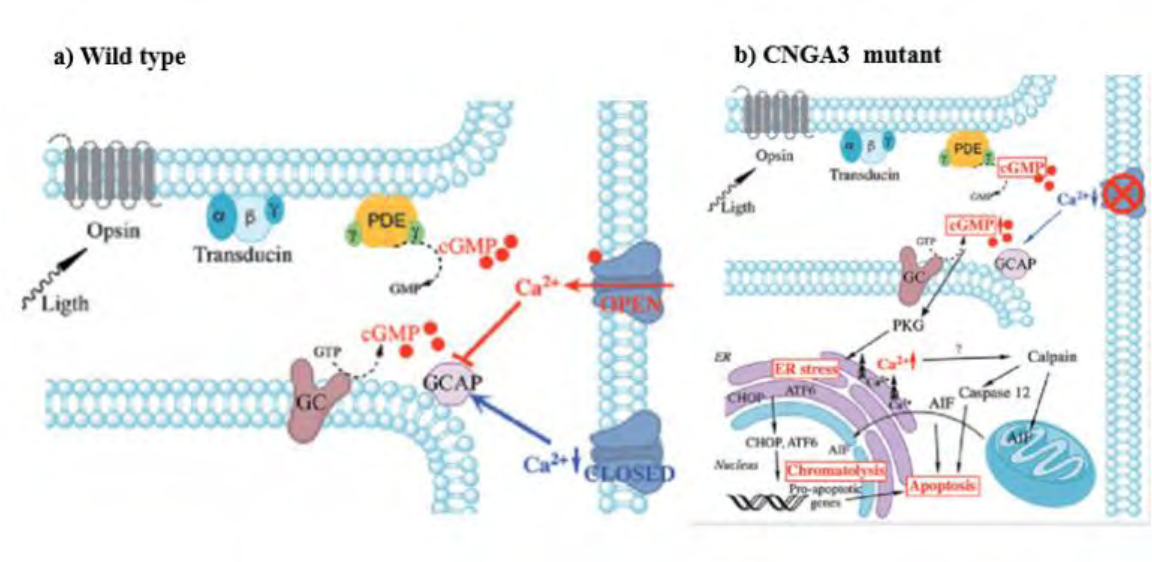

Figure 1.5: Representation of the phototransduction pathway in photoreceptors with wild type *CNGA3* **(a)** with mutant *CNGA3* mice **(b)** (Iribarne & Masai, 2017).

1.4. Stargardt Disease (STGD)

Stargardt disease (STGD), also termed as Stargardt's macular dystrophy or juvenile macular degeneration, is the most prevalent form of macular atrophy with autosomal recessive pattern of inheritance (Rotenstreich et al., 2003; Walia & Fishman, 2009; Lu et al., 2017;). It is clinically and genetically heterogenous with an estimated prevalence of 1 in 8,000 – 10,000 (Michaelides et al., 2003; Fujinami et al., 2013; Molday, 2015; Fujinami et al., 2015; Strauss et al., 2016). The term stargardt is coined after the German ophthalmologist, Karl Stargardt, who first described the disease in 1909 (Stargardt, 1909). It is characterized by the irreversible degeneration of macular RPE and loss of photoreceptors that results in the deposition of lipofuscin which appears as white yellow flecks (Rotenstreich et al., 2003).

Firstly STGD is confused with the term fundus flavimaculatus introduced by Franceschettiin in 1963, which is also described by the appearance of white yellow flecks (Sautter, 1963). Later on, it was found that both these conditions were same (Irvine & Wergeland Jr, 1972; Krill & Deutman, 1972; Hadden & Gass, 1976; Noble & Carr, 1979). Patients with early onset of disease have worst visual outcomes and poor prognosis as compared to late onset of disease (Lois et al., 2001; Fishman, 2001; Rotenstreich et al.,

2003; Simonelli et al., 2005).

1.4.1. Clinical Features of STGD

Abnormal deposition of lipofuscins and intermediates of vitamin A is the main clinical feature of STGD (Birnbach et al., 1994; Koenekoop, 2003). Accumulation of these metabolites damage the RPE and photoreceptors which ultimately leads to the degeneration of macula resulting in the loss of central vision (Sparrow & Boulton, 2005; Lee et al., 2014). These depositions initially appear as white dots (Fujinami et al., 2014; Lee et al., 2014) but later appears yellowish flecks on fundus images of the macula (Fujinami, Sergouniotis, et al., 2013; Fujinami et al., 2015; Khan et al., 2018; Tanna et al., 2018; Tanna et al., 2019; Gill et al., 2019).

In some cases, bull's eye maculopathy is also detected by fundus autofluorescence (FAF) (Gomes et al., 2009: Fujinami et al., 2013). Patients also present with clinical features of central vision loss, slow dark adaptation, color vision issues, scotoma and photophobia (Fujinami, Lois, Mukherjee, et al., 2013; Lambertus et al., 2015; Tanna et al., 2018).

1.4.2. Genetic Causes of STGD

STGD is mainly inherited in autosomal recessive pattern. However, it is also inherited in autosomal dominant manner and linked with different genes as discussed below:

1.4.2.1. STGD1

Autosomal recessive STGD1(MIM #48200) is mostly associated with mutations in ABCA4 (Allikmets et al., 1997) but in some cases with CNGB3 (Nishiguchi et al., 2005).

1.4.2.2. STGD3

STGD3 (MIM #600110) is mostly linked with mutations in *ELOVL4* with dominant pattern of inheritance (Griesinger et al., 2000; Bernstein et al., 2001; Zhang et al., 2001).

1.4.2.3. STGD4

STGD4 (MIM #603786) is a autosomal dominant disease linked with *PROM1* mutations (Yang et al., 2008).

1.4.3. Structure of *ABCA4* protein

ABCA4 (MIM 601691) belongs to the superfamily of ATP binding cassette (ABC) transporter gene that encodes the retinal specific transmembrane ATP-binding cassette, sub-family A (ABC1), member 4 (Cideciyan et al., 2004; Tsybovsky et al., 2010; Issa et al., 2013). It is a high molecular weight protein (~290,000 Da) and was identified by Papermaster and his colleagues (1978). It contains 2273 amino acids and mainly present in the rim of the rod and cone outer segment discs (Papermaster et al., 1978; Papermaster et al., 1982).

ABCA4 transporter comprise of four major core domains:, two nucleotide binding domains (NBD1, NBD2) that hydrolyze ATP (Rees et al., 2009) capped with two regulatory (RD1,RD2), two transmembrane domains (TMD1, TMD2) that binds substrates along with two glycosylated extracellular domains (ECD1, ECD2) (Molday, 2015; Qian et al., 2017). Each TMD, comprise six transmembrane segments, also contains an helix-turn-helix structure termed as extracellular helix pair (EH), that partially penetrates ABCA4. The motif EH1-EH2 and EH3-E4 form V-shaped structures present between TM5 and TM6, as well as TM11 and TM12, respectively (Garces et al., 2020). Four short transverse intracellular helices (IH1, IH2, IH3 and IH4) are located at the interface of TMD and NBD, and help to bring the conformational changes in these domains (Kim & Chen, 2018). Mutations in any of these domains can affect the functionality of ABCA4 and results in STGD (Garces et al., 2020).

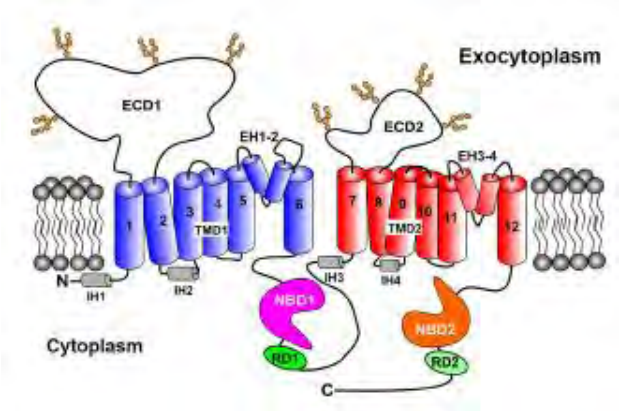

Figure 1.6: Topological model of ABCA4 showing different domains (Molday et al., 2022).

1.4.4. Role of *ABCA4* in Visual Cycle

Retinal is an important molecule for vision, but its aldehyde group allows to move out of the outer segment compartmentant, making it toxic for the cells. So retinal is converted into retinol to encounter its toxic effects. In some cases, a compound known as N-retinylidene-phosphatidylethanolamine (N-Ret-PE) is formed by the reversible reaction of retinal and phosphatidylethanolamine (PE) (Anderson & Maude, 1970; Molday et al., 2022). N-Ret-PE has ability to form toxic bis retinoids like Pyridinium bis-retinoid A2E by reacting with other retinoids if not cleared properly from lumen (Eldred & Lasky, 1993; Sakai et al., 1996; Parish et al., 1998; Mata et al., 2000; Kim & Sparrow, 2021).

Thus, removal of all trans and cis forms of retinoids by *ABCA4* is important to prevent the accumulation of unwanted metabolites. It basically prevents the deposition of toxic retinoid compounds by actively translocating the retinoids like N-Ret-PE, the Schiff base adduct of retinal and phosphatidylethanolamine, from photoreceptor to RPE (figure 1.7) (Quazi et al., 2012; Quazi & Molday, 2014; Tanna et al., 2017). Deposition of these toxic compounds in retinal cells, leading towards degeneration of cones and rods is linked with loss of function mutation in *ABCA4* (Sparrow et al., 2012).

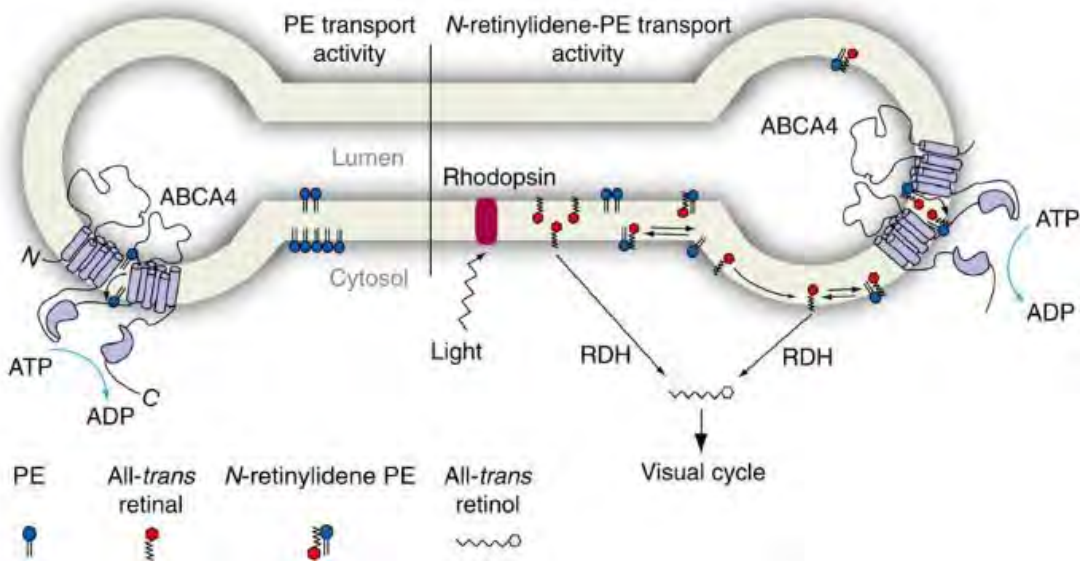

Figure 1.7: Schematic representation of *ABCA4* role in the translocating of N-retinylidene-PE and PE across the disc membrane of rod outer segment (ROS) (Quazi et al., 2012).

1.5. Glaucoma

Glaucoma originates from Greek word glaukos, meaning bluish-green gleam (Simpson & Weiner, 1989). It belongs to the group of neurodegenerative disorder, characterized by retinal nerve fiber layer (RNFL) thinning, optic disc progressive excavation, the gradual deterioration of retinal ganglion cells (RGS), leading towards the optic nerve atrophy and ultimately results in visual impairment and blindness (Jonas, 2005; Weinreb et al., 2014; Schuster et al., 2020).

The progressive degeneration affects the secretions of cell and raise the intraocular pressure (IOP) within the cell. This elevated pressure builds up the mechanical stress across the adjacent tissues and lamina cribrosa (collagen containing sieve-like structure made up of axons and blood vessels). This stress ultimately disrupts the structure of lamina cribrosa, so the visual signal transmission carried by axons via optic nerve to the brain is impaired (Weinreb et al., 2014; Tian et al., 2017; Schuster et al., 2020).

Initially, it was confused with the cataract (Westerlund, 1947) but later on the term buphthalmos, the enlargement of the ocular globe, was introduced and it was inferred that elevated IOP is the hallmark feature of glaucoma (Anderson & Parsons, 2013).

1.5.1. Classification of Glaucoma

Glaucoma can be classified based on etiology, age of onset, structural changes , and pathogenesis as mentioned in figure 1.8. Glaucoma has been categorized in three types on the basis of modern classification:

1.5.1.1. Primary Open Angle Glaucoma (POAG)

This condition is characterized by the opening of the anterior chamber drainage angle due to which the fluid is unable to drain through normal intact trabecular meshwork (TM) and raises the IOP. It usually occurs after the age of 40 (Mahabadi et al., 2017).

1.5.1.2. Primary Angle Closure Glaucoma (PACG)

This condition results due to obstruction of the angle between the iris and the cornea that don't allow the proper drainage of aqueous humor, leading to elevation of IOP in the eye. Its prevalence is more in females as compared to males (Khazaeni & Khazaeni, 2017).

1.5.1.3. Primary Congenital Glaucoma (PCG)

It is a developmental disorder of anterior chamber angle of eye, occurring at the time of birth or within first three years of life (Ho & Walton, 2004), with the highest prevalence rate in Asia (Tham et al., 2014). Aqueous humor that maintains the pressure within eye is not properly drained , damages the optic nerve and resulting in impaired vision (Maumenee, 1958; Anderson & Maude, 1970; Kupfer & Kaiser-Kupfer, 1979).

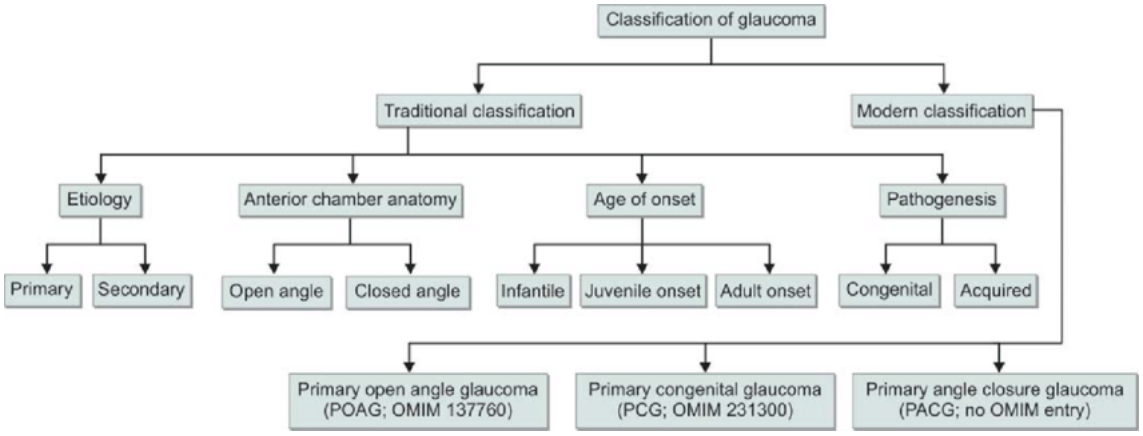

Figure 1.8: Classification of glaucoma (Faiq et al., 2013).

1.5.2. Clinical Features of PCG

Patients of PCG manifest the symptoms of IOP > 21 mmHg, excessive tearing (epiphora), hypersensitivity to light (photophobia), eyelids inflammation (blepharospasm), large eye ball (buphthalmos), hazy cornea, edema, descemet membrane breakdown, optic disc impairment, dysgenesis of anterior segment of eye and trabecular meshwork (TM) (Francois, 1980; Allingham et al., 2005; Faiq et al., 2013; Cascella et al., 2015; Abu-Amero & Edward, 2017; Badawi et al., 2019).

1.5.3. Genetics of PCG

PCG is inherited in both autosomal recessive and dominant form of inheritance. The autosomal recessive PCG is mainly linked with mutations in *CYP1B1* and *LTBP2* genes. (Fan & Wiggs, 2010). In Pakistan, first genetic case of PCG with pathogenic variant in CYP1B1 was reported in 1997 (Stoilov et al., 1997). However, dominant form is associated with pathogenic variants in *TEK* (Souma et al., 2016; Abu-Amero & Edward, 2017). In

some cases, the development of this disease has been linked with mutations in *MYOC*, *FOXC1* and *BMP4* genes (Kaur et al., 2005; Khan, 2011; Traboulsi, 2012).

1.5.4. Structure of *CYP1B1*

The *CYP1B1* gene encodes a 543-amino acid-long protein cytochrome P450, family 1, subfamily B and polypeptide 1 (*CYP1B1*). It is a member of the B subfamily of cytochrome P450 1 and shows expression in the iris, retina, cornea and ciliary body and is involved in the formation of TM (Faiq et al., 2015; Souzeau et al., 2019).The CYP1B1 comprise of

a) N-terminal region that binds to membrane

b) 10-residue-long proline-rich region termed as hinge and

c) A highly conserved cytosolic globular domain containing J-helix, a K-helix, and a region that binds to heme (Vasiliou & Gonzalez, 2008). Mutation in any of these regions would affect the catalytic activity of CYP1B1 (Sarfarazi & Stoilov, 2000)

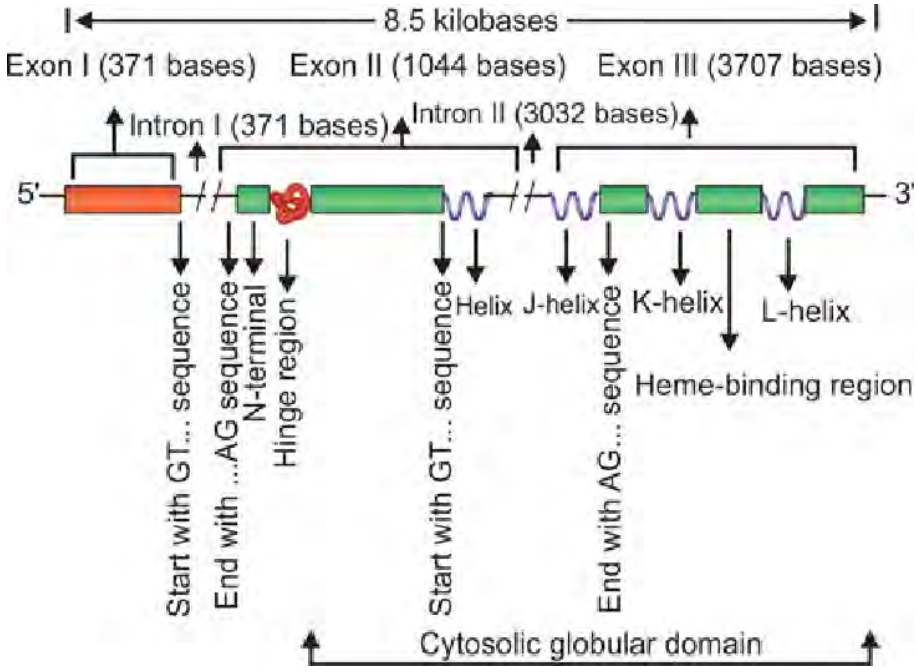

Figure 1.9: Schematic representation of *CYP1B1* (Faiq et al., 2013).

1.5.5. Role of *CYP1B1* in Eye Development

CYP1B1 encodes NADH dependent monooxygenase which is involved in catalytic oxidation of xenobiotics and many endogenous compounds such as 17 β-estradiol, retinal,

arachidonic acid, and melatonin (Cvekl & Wang, 2009; Duester, 2009). It is also involved in the oxidation of many metabolites which act as signaling molecules in the development of ocular structures. Many studies have been carried out to understand the pathogenetic role of CYP1B1 in PCG. More *CYP1B1* expression was observed in fetal eyes as compared to adult eyes, highlighting its importance in the ocular differentiation (Wirtz et al., 2002). *CYP1B1* knock out mice was created and developmental defects of TM and Schlemm's canal (**SC**) in eye tissue were observed, indicating the potential role of *CYP1B1* in the formation of these ocular structures (Libby et al., 2003). It was demonstrated that mutations in *CYP1B1* like R48G, A119S, and V432L affect its enzymatic activity for hydroxylation of estradiol (Shimada et al., 2001; Aklillu et al., 2002)

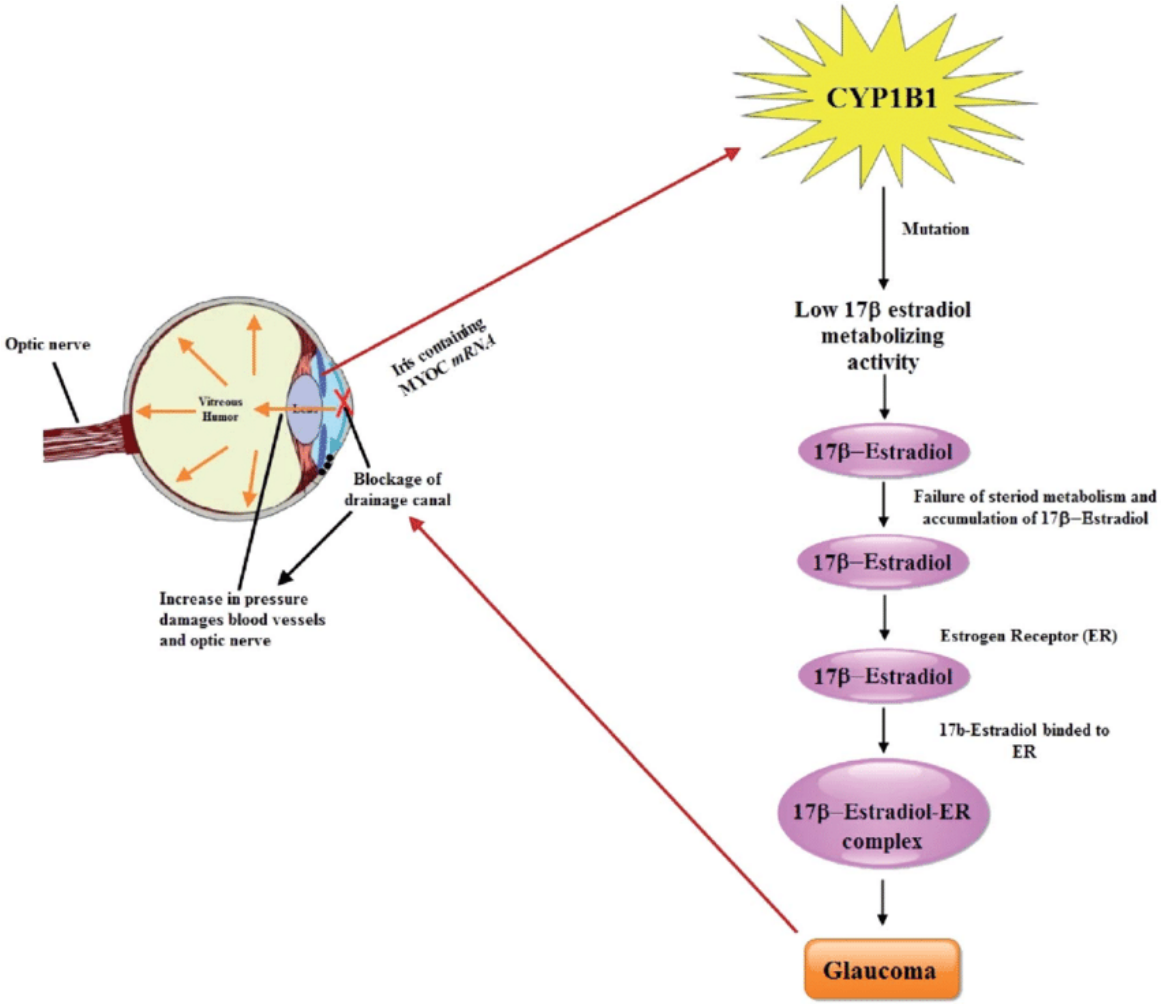

Figure 1.10 Schematic representation of the pathway in the pathology of glaucoma by *CYP1B1* (Shah et al., 2019).

1.6.Treatment

Different treatment options are available for the betterment of congenital ocular patients depending upon the genetic cause. These treatments help to minimize the symptoms and allow the patients to live a better life.

1.6.1. Pharmacologic Therapy

Researchers are working on the development of drugs for STGD1 that has the potency to reduce the accumulation of lipofuscin and other metabolites of vitamin A. For example A1120 (a non-retinoid RBP4 antagonist), fenretinide (a retinoid based RBPS antagonist) and ALK-001 (deuterated vitamin A) are under evaluation for STGD1 (Lu et al., 2017). Similarly the drugs like brinzolamide (inhibitor of carbonic anhydrase), brimonidine (alpha-adrenergic agonists) or timiol (beta-blockers) are used to reduce aqueous humor production in case of glaucoma (Kaur & Gurnani, 2022).

1.6.2. Surgery

Various surgical procedures are done to treat some ocular disease like laser therapy and filtering procedures are used for glaucoma patients. Laser trabeculoplasty or cyclophotocoagulation is an option for open-angle glaucoma patients. In this, a small laser beam is used to clear the obstructed pathways in the trabecular meshwork (Aquino et al., 2015; Gulati et al., 2017).

In filtering surgery, a procedure termed as trabeculectomy, an incision is created in the sclera and a part of the trabecular meshwork is removed. Simply a drainage device is placed in Minimally Invasive Glaucoma Surgery (MIGS). It seems to have fewer side effects but IOP is reduced by a lesser amount as it is performed in combination with cataract (Malvankar-Mehta et al., 2015; Pillunat et al., 2017; Agrawal & Bradshaw, 2018).

1.6.3. Stem Cell Therapy

Scientists are putting their efforts to use the therapeutic potential of stem cells to regenerate the RCs. Harrel and his colleagues have used the dental pulp as a source for mesenchymal stem cells (DP-MSCs). They have observed the survival and regeneration of injured axons and RGCs when DP-MSCs are transplanted intravenously (Harrell et al., 2019). Improved

vision function was observed in preclinical studies, when hESC-derived RPE cells were injected in mouse models of retinal degeneration (Lu et al., 2009).

1.6.4. Gene Therapy

The main goal of gene therapy is to introduce a functional gene within the cell to restore the normal function of the particular protein. As 90% of STGD1 cases are linked with ABCA4, so a StarGen^{TM} (Oxford Biomedica, Sanofi), a lentivirus-based vector carrying the *ABCA4* gene is under clinical trials. Positive outcomes were seen in a preclinical trials of StarGen^{TM} in a *Abca4* $^{-/-}$ knockout mouse model of Stargardt disease (Kong et al., 2008; Lu et al., 2017).

1.7. Mutations Reported in Pakistani Population

After doing literature review, genetic data was gathered that showed 56 genetic studies comprising of 466 patients from 103 families with retinal dystrophies. On the basis of data gathered, it was observed that most common mutations in *CNGA3*, and *CNGB3* genes were detected in Pakistani patients with macular atrophy (Khan et al., 2014). Mutations reported in Pakistani population with CORD are listed in table 1.1.

Approximately 270 mutations have been reported in exon 2 and 3 of *CYP1B1* collectively, making up a significant percentage of the genetic burden in both familial and sporadic instances of PCG (Leiden Open Variation Database (LOVD) (www.lovd.nl/ABCA4) ; (Firasat et al., 2018). Mutations reported in Pakistani glaucoma patients so far are listed in table 1.2.

Approximately more than 13 studies have been carried on PCG, comprising data of more than 70 families. Based on this data, it is observed that mutations in *CYP1B1* and *LTBP2* are associated with PCG in Pakistan. Exon 2 and 3 in *CYP1B1* are hot spot regions for mutations in patients of PCG and p.Arg390His is the most frequent pathogenic variant observed in Pakistani patients (Sheikh et al., 2014; Micheal et al., 2015; Bashir et al., 2015; Rauf et al., 2016; Waryah et al., 2019; Rashid et al., 2019; Khan et al., 2019; Afzal et al., 2019).

In 2017, Lee screened out the *ABCA4* variants in 38 patients of South Asian descent,

notably from India, Pakistan, Bangladesh and Sri Lanka and reported that half of the patients in his study carried the pathogenic variant in exon 42 c.5882G>A, p.(G1961E) (Lee et al., 2017). Based on this data, there is a need for the genetic screening of ocular disorders in Pakistan.

Table 1.1: Mutations Reported in Pakistani patients with CORD

Genes	Exon	Nucleotide Change	Protein Change	Citation
CNGA3	7	c.822G>T	p. R274S	(Azam et al., 2010)
	7	c.827A>G	p. N276S	(Saqib et al., 2011)
	8	c.955T>C	p.C319R	(Sheikh et al., 2014)
	8	c.1306C > T	p. R436W	(Arshad et al., 2019; Saqib et al., 2015)
	8	c.991G > C	p. G331R	(Saqib et al., 2015)
	8	c.1540G>A	p. D514N	(Arshad et al., 2019)
	8	c.847 C>T	p. R283W	(Ur Rehman et al., 2019)
CNGB3	6	c.646C > T	p. R216X	(Saqib et al., 2015)
	16	c.1825delG	p.V609W*fsX9	(Azam et al., 2010)
RPGRIP1	13	c.1639G>T	p. A547S	(Hameed et al., 2003)
	16	c.2480G>T	p. R827 L	(Hameed et al., 2003)
	17	c.2656C > T	p. L886F	(Saqib et al., 2015)
ABCA4	3	c.214G>A	p. G72R	(Ur Rehman et al., 2019)
	21	c.3081T>G	p.Y1027Ter	(Ur Rehman et al., 2019)

Table 1.2: Mutations reported in Pakistani patients with PCG

Genes	Exon	DNA Position	Protein Position	References
CYP1B1	2	c.457C>G	p. R153G	(Tehreem et al., 2022)
	2	c.516C>A	p. S172R	(Tehreem et al., 2022)
	2	c.629dup	p.G211Rfs*13	(Tehreem et al., 2022)
	2	c.722T>A	p.V241E	(Tehreem et al., 2022)
	2	c.732G>A	p.M244I	(Tehreem et al., 2022)
	2	c.287dup	p.L97Afs*127	(Tehreem et al., 2022)
	2	c.662dup	p.R222Pfs*2	(Tehreem et al., 2022)
	2	c.247del	p.D83Tfs*12	(Tehreem et al., 2022)
	2	c.758-759insA	p.V254Gfs*73	(Tehreem et al., 2022)
	2	c.740T>A	p.Leu247Gln	(Tehreem et al., 2022)
	2	c.37C>T; c.38T>A[a]	p.L13*	(Waryah et al., 2019)
	2	c.789dup	p.L264Afs*63	(Tehreem et al., 2022)
	2	c.724G>c	p.D242H	(Tehreem et al., 2022)
	2	c.107G>A	p.G36D	(Sheikh et al., 2014)
	2	c.109C>T	p.Q37*	(Rauf et al., 2016)
	2	c.182G>A	p.G61E	(Afzal et al., 2019; Bashir et al., 2015; Yousaf et al., 2022)
	2	c.198_209del12	p.G67-A70del	(Sheikh et al., 2014)
	2	c.840C/A	p.C280*	(Zahid et al., 2023)
	2	c.241T>A	p.Y81N	(Rauf et al., 2016)
	2	c.746G>C	p.A115P	(Sheikh et al., 2014)
	2	c.542T>A	p.L18Q	(Rashid et al., 2019)
	2	c.693C>A	p.F231L	(Zahid et al., 2023)
	2	c.685G>A	p.E229K	(Afzal et al., 2019; Firasat et al., 2008; Sheikh et al., 2014; Zahid et al., 2023)
	2	c.736_737insT	p.Y246Lfs81* p.E299K	(Bashir et al., 2015; Rauf et al., 2016;

				Sheikh et al., 2014)
	2	c.862G>C	p.A288P	(Micheal et al., 2015)
	2	c.725A>C	p.D242A	(Micheal et al., 2015)
	2	c.530T>G	p.L177R	(Firasat et al., 2008)
	2	c.868dupC	p.R290Pfs*37	(Micheal et al., 2015; Rashid et al., 2019; Sheikh et al., 2014; Tehreem et al., 2022)
	Intron 2	c.1044-1G>C	p.Y349Lfs*73	(Afzal et al., 2019)
	3	c.1460T>C	p.L487P	(Firasat et al., 2008)
	3	c.1122C>G	p.D374EE	(Firasat et al., 2008)
	3	c.1048C>A[a] & c.1090G>A	p.P350T& p.V364M	(Waryah et al., 2019)
	3	c.1063C>T	p.R355 *	(Afzal et al., 2019; Micheal et al., 2015)
	3	c.1103G>A	p.R368H	(Afzal et al., 2019; Bashir et al., 2015; Rauf et al., 2016)
	3	c.1168C>T	p.R390C	(Rashid et al., 2019)
	3	c.1169G>A	p.R390H	(Afzal et al., 2019; Bashir et al., 2015; Khan et al., 2019; Micheal et al., 2015; Rashid et al., 2019; Rauf et al., 2016; Sheikh et al., 2014; Waryah et al., 2019)
	3	c.1263 T>A	p.F421L	(Tehreem et al., 2022)
	3	c.1209InsTCATGCCACC	p.T404Sfs*30	(Rashid et al., 2019; Rauf et al., 2016)
	3	c.1294G>C	p. V432L	(Khan et al., 2019)
	3	c.1300T>C	p.Y434R	(Firasat et al., 2008; Rauf et al., 2016)
	3	c.1310 or c.1311 C>T	p.P437L	(Rashid et al., 2019; Waryah et al., 2019)

	3	c.1325delC	p.P442Efs*15	(Rashid et al., 2019; Rauf et al., 2016)
	3	c.1331G>A	p.R444Q	(Rauf et al., 2016)
	3	c.1358A>G	p. N453S	(Khan et al., 2019)
	3	c.1405C>T	p.R469W	(Rauf et al., 2016)
	3	c.1436A>G	p.Q479R	(Rashid et al., 2019)
LTBP2	1	c.412delG	p.A138Pfs*278	(Ali et al., 2009)
	1	c.331C>T	p.Q111*	(Ali et al., 2009)
	4	c.895C >T	p.R299*	(Ali et al., 2009)
	6	c.1243-1256 del	p.E415RfsX596	(Ali et al., 2009)
	19	c.3028G>A	p.D1010N	(Rauf et al., 2020)
	23	c.3427delC	p.Q1143Rfs*35	(Rauf et al., 2020)
	27	c.4031_4032insA	p.D1345Gfs*6	(Micheal et al., 2016)
	34	c.4934G>A	p.R1645E	(Micheal et al., 2016)
	35	c.5270G>A	p.C1757Y	(Rauf et al., 2020)

1.8. Aim and Objectives of Study

This study was designed to investigate four families suffering from rare eye disorders with the following objectives:

1. To recruit the families suffering from inherited eye abnormalities.
2. To identify the most prevalent genes and mutations in Pakistani families with eye disorders.
3. To perform the genetic analysis to identify variants in the recruited families.

2. Materials & Methods

2.1. Study Approval

Permission was granted by the Bioethical Committee (BEC) of the Faculty of Biological Sciences, Quaid-I -Azam University, Islamabad, to carry out this study at the laboratory of Genomics, Department of Biochemistry. The families signed an BEC approved consent before granting permission to use their blood samples and medical records for the research purpose.

2.2. Family Enrolment

Four families with inherited ocular disorders were recruited from different areas of Pakistan. These families were labeled as A, B, C, and D.

2.3. Evaluation of Clinical Features

Maximum information was gathered from the families regarding the type of ocular disorders. Demographic characteristics like ages, genders etc were noted down. Ocular as well as non-ocular features like hearing, speaking, facial features, and behavioural characteristics were observed. We asked about birth history and growth of children from mother either it was normal or any other complication during pregnancy or infancy. Questions were asked regarding medical history, initial symptoms, age of onset of disease, current vision status, any diagnostic tests of eye and treatments recommended by physician. The apparent eye features were observed and captured in photos.

2.4. Pedigree Design

Information regarding generations were collected and pedigree of all these families were designed using haplopainter in order to understand the pattern of inheritance. In 2008, Bennet proposed the standard guidelines to design the pedigree (Bennett et al., 2008). Empty squares and circles showed the normal males and females respectively, whereas filled squares and circles represented the affected males and females respectively. Cross symbols represent the deceased individuals and consanguinity among two individuals is shown by double lines.

2.5. Sample Collection

7ml of intravenous blood was withdrawn from affected and healthy individuals (Parents and one normal sibling) from each family by using BD Precision Glide™ Sterilized Needle, (0.8mm X 38mm, 21G, 1.5TW, Singapore). All necessary safety measures were taken according to phlebotomy protocol and blood was collected into the K3 EDTA (ethylene diamine tetra acetic acid) tubes to prevent the blood clotting and labelled with specific numbers, assigned to an individual in the respective family. Butterflyneedles were used to collect blood from the children. These blood tubes were stored at 4◦C in a refrigerator.

2.6. DNA Extraction

The DNA of each individual was extracted by using organic method, also termed as phenol chloroform method (Sambrook & Russell, 2006). The composition and concentrations of all the chemicals used in this protocol are mentioned in table 2.1.

2.6.1. Day 1

- 750µl blood of each individual was taken from EDTA tubes and transferred in 1.5ml microcentrifuge tubes (Gene Era Biotech Co.®, California, USA) followed by addition of 750µl solution A to each tube and 15 minutes incubation at room temperature respectively with several tube inversions to speed up the lysis of blood.
- After the completion of incubation time, the centrifugation was carried out for 1 minute at a speed of 12000rpm (revolution per minute) in a microcentrifuge (Hettich Zentrifligen®, Mickro 120, Germany) resulting in the formation of two layers, the upper one (supernatant) and the lower one (pellet). The supernatant was poured out in 10% bleach solution to destroy the pathogens and the nuclear pellet was dissolved in 400µl of solution A. The tubes were centrifuged again for one minute at a speed of 12000rpm to allow the DNA to settle down at the bottom of the tube.
- Again the supernatant was poured out and the pellet was redissolved by adding 400µl of solution B, 12µl of sodium dodecyl sulfate (20% SDS), and 5µl of proteinase-K (10 mg/ml). The tubes were incubated overnight in an incubator (HeraTherm™ Thermo Scientific, USA) at 37˚C

2.6.2. Day 2

- On the second day, firstly solution C+D of equal volume was prepared to contain solution C (Saturated Phenol) and solution D (Isoamyl alcohol and chloroform) in a ratio of 1:1. Then 500µl of solution C+D was added in the incubated tubes followed by centrifugation for 10 minutes at 12000rpm, which separated the mixture in two layers, the upper one containing DNA was picked by pipette carefully to avoid mixing with the lower layer and shifted into a new microcentrifuge tube and the lower layer was discarded carefully.
- 500µl of solution D was added, followed by centrifugation for 10 minutes at 12000rpm again resulted in two layers, the upper one containing the DNA was shifted into a new microcentrifuge tube and the lower layer was discarded carefully. The DNA was precipitated by adding 55µl of sodium acetate (3M, pH=6) and 500µl of chilled isopropanol and the tubes were inverted following the centrifugation for 10 minutes at 12000rpm.
- After centrifugation the supernatant was decanted, and the pellet was washed with 200µl of 70% ethanol. The centrifugation was carried out at 8000rpm for 7 minutes. The supernatant was poured out again and the tubes containing DNA pellets were kept at room temperature for 30 minutes to dry. After drying, the DNA pellets were dissolved in 80-150µl of Tris-EDTA (TE) buffer depending upon the size of the pellet. The tubes were kept in an incubator for overnight incubation at 37°C.

2.6.3. Day 3

- The tubes containing DNA were taken out from incubator and stored at 20°C. Further, the quantity and quality of DNA was checked as mentioned below:

2.6.4. Quantitative Analysis of DNA

The concentration of DNA was determined via Nanodrop (Colibri Titertek Berthold, Germany). The DNA concentrations (ng/µl) were quantitatively analyzed along with the plotted graph. The plotted graph showed the absorbance values (A260/A280) and (A260/A230) indicating the protein, and other organic and inorganic contaminations respectively. The absorbance value within the range of 1.8-2.05 shows that the quality of DNA was good enough. 20-40ng/µl concentration of DNA is considered the best-known DNA concentration for polymerase chain reaction (PCR). Dilutions were made by using

the dilution formula in case of concentration of any DNA sample higher than 50ng/µl.

$$C_1V_1=C_2V_2$$

2.6.5. Qualitative Analysis of DNA

The qualitative analysis of extracted DNA was done by using 1% agarose gel. The chemical composition of agarose gel is given in table 2.2.

- For gel electrophoresis, 1X tris borate EDTA (TBE) was used to prepare the agarose gel (1%). The same buffer was used to run the DNA.
- A stock solution of TBE buffer (10X) was prepared and the gel was made by dilution of the stock solution with distilled water in 1:10.
- For 1% agarose gel preparation, 1g of agarose was taken and added in 100 ml of 1X TBE in a conical flask. The solution was heated in a microwave for almost 2 minutes.
- After cooling, 10µl of ethidium bromide was added and mixed well. Now the agarose solution was poured into the casting tray and combs were inserted in it. The gel was allowed to solidify for almost 20-25 minutes.
- When the gel was solidified, the 1X TBE (1L) was added to the gel tank and the gel was transferred into it after removing combs.
- 3µL of DNA from each sample along with 3µL of loading dye (6X) was loaded in wells and run at 100 voltage for 60 minutes to analyze the DNA.
- Gel was visualized through Gel Doc System (INGENIUS SYNGENE Bio Imaging®, UK). The intensity and intactness of the bands on the gel are roughly proportional to DNA quality and quantity respectively.

2.7. Candidate Gene Selection

Genes were chosen for each family by following pipeline mentioned in figure 2.1

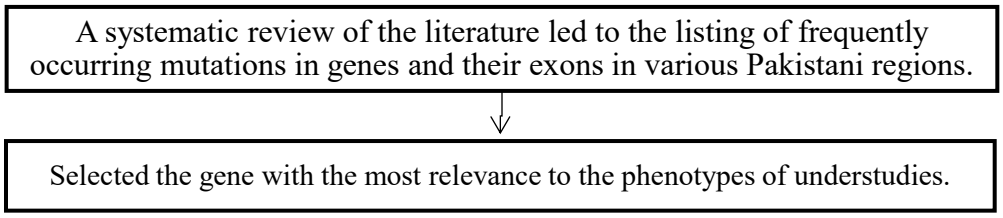

Figure 2.1: Flowchart for the selection of candidate gene .

2.8. Primer Designing

Primers are 18-24bp oligonucleotides, used to amplify specific marked regions of the DNA through PCR. Various browsers and bioinformatics tools were used to design primers for selective exons of each gene.

2.8.1. Ensemble Genome Browser

Firstly, the sequences of ***ABCA4*** **(NM_014336.5),** ***CNGA3*** **(NM_201253.3),** ***CNGB3*** **(NM_019098.5),** ***RPGRIP1*** **(NM_020366.4)** and ***CYP1B1*** **(NM_000104.4)** genes in FASTA format were downloaded from the Ensemble Genome Browser by selecting the longest transcript with specific NMID. The list of all the primers used in this study were designed by the following software as discussed below:

2.8.2. Primer 3 Input

Primer3 input browser (https://primer3.ut.ee/) was used to design the primers of the selected exon by choosing specific conditions like Primer length (18 – 22), GC Content (40-60%), Tm (56-64◦C) and Tm difference (<1◦C) (Untergasser et al., 2012).

2.8.3. In Silico PCR

It (https://genome.ucsc.edu/cgi-bin/hgPcr) provided information about the size of a hypothetical amplicon. Sensitivity, efficiency, and performance of primers under optimum temperature was evaluated. Various in silico tools were used to evaluate the quality of primers as discussed below:

2.8.4. Human Blat Search UCSC Genome Browser

It (https://genome.ucsc.edu/cgi-bin/hgBlat) was used to confirm the specificity of primers that whether each primer had a single hit in the genome or not.

2.8.5. Oligo Calc

It (http://biotools.nubic.northwestern.edu/OligoCalc.html) was used to investigate the various properties of designed primers like hairpin loop formation, self-complementarity, and mismatch like the binding of primer at any other place than selective exon through 3' end complementarity.

2.9. PCR

PCR, used to amplify the small size of DNA fragment, comprising of three steps i.e. denaturation, annealing and extension (Mullis and Faloona, 1987). Thermocycler (Biometra®,Germany) was used to carry out the PCR. After preparing and adding the reagents, the PCR tubes were vortexed following the short spin. These PCR tubes were shifted in the thermocycler (Biometra®, Germany) under specific annealing conditions for each primer and extension time required for desired product formation. Primers of ***ABCA4*** **exon 3, 11, 12, 17, 21, 22, 39, 42, 43 ,48;** ***CNGA3*** **exon 7, 8 ;** ***CNGB3*** **exon 16;** ***RPGRIP1*** **exon 13,16,17** and ***CYP1B1*** **exon 3** were amplified by using open reagent PCR as size of amplicons in all these exons is less than 1000bp. The PCR reagents composition and profile is given in table 2.8 and 2.9 respectively.

2.9.1. PCR by using HOTSTART Taq Master Mixture

The PCR regents and conditions were optimized on the basis of hypothetically achieved product length determined by In-Silico PCR and efficiency of each primer set. Like primers of ***CYP1B1*** **exon 2** was amplified by using commercially available HOTSTART Taq Master Mixture (Qicgen, USA) as amplicon size was greater than 1000bp. The constituents of master mix and PCR profile is mentioned in table 2.10 and 2.11 respectively.

2.9.2. Touch Down PCR

Touch down program was used to amplify the exon 2 of *CYP1B1* in order to reduce off-targeting of primers and to increase the yield of required product under different conditions. For this purpose dimethylsulphoxide (DMSO) and $MgCl_2$ (1µl) were added in the reaction mixture (13µl) to make the primers highly specific for product formation. The constituents used in this mixture and profile is mentioned in the table 2.12 and 2.13 respectively.

2.9.3. Agarose Gel Electrophoresis

The quality and estimated size of the PCR product was checked by visualizing the bands in the Gel Doc System (INGENIUS SYNGENEBio Imaging®, UK) after running it on 2% agarose gel at voltage of 120V for 20 minutes. This image was saved in the connected database with Gel Doc System. The chemical composition of 2% gel is given in table 2.2.

2.9.4. PCR Product Purification

Purified product was required for the applications like sanger sequencing. The non specific products like primer dimers, dNTPs, and enzymes were removed by using different protocols mentioned below:

2.9.4.1. EXOSAP-IT™ Purification

Equal volume of ExoSAP and water was mixed for each reaction. 2µl of EXOSAP IT™ reagents (Thermo Scientific) from mixture and 6µl of PCR product were added and tubes were placed in thermocycler (Biometra®, Germany). The profile was selected that consists of 15 minutes incubation at 37°C to hydrolyze the excessive primers and nucleotides in a single enzymatic reaction and 15 minutes incubation at 80°C to inactivate the ExoSAP-IT ™ reagents. After this procedure of 30 minutes, the bands of purified products were examined on the 2% agarose gel under UV light. Clear and bright bands confirmed the quality of purified product for sequencing.

2.9.4.2. Gel Purification

The nonspecific products were present in the amplicon of exon 8 of *CNGA3*, exon 3, 12 and 48 of *ABCA4* and exon 2 of *CYP1B1*. Gene Jet Purification Kit (Thermo Scientific, USA) was used to purify these amplicons. The procedure is as follow:

- The 1.5 ml microcentrifuge tubes were pre-weighed and sterilized blade was used to cut the gel containing desired PCR product. The difference between the pre-weight and post-weight readings was used to calculate the weight of the gel slice. The gel mixture was combined with an equal volume of binding buffer (1:1) and incubated at 60 °C in the incubator until the gel slice was fully dissolved. The tube was inverted several times. The solution's yellow color indicated a pH level that is optimal for DNA binding.
- The tubes were inverted several times and the gel mixture was transferred on the Gene JET purification column and centrifuge at 8000rpm for 1 minute. The column was put back into the same collection tube after the flow-through was discarded. 100µL of binding buffer was added to the column and centrifuged it for 1 min. The column was kept in the same collection tube again after discarding flow through. 700µL of wash buffer (diluted with ethanol) was added to the column and centrifuged it for 1 min.

Impurities from the walls of column were removed via repeated centrifugation

- Column was repositioned into new 1.5ml microcentrifuge tube. Elution buffer was added to the column depending upon the volume required followed by centrifugation for 1 minute. The DNA obtained in flow through was qualitatively analyzed by running on 2% agarose gel. Clear and bright bands according to estimated size confirmed the quality of purified product for sequencing. Now, samples were proceeded further for Sanger sequencing.

2.10. Gene Sequencing

Purified products of PCR with clear bands were further proceeded for Sanger sequencing. 4µl of Terminator Ready Reaction Mix, 4µl of DNA template (30-90ng), 1µl of primer and 1µl of ddH_2O were added in 0.2ml of micro-map tubes followed by short spin. Tube were placed in the thermocycler and profile was set comprising of 25 cycles with incubation 96°C for 10 seconds, then 50°C for 10 seconds and 60°C for 4 minutes, and stored at 4°C.

40µL (75%) and 30µL (100%) of isopropanol were mixed in a 1.5ml of microcentrifuge tube in order to purify the sequencing products followed by incubation of 15 minutes at room temperature .The samples were centrifuged, and supernatant were discarded. 75% isopropanol was used to wash DNA pellet followed by centrifugation for five minutes. Again supernatant was discarded and the sample was placed in a vacuum centrifuge tube for 10-15 minutes and stored at 20°C. The pellet of the sample was dissolved in 3µL of loading buffer, centrifuged, and heated at 95°C for 2-3 minutes. Finally, tubes were put on chilled ice, and the purified product was sequenced.

2.11. In Silico Analysis of Sequencing Data

2.11.1. Bio Edit Software

The sequencing results were analyzed on the **Bio edit Software** (Hall, 1999) by aligning the sequence results with consensus sequence of each gene downloaded from the Ensemble Genome Browser using the ClustalW Multiple Alignment Option (Thompson et al., 1994). Any changes in the chromatogram and nucleotide bases were examined properly. The variants identified in data were further investigated through different bioinformatics tools.

2.11.2. Mutation Taster

This tool predicts about the pathogenic nature of the variant that either it is disease causing or not (Schwarz et al., 2014). It gives us the PhastCons and PhyloP scores that help us to determine the grade of conservation of given nucleotides and the level of pathogenicity. The phastCons values lie within range of 0 to 1 (the closer the value is to one, the more likely the nucleotide is conserved, and the variation is pathogenic). PhyloP scores from -14 to +6. In comparison to a negative score, a positive score indicates slower evolution than expected under neutral drift, but also acceleration. (Siepel et al., 2005).

2.11.3. Sorting Intolerant from Tolerant (SIFT)

This tool helps to predict the functional change in protein due to amino acid substitution on the basis of phylogenetic tree and physical characteristics of amino acids. It is used for non-synonymous polymorphisms and missense mutations Its scores show the respective data. If this score is lower than 0.05 then this shows a damaging (D) effect of substitution on the protein function, and if it is less than 0.05 it is considered to be tolerant (T); thus does not affect function of the protein (Vaser et al., 2016).

2.11.4. Polymorphism Phenotyping v2 (POLYPHEN-2)

It predicts the effect of variation in protein function depending upon modification of amino acids in the protein structure.This software accurately checks whether the variation affects both structure and function of protein, taking into the account the physical properties as well. Based on the training sets inbuilt in this software, the values fall in **0.85-1** to render the substitution as probably damaging (D), **0.15-1** as possibly damaging (P), **0.0-0.15** as benign (B) (Adzhubei et al., 2010).

2.11.5. Human Splice Site Finder (HSF)

The Human Splice SIE Finder is a tool that uses combination of 12 different algorithms to analyze the impact of mutations on branch site, acceptor, and donor splice sites. It also helps us to determine the effect of mutations on exonic splicing enhancers (ESE) and exonic splicing silencers (ESS) that either promote or suppress splicing. (Desmet et al., 2009).

2.11.6. Combined Annotation Dependent Depletion (CADD)

This tool was used to analyze the deleteriousness of SNVs including indels in the human genome. Positive CADD raw scores show that variant is deleterious (D), negative scores how that it is neutral (Rentzsch et al., 2019).

2.11.7. Varseak

This tool helps us to determine the impact of mutation on splice site. It predicts the score as splice site prediction class from 1 to 5 ranking it as no, likely no, unknown, likely and 100 % splicing effect respectively (Witsch-Baumgartner et al., 2022).

2.11.8. SNPs and GO

It is an online server that helps to determine the effect of missense variants on the functional properties of protein by using different algorithms (Capriotti et al., 2013).

2.11.9. Varsome

Varsome is an effective annotation tool and human genome variation search engine. By using the guidelines of American College of Medical Genetics and Genomics (ACMG), it assists us in categorizing the variant as 'pathogenic', 'likely pathogenic', 'benign', or 'uncertain importance' (Kopanos et al., 2019).

2.11.10. Panther-PSEP (Position-Specific Evolutionary Preservation)

This tool calculates the length of the amino acid's preservation time and aids in determining the influence of variation on protein function. The longer the preservation time, the greater the possibility of functional influence (Tang & Thomas, 2016).

2.12. In silico Analysis of Structural Changes in Protein

Different bioinformatic tools were used to determine changes in the primary, secondary and tertiary structure of protein because of pathogenic mutation. The pipeline for all those tools were mentioned in figure 2.2.

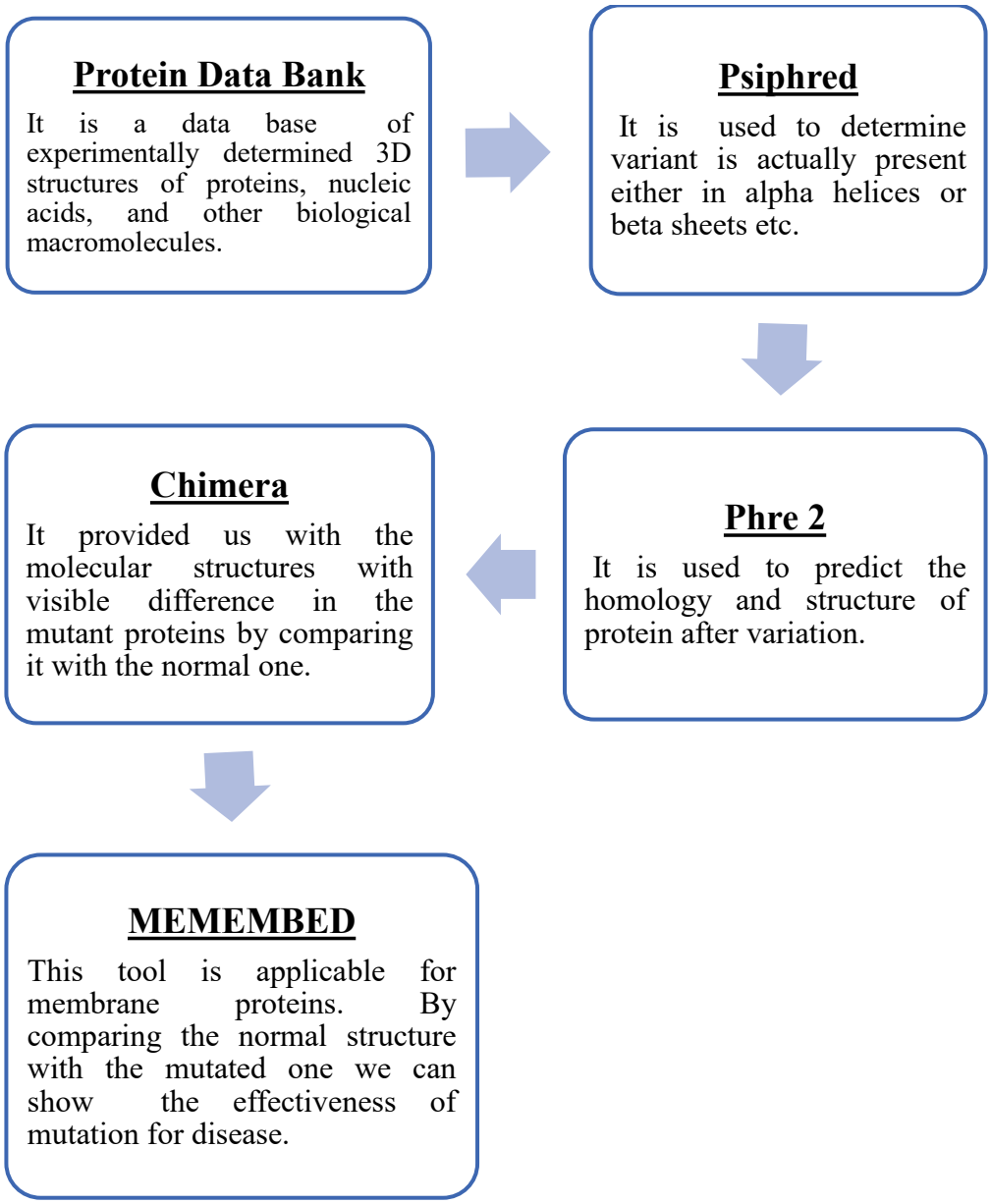

Figure 2.2: Schematic representation of all the tools used in in silico analysis of structural changes in protein (McGuffin et al., 2000; Pettersen et al., 2004; Gasteiger et al., 2005; Kelley et al., 2015).

Table 2.1: Chemical composition and concentrations of DNA extraction stock solutions and buffers

Stock Solution	Chemical Composition	Concentrations
Solution A	Sucrose	0.32M
	Tris HCl (pH= 7.5)	10mM
	Magnesium Chloride ($MgCl_2$)	5mM
	Triton X-100 (v/v)	1%
Solution B	Tris HCl (pH= 7.5)	10mM
	Sodium Chloride (NaCl)	400mM
	EDTA (pH= 8)	2mM
Solution C	Saturated Phenol	
Solution D	Chloroform	24 volumes
	Isoamyl alcohol	1 volume
20% SDS	SDS	10g
	Water	50mL
Loading Dye	Sucrose	40g
	Bromophenol	0.25g
10X TBE	Tris	0.89M
	Boric Acid	0.89M
	EDTA (pH= 8)	0.89M

Table 2.2: Composition of agarose gel electrophoresis

Sr. No.	Reagents	Volume/Reaction
1.	Agarose	1 – 2 %
2.	1X Tris-EDTA-Boric acid (TBE) Buffer	100ml
3.	Ethidium Bromide	Upto 10ml

Table 2.3: List of primers of *CNGB3* exon 16

Exon Name	Primer Sequences	Tm (°C)	Product Size (bp)
CNGB3 Ex-16F	ACACTCTCTGCACAATCACC	58.4	544
CNGB3 Ex-16R	AGCACTCTGTGGGTAAGAGAG	61.3	

Table 2.4: List of primers of *CNGA3*

Exon Name	Primer Sequences	Tm (°C)	Product Size (bp)
CNGA3 Ex-7F	GGGGTGATTACACTGAGGTAG	61.3	356
CNGA3 Ex-7R	GGTCAAGGGTAGGTAATGTCC	61.3	
CNGA3 Ex-8AF	GGGACAGACTCCTGGGTCTAC	60	904
CNGA3 Ex-8AR	ACCTTGAGGAGAAAGTG	59.8	
CNGA3 Ex-8DF	CCTCAGCGATGGCAGCTACT	61.2	548
CNGA3 Ex-8DR	CAAGTTCCATGCCACACAGC	58.4	

Table 2.5: List of primers of *ABCA4*

Exon Name	Primer Sequences	Tm (°C)	Product Size (bp)
ABCA4 Ex-3F	TGCTGAGAATGAAGGAGGACA	62.4	641
ABCA4 Ex-3R	CTGTCCAGGTTGATCAGGGT	64.5	
ABCA4 Ex-11F	CATGGACTTGGGGAAATGGG	61	597
ABCA4 Ex-11R	GGAGATGTGAAGAGGAAACCG	59	
ABCA4 Ex-12F	GGACAGCAGCCCTTATCCTG	64.5	859
ABCA4 Ex-12R	AGGATCGCGAACTTCAGACTC	62.6	
ABCA4 Ex-17F	GGGTAGTCTTTCTGGGAGCC	64.5	348
ABCA4 Ex-17R	ACTCATCAGGAATCACACCGT	60.6	
ABCA4 Ex-21F	TGAGCATCTTGATTGCCAAA	56.3	589
ABCA4 Ex-21R	GGTTTGGTGCTGCCTCTTAG	62.4	
ABCA4 Ex-22F	CTAAGAGGCAGCACCAAACC	58	420
ABCA4 Ex-22R	TGATAAACCCCCTTCTGAGTG	61	
ABCA4 Ex-39F	GTCTGGCTGCAAGGACTCTC	64.5	826
ABCA4 Ex-39R	AAACATTGTGGAGTGGGGCT	60.4	
ABCA4 Ex-42F	GGAAAGGACAGTGCCAAGGA	62.4	753
ABCA4 Ex-42R	GCACAAGAGCTGATGTTCGG	62.4	
ABCA4 Ex-43F	ACACACACACTTACCCTGGG	62.4	288
ABCA4 Ex-43R	GCCTCAGAGCCACCCTACTA	64.5	
ABCA4 Ex-48F	GACAGGGTCTTTCTTGTTGCC	62.6	560
ABCA4 Ex-48R	ATCGGGAATGTTATGCCTCC	60.4	

Table 2.6: List of primers of *CYP1B1*

Exon Name	Primer Sequences	Tm (°C)	Product Size (bp)
CYP1B1 Ex-2AF	TCTTCTCCAAGGGAGAGTG	55.3	1326
CYP1B1 Ex-2CR	GATCTTGGTTTTGAGGGGTG	62.6	
CYP1B1 Ex- 3AF	AGTCATGCAAGGCCTATTAG	58.4	917
CYP1B1 Ex-3BR	TGAGAAGCAGCACAAAAGG	60.6	

Table 2.7: List of primers of *RPGRIP1*

Exon Name	Primer Sequences	Tm (°C)	Product Size(bp)
RPGRIP1 Ex13AF	GGGTCTGCAAGGAAATCAAA	60	365
RPGRIP1 Ex13AR	AGTGGAACACAGGCGTTAGC	62	
RPGRIP1 Ex-16F	GTTTGCAGGCAGGTGAAGAT	61	650
RPGRIP1 Ex-16R	TTCTGCTCTGTTGCTCTTGACA	59	

Table 2.8: Polymerase Chain Reaction reagents (open reagent)

Sr. No.	PCR Reagents	Volume Per Reaction
1	10X Taq Buffer (NH4)2SO4 or 10X Taq Buffer KCl (ThermoScientific)	2.5µl
2	MgCl2 (Thermo Scientific)	0.8-1µl
3	dNTPs (10mM, Thermo Scientific)	0.5µl
4	Taq. Polymerase (Thermo Scientific)	0.2µl
5	Template DNA (50-100ng)	1µl
6	Forward Primer (10µM)	1µl
7	Reverse Primer (10µM)	1µl
8	Nuclease free water	up to 25µl

Table 2.9: General PCR profile

Steps	Cycles	Temperature (˚C)	Time Duration
Initial Denaturation		95.0	10 min
Denaturation	40 Cycles	95.0	1 min
Annealing		58.0-64.0	1-1.5 min
Extension		72.0	1-2 min
Final Extension		72.0	10 min
Pause		4.0	∞

Table 2.10: HOTSTART Taq Master Mix PCR reagents

Sr. No.	PCR Reagents	Volume Per Reaction
1	HOTSTART Taq Master Mix	3.0µl
2	Template DNA (50-100ng)	1µl
3	Forward Primer (10µM)	1µl
4	Reverse Primer (10µM)	1µl
5	Nuclease free water	Up to 13µl

Table 2.11: HOTSTART Taq Master Mix PCR profile

Steps	Cycles	Temperature (˚C)	Time duration
Initial Denaturation		95.0	15 min
Denaturation	40 Cycles	95.0	1 min
Annealing		60.0	1 min
Extension		72.0	1-2 min
Final Extension		72.0	10 min
Pause		4.0	∞

Table 2.12: Touch down PCR reagents

Sr. No.	Reagents	Volume per reaction
1	HOTSTART Taq Master Mix	4.0µl
2	Template DNA (50-100ng)	1.3µl
3	Forward Primer (10µM)	1µl
4	Reverse Primer (10µM)	1µl
5	DMSO	1.5µl
6	$MgCl_2$ (Thermo Scientific)	1µl
7	Nuclease free water	Up to 13µl

Table 2.13: Touch down PCR profile

Steps	Cycles	Temperature (˚C)	Time duration
Initial denaturation		95.0	15 min
Denaturation	2x18 Cycles	95.0	1 min
Annealing		64.0	1 min
Extension		72.0	2 min 30 sec
Denaturation		95.0	1 min
Annealing	5x39 Cycles	59.0	1 min
Extension		72.0	2 min 30 sec
Final Extension		72.0	10 min
Pause		4.0	∞

3. Results

3.1. Clinical Profile of Families

Four families (Family A, B, C and D) with different type of inherited eye disorders were recruited from the different areas of Pakistan. Patients of family A were suffering from STGD1, whereas affected individuals of family B & D were presented with symptoms of CORD. Affected individuals of family C were suffering from PCG.

3.1.1. Family A

Patients of family A presented the symptoms of STGD1. The autosomal recessive pattern of inheritance was observed in the generation pedigree (Figure 3.1). Three individuals (two males and one female) are affected in fourth generation. The samples were collected from affected individual VI:1 along with parents and available siblings.

During physical examination, we observed the apparent features of both eyes of patient. The eyes of affected patient VI:1 were normal as observed in figure 3.2. The patient was born normal. The symptoms started appearing at the age of 8 years. It was observed that bright light irritates the affected patients and makes his eyes red. He can see but unable to read or see the faces clearly. He observed blurriness in his central vision and scotoma is indicated. He was able to differentiate between different colors indicating no color blindness. Nystagmus was not observed in any of the individual. No other issues like hearing, facial abnormalities or other neurological problems were detected, indicating it as a non-syndromic case.

The spectral domain optical coherence tomography (SD-OCT) showed the foveal atrophy and the appearance of drusens in fundoscopic images which corelated with STGD1 (Figure 3.3). Clinical features of family A are listed in the table 3.1. All the affected patients presented the same symptoms. Not even a single symptom of STGD1 was observed in parent, indicating them as completely normal.

3.1.2. Family B

Patients of family B were suffering from CORD. The analysis of 4 generation pedigree clearly indicated the autosomal recessive pattern of inheritance (Figure 3.4). Two females are affected in fourth generation. The patient IV:2 was recruited to take her blood sample.

During a recent physical examination, apparently both eyes looked normal (Figure 3.5) and no other abnormality was seen indicating the non-syndromic nature of disease. It was observed that patient can perceive little bit of light. She was unable to see and differentiate between colors which lead to the diagnosis of achromatopsia. She also presented scotoma and responded mostly based on hearing and using white cane to move. During night, she has no vision.

SD-OCT showed the severe macular atrophy indicating the loss of both cone and rod cells and lead to diagnosis of CORD (Figure 3.6). Clinical features of family B are listed in the table 3.2. Her elder sister IV-2 also presented the similar symptoms.

3.1.3. Family C

Patients of family C were diagnosed with PCG. Autosomal recessive inheritance of PCG was observed in the 4-generation pedigree (Figure 3.7). Two males IV:2 and IV:4 are affected in the fourth generation. The affected individual IV:2 was recruited to collect the blood.

The apparent features of patient IV:2 were noticed during physical examination. Previously, suffered from bulging of eyes due to high intraocular pressure and corneal opacity with no visual acuity. The surgery of this patient IV:2 was carried out twice at a local hospital to overcome this issue, but it remained unsuccessful to restore vision.

The eye images of affected individual IV:2 showed the bluish discoloration (Figure 3.8). He was unable to perceive light, so bright light didn't affect him. Patients' gestures and postures were examined to confirm that there was not any syndrome associated with the disease. Clinical features of family C are listed in the table 3.3. Other patient also exhibited the similar clinical symptoms. Physical examination of parents revealed that they had normal vision and did not have any symptomof primary congenital glaucoma.

3.1.4. Family D

Patients of family D presented the symptoms of macular atrophy. The analysis of 4 generation pedigree clearly indicated the autosomal recessive pattern of inheritance (Figure 3.9). Three females are affected in fourth generation. The blood sample was collected from affected individual IV:4 along with parents and available siblings.

Apparently both eyes looked normal (Figure 3.10) and no other abnormality was observed indicating it as a non-syndromic case, during physical examination. The

patient IV:4 initially presented the symptoms at the age of 4 years. She was unable to differentiate between colors. Her central vision was also affected .

The deposition of pigments is observed in fundoscopic images of the affected patient IV:4 , indicating the macular atrophy (Figure 3.11). Clinical features of family D are listed in the table 3.4. Other affected patients also showed the similar clinical profile. Parents didn't exhibit the symptoms of macular degeneration.

3.2. Candidate Gene Analysis

A detailed systematic review was carried out to screen out the genes that were correlated with the phenotype. Mutations in various genes which are involved in maintaining the intricate architecture and proper functioning of ocular tissues have been reported. Out of which mutations in *ABCA4*, *CNGA3*, *CNGB3* and *RPGRIP1* are more frequent and correlated with the phenotype (Figure 3.12). Some of the most frequent mutations reported in various exons of *ABCA4* internationally were also screened out like exon 3, 12, 17, 21, 22, 43 and 48 (Figure 3.13).

3.2.1. Family A

Family A, suffering from STGD1 was screened for various exons of *ABCA4*, *CNGA3*, *CNGB3* and *RPGRIP1*. The sanger sequencing of all these exons identified two heterozygous variants i.e., c.1694C>T (p.T565M) in exon 8 of *CNGA3* and c. 1678A>T (p.R560W) in exon 13 of *RPGRIP1* in affected individual VI:I of family A (Figure 3.14 and 3.15). Further in silico analysis of these variants is summarized below:

3.2.1.1. CNGA3 variant

A heterozygous missense variant was identified at the physical location chr2:99013327C>T and DNA position c.1694C>T. This change in nucleotide results in substitution of amino acid threonine (T) into methionine (M) at 565 position (p.T565M). This variant is reported in ExAC with reference ID 201747279. The phastCons score is equal to 1 and phyloP score is positive indicating that amino acid at this position is highly conserved and can affect protein function. The HumDiv and HumVar score of p.T565M is 0.999 and 0.999 respectively, predicting it probably damaging. So, it is predicted to be pathogenic on basis of score calculated by Mutation Taster, PolyPhen-2, CADD, SNPs & GO, SIFT, PROVEAN, HSF, REVEL, VARSEAK and PANTHER-PSEP. ACMG also classify it as pathogenic (Table 3.5).

3.2.1.2. RPGRIP1 Variant

A heterozygous missense variant was identified at the physical location chr14:21790079A>T and DNA position c. 1678A>T. This change in nucleotide results in substitution of amino acid arginine (R) into tryptophan (W) at 560 position (R560W). Mutation taster predicted this missense variation as polymorphism. The variant is not reported in ExAC and 1000G. The phastCons score is less than 1 and phyloP score is positive but indicating that amino acid at this position is not highly conserved. It is predicted to have benign effect by CADD, SNPs & GO, HSF and VARSEAK, however SIFT and PolyPhen-2 predict it as pathogenic. According to ACMG, the variant is of uncertain significance (Table 3.5).

3.2.2. Family B

Family B, suffering from CORD was screened for various exons of *ABCA4*, *CNGA3*, *CNGB3* and *RPGRIP1*. Three variants were identified including a homozygous deletion c.1298_1298delT (p. L433Wfs*32) and a homozygous variant g.49583T>A (no protein change) in exon 8 of *CNGA3* and a heterozygous variant c.3288G>A (no protein change) in exon 22 of ABCA4 was identified in affected individual IV:2 (Figure 3.16 - 3.18). Further in silico analysis of these variants is mentioned below:

3.2.2.1. CNGA3 Variants

A homozygous deletion was identified at the physical location chr2:99012931_ 99012931delT, and DNA position c.1298_1298delT. This deletion results in frameshift of protein, might cause nonsense mediated decay (NMD). Mutation taster predicted this variation as disease causing and it may affect the protein and splice site features. The variant is not reported in 1000G and ExAC but reported in HGMD with ID CM084799. According to ACMG classification, this variant is likely pathogenic (Table 3.5).

Normal and mutated structure of CNGA3 (c.1298_1298delT) was generated by using phyre 2. Then both structures are superimposed via chimera, and it is observed that some part of mutated *CNGA3* is missing, indicating that the deletion of T is expected to cause premature termination codon and results in truncated protein as indicated in figure 3.19. The interaction of both normal and truncated protein with membrane were assessed by using MEMEMBED Prediction. It is observed that initial part of the CNGA3 chain is normal and interacting with membrane, but missing part is required to

form channels with *CNGB3,* ultimately it results in loss of function (Figure 3.20) .

Another homozygous variant was identified at the physical location chr2:99012200T>A and g.49583T>A. This variation is present in intronic region and Mutation taster predicted it as polymorphism. The phastCons score is less than 1 and phyloP score is 0 indicating that it might not affect the function of protein (Table 3.5).

3.2.2.2. ABCA4 Variant

A homozygous variant was identified at the physical location chr.1:94508357C>T and DNA position c.3288G>A. This is a non-synonymous mutation having no change in amino acid. Mutation taster predicted this variant as polymorphism. The variant is reported in ExAC. It is predicted to be benign by CADD, HSF and VARSEAK (Table 3.5).

3.2.3. Family C

Family C, suffering from PCG was screened for *CYP1B1* gene. The sanger sequencing of *CYP1B1* identified two homozygous missense variants i.e., c.142C>G (p.R48G) and c. 355G>T (p.A119S) in IV:2 affected member of family C

(Figure 3.21 & 3.22). Various in silico tools were used to determine the nature of these variants as mentioned below:

3.2.3.1. CYP1B1 Variants

A homozygous missense variant was identified at the physical location Chr.2:38302390G>C and DNA position c.142C>G. This substitution results in change of amino acid arginine (R) into glycine (H) at 48 position (p.R48H). This variant is already reported in both homozygous and heterozygous forms in the 1000G and ExAC and designated as rs10012. The phastCons score is equal to 0 and phyloP score is negative indicating that amino acid at this position is not highly conserved and not going to affect the structure of protein.

Another homozygous missense variant was identified at the physical location chr2:38302177C>A and DNA position c.355G>T. This substitution results in change of amino acid alanine (A) into serine (S) at 119 position (p.A119S). It is already reported in both homozygous and heterozygous forms in the 1000G and ExAC and designated as rs1056827. The phastCons score is less than 1 and phyloP score is negative indicating that amino acid at this position is not highly conserved and not

going to affect the structure of protein. Both variants are predicted to be benign by Mutation Taster, Mutation Accessor, PolyPhen-2, CADD, SNPs & GO, SIFT, PROVEAN, HSF, REVEL, VARSEAK and PANTHER-PSEP. ACMG also classify them as benign (Table 3.5).

3.2.4. Family D

Family D, suffering from macular atrophy was screened for various exons of *ABCA4*, *CNGA3*, *CNGB3* and *RPGRIP1*. The sanger sequencing of all these exons identified one heterozygous variant c.6004A>T (p.S2002C) in exon 43 of ABCA4 in affected individual IV:4 of family D (figure 3.23). Further in silico analysis was performed to determine the pathogenic level of the variant as summarized below:

3.2.4.1. ABCA4 Variant

A heterozygous missense variant was identified at the physical location Chr.1:94473191T>A and DNA position c.6004A>T. This change in nucleotide results in substitution of amino acid serine (S) into cytosine (C) at 2002 position (p.S2002C). The variant is novel. The phastCons score is equal to 1 and phyloP score is positive indicating that amino acid at this position is highly conserved and will impact its effect on protein structure. It is predicted to be disease causing by Mutation Taster, Mutation Accessor, PolyPhen-2, CADD, SNPs & GO, SIFT, HSF, REVEL, VARSEAK and PANTHER-PSEP. According to PROVEAN, the variant is of uncertain significance, but ACMG classify it as pathogenic (Table 3.5).

Normal structure of *ABCA4* was downloaded from protein data bank (PDB) and mutated structure of *ABCA4* was generated by using phyre 2. Then both structures are superimposed via chimera, and some differences are observed because of mutation (Figure 3.24). The interactions of both normal and truncated protein with membrane were assessed by using MEMEMBED Prediction. It is observed that mutated protein is showing more interactions as compared to normal one (Figure 3.25).

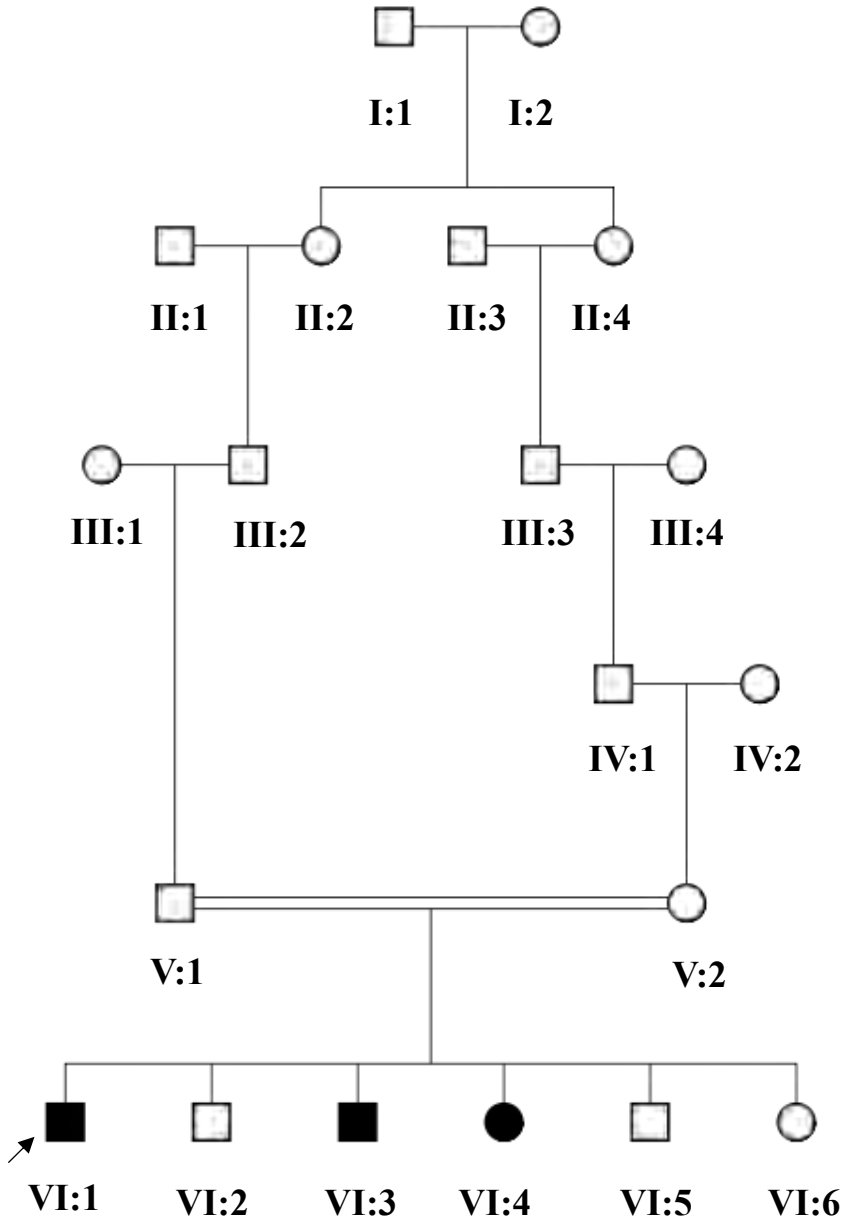

Figure 3.1: Pedigree of family A, designed by haplopainter, showing the autosomal recessive pattern of inheritance.

Table 3.1: Clinical profile of family A

Family	**A**		
No. of affected patients	3		
OCT Findings	Macular / Foveal Atrophy		
Patient ID	VI:1	VI:3	VI:4
Gender	Male	Male	Female
Age of onset	8 years	8 years	9 years
Age	29 years	25 years	30 years
Photophobia	Yes	Yes	Yes
Scotoma	No	No	No
Nystagmus	No	No	No
Blurriness of central vision	Yes	Yes	Yes
Night Blindness	No	No	No
Achromatopsia	No	No	No
Legally Blind	No	No	No

Figure 3.2: The affected individual VI:1 of family A, suffering from STGD1.

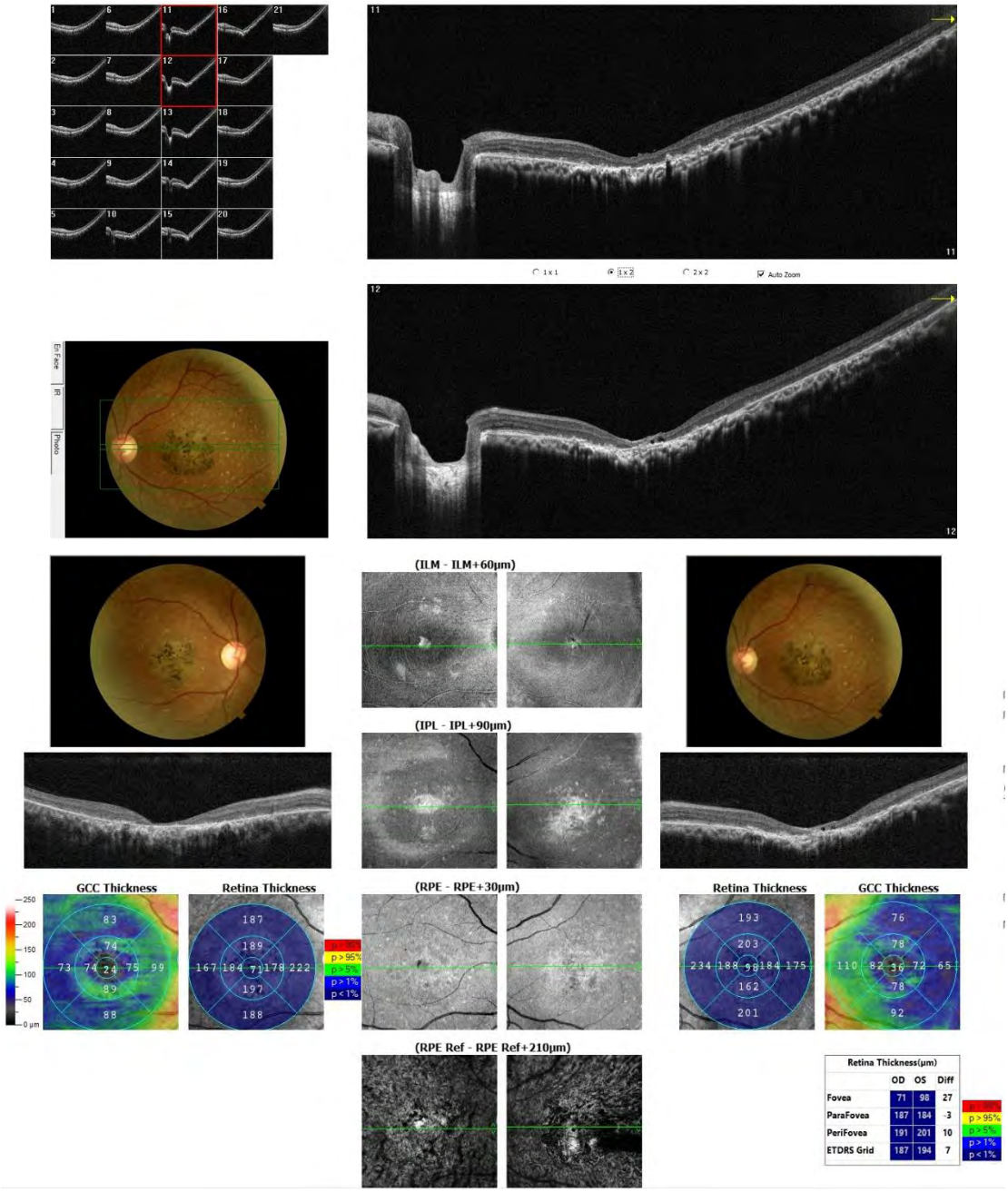

Figure 3.3: SD-OCT Macular analysis of affected individual VI:1 of family A. The architecture of the inner retinal layers is intact. However, gross degeneration of the outer retina including the ellipsoid zone, interdigitation zone, external limiting membrane (ELM) and the outer nuclear layer is seen in the foveal area. The RPE in this region is stippled.

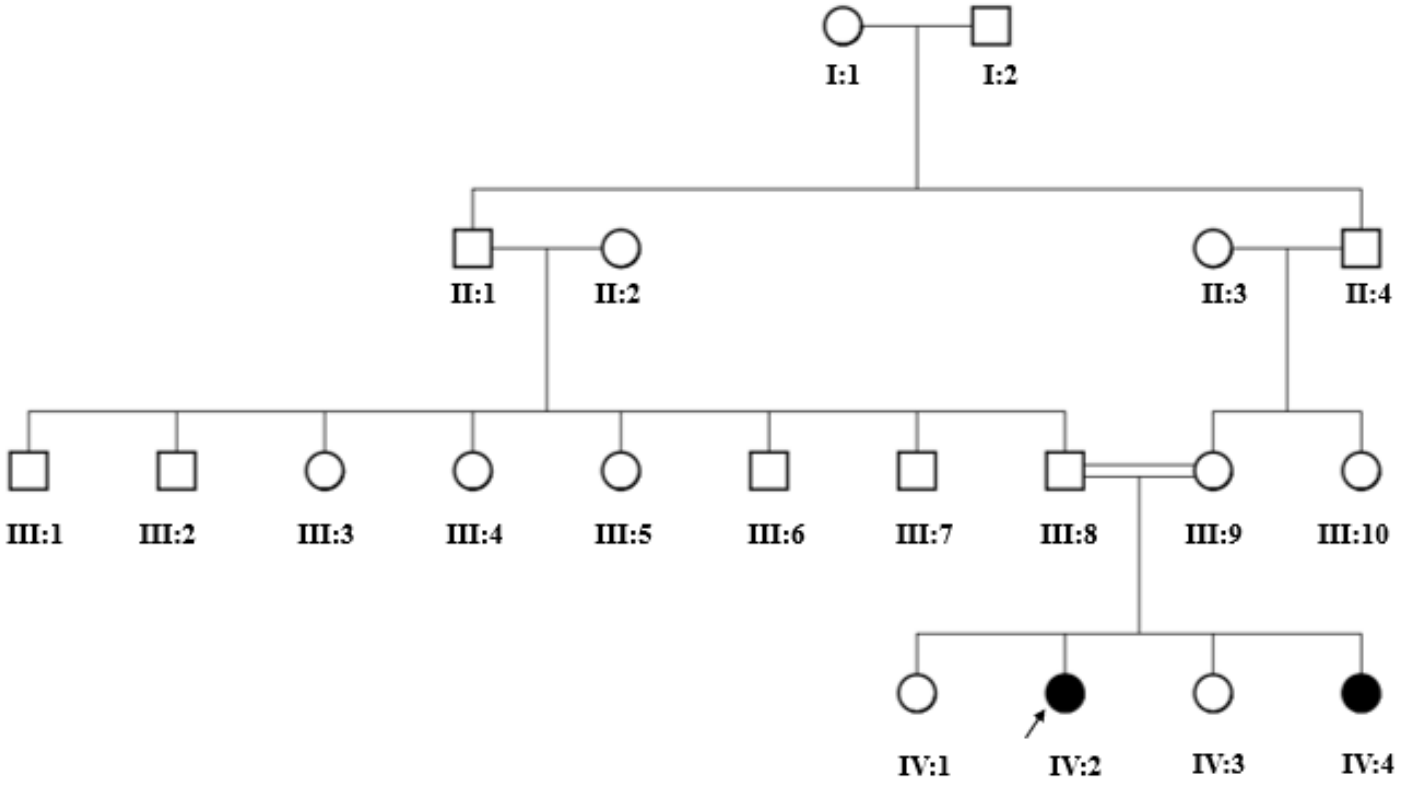

Figure 3.4: Pedigree of family B, designed by haplopainter, showing the autosomal recessive pattern of inheritance.

Table 3.2: Clinical profile of family B

Family	B	
No of affected patients	2	
OCT findings	Macular Atrophy	
Patient ID	IV:2	IV:4
Age of onset	Congenital	Congenital
Age	21 years	22 years
Photophobia	Yes	Yes
Scotoma	Yes	Yes
Nystagmus	No	Yes
Loss of central vision	Yes	Yes
Night blindness	Yes	Yes
Achromatopsia	Yes	Yes
Perception of light	Yes	Yes
Legally Blind	No	No

Figure 3.5: The affected individual IV:2 of family B, suffering from CORD.

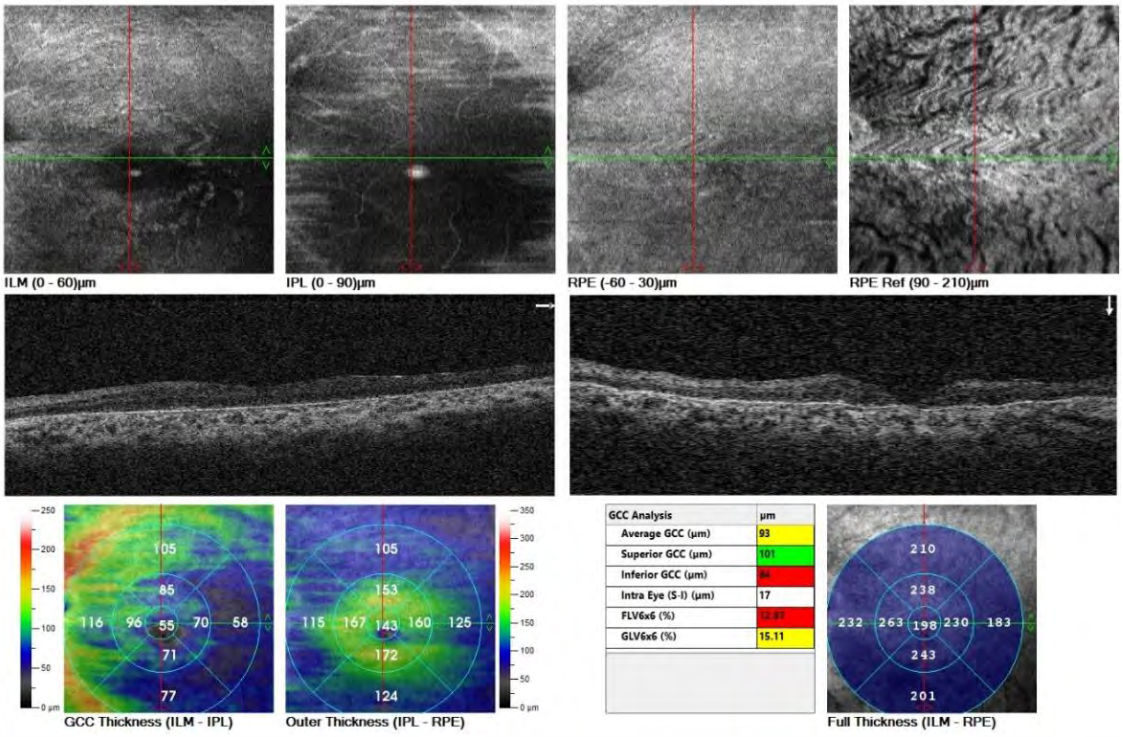

Figure 3.6: SD-OCT Macular analysis of affected individual VI:2 of family B. There is generalized diffuse degeneration of the outer retinal elements in the macular area. The retinal tissue is showing distortion and severe thinning.

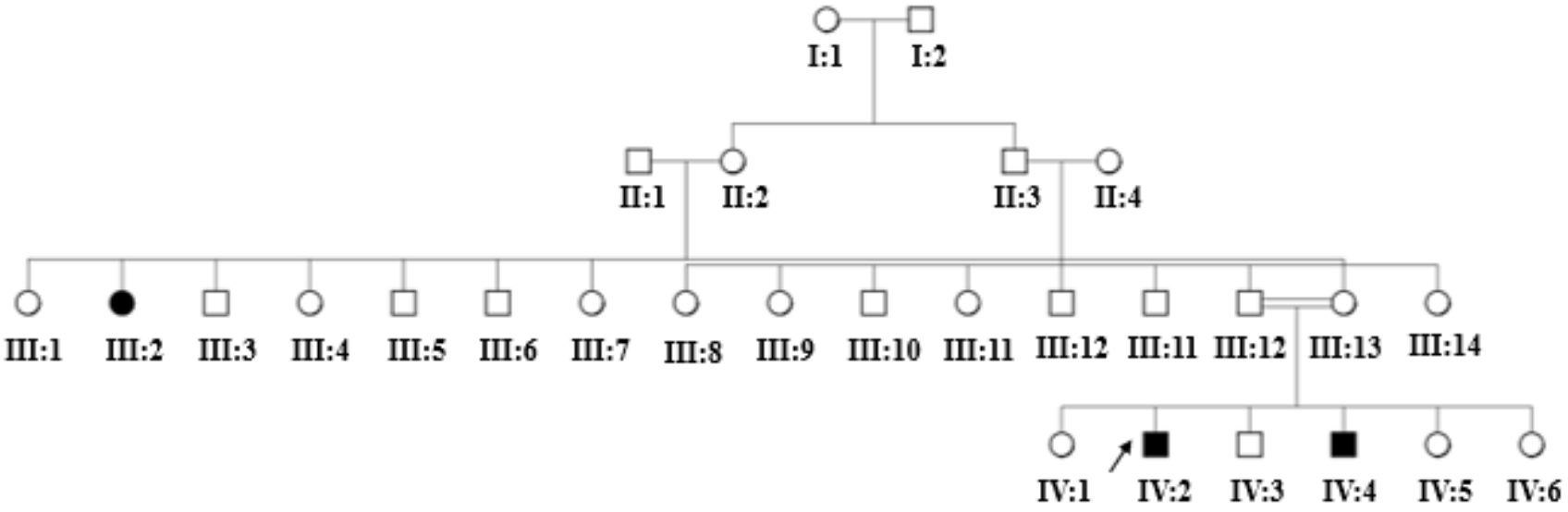

Figure 3.7: Pedigree of family C, designed by haplopainter, showing the autosomal pattern of inheritance.

Table 3.3. Clinical profile of family C

Family	C	
No. of affected patients	2	
Patient ID	IV:2	IV:4
Gender	Male	Male
Onset of disease	Congenital	Congenital
Age	21	31
Photophobia	No	No
Optic nerve deterioration	Yes	Yes
Nystagmus	No	No
Discoloration of eye	Yes	Yes
Corneal opacity	Yes	Yes
Unilateral/bilateral	Yes	Yes
Perception of light	No	No
Legally Blind	Yes	Yes

(a)  (b) 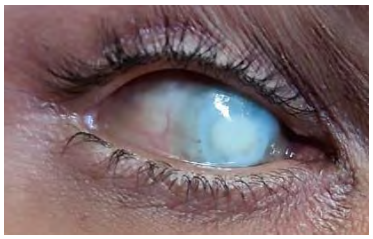

Figure 3.8: The affected individual IV:2 of family C, suffering from PCG. Discoloration of eyes is observed **(a,b).**

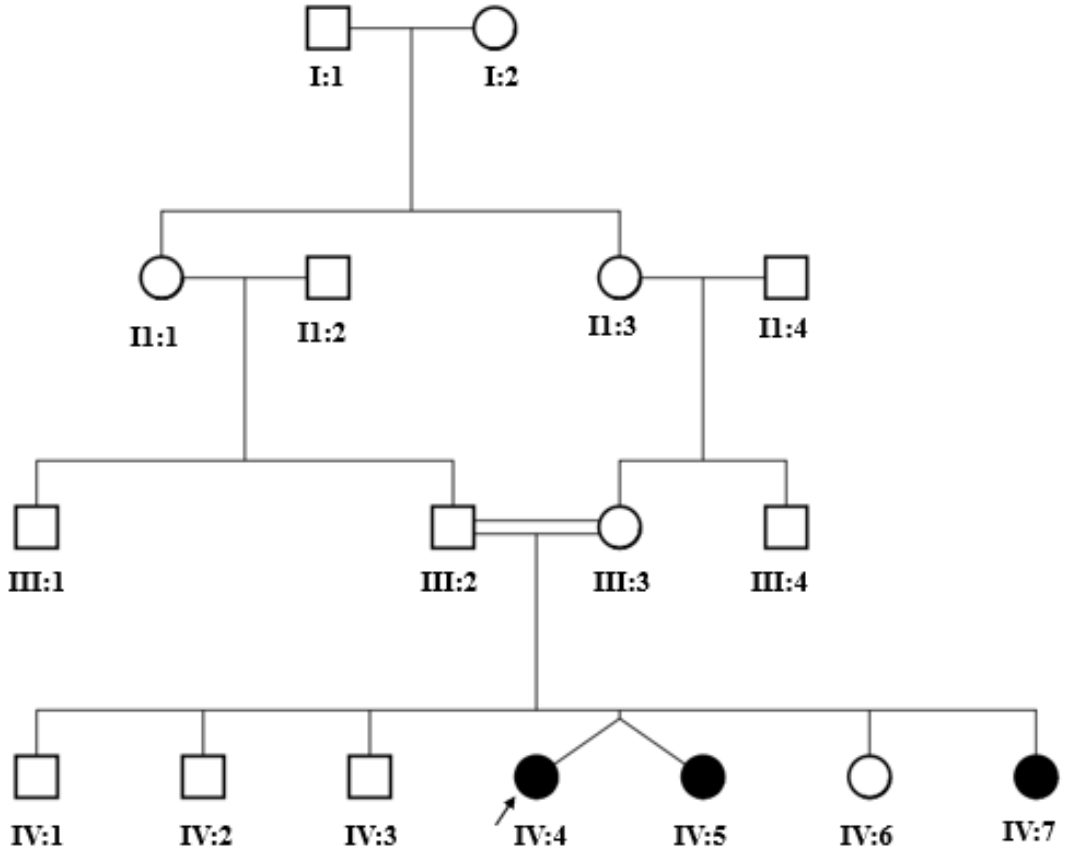

Figure 3.9: Pedigree of family D, designed by haplopainter, showing the autosomal recessive pattern of inheritance.

Table 3.4: Clinical profile of family D

Family	**D**		
No. of affected patients	3		
OCT Findings	Macular Atrophy		
Patient ID	VI:4	VI:5	VI:7
Gender	Female	Female	Female
Age of onset	4 years	4 years	4 years
Age	13 years	13 years	4 years
Photophobia	Yes	Yes	Yes
Scotoma	Yes	Yes	Yes
Nystagmus	No	No	No
Blurriness of central vision	Yes	Yes	Yes
Night Blindness	No	No	No
Achromatopsia	Yes	Yes	Yes
Legally Blind	No	No	No

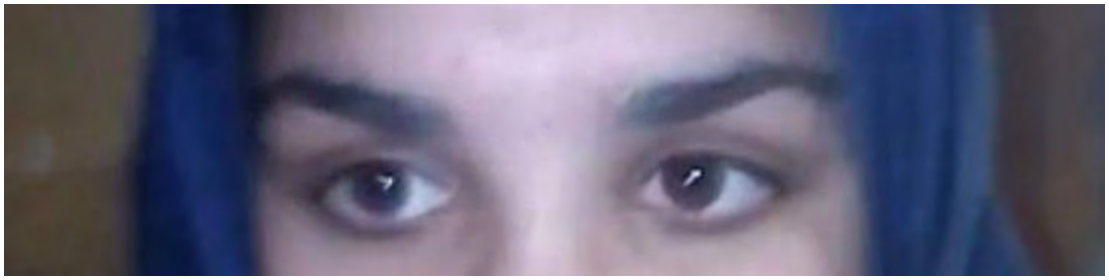

Figure 3.10: Affected individual IV:4 of family D, suffering from macular atrophy.

Figure 3.11: Fundoscopic image of affected individual VI:4 showed deposition of pigments in macular region.

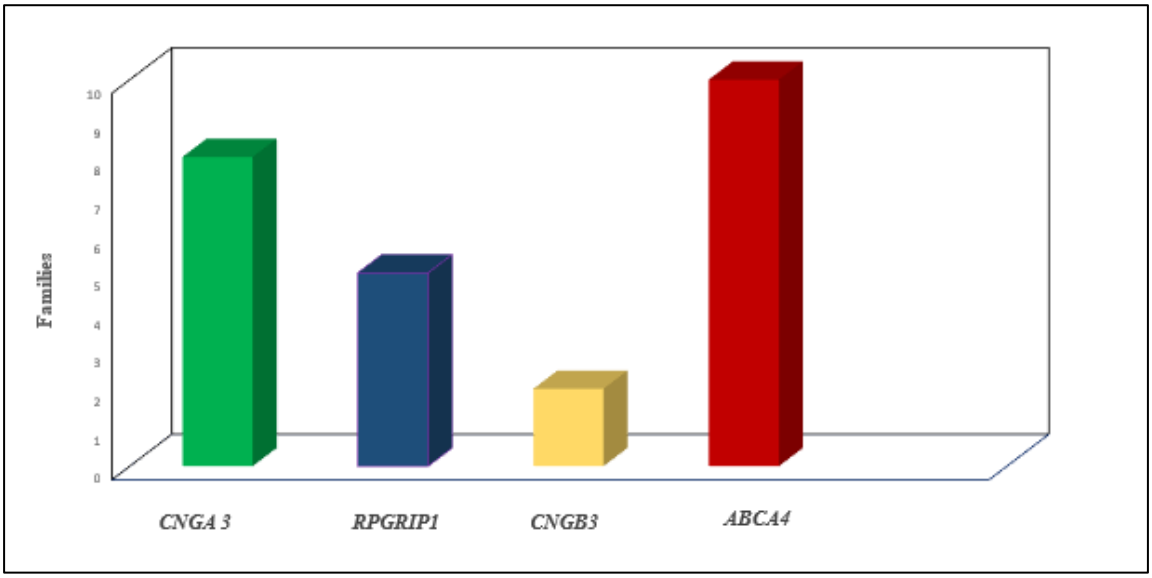

Figure 3.12. Graphical representation of most mutated genes in Pakistani Patients with CORD.

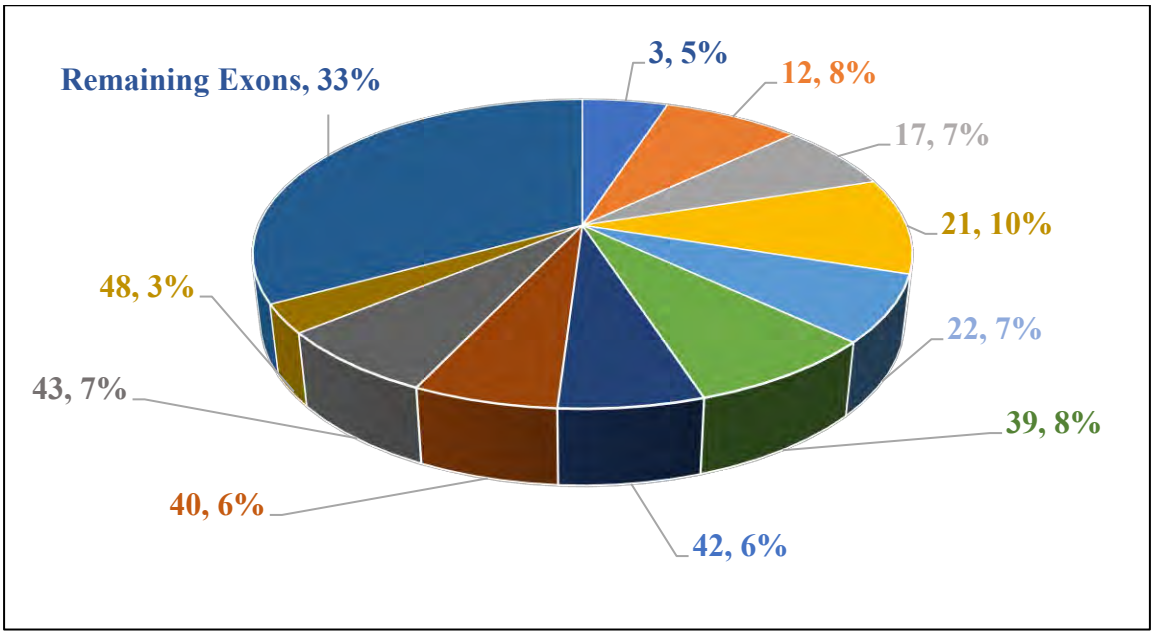

Figure 3.13: Graphical representation of most frequent mutated exons of *ABCA4*.

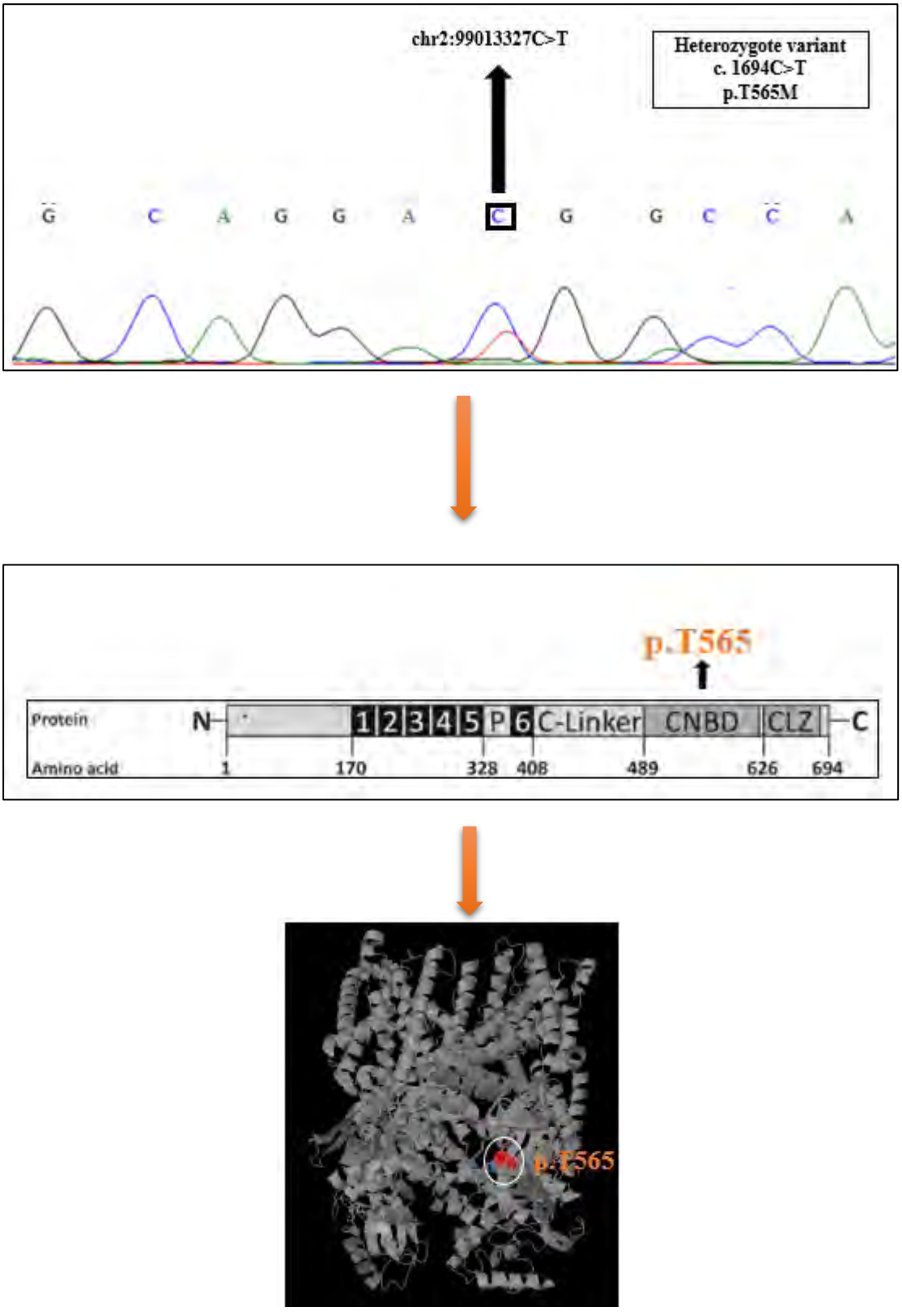

Figure 3.14: Sequencing chromatogram showing heterozygous nucleotide variant c.1694C>T in the affected individual VI:1 of family A. The p.T565M is present in cGMP binding domain of CNGA3 protein.

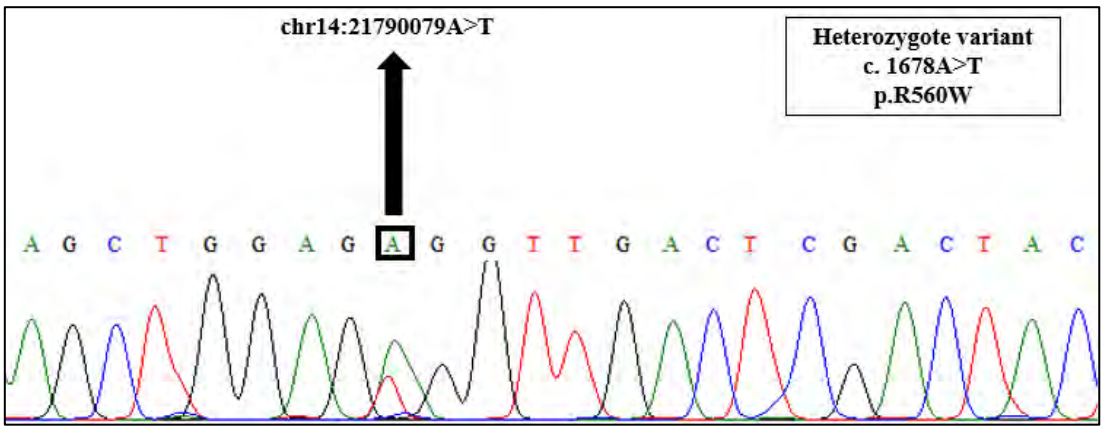

Figure 3.15: Sequencing chromatogram showing heterozygous nucleotide variant c.1678A>T in the affected individual VI:1 of family A. This variant results in change of arginine into tryptophan at 560 position (p.R560W) in *RPGRIP1* protein.

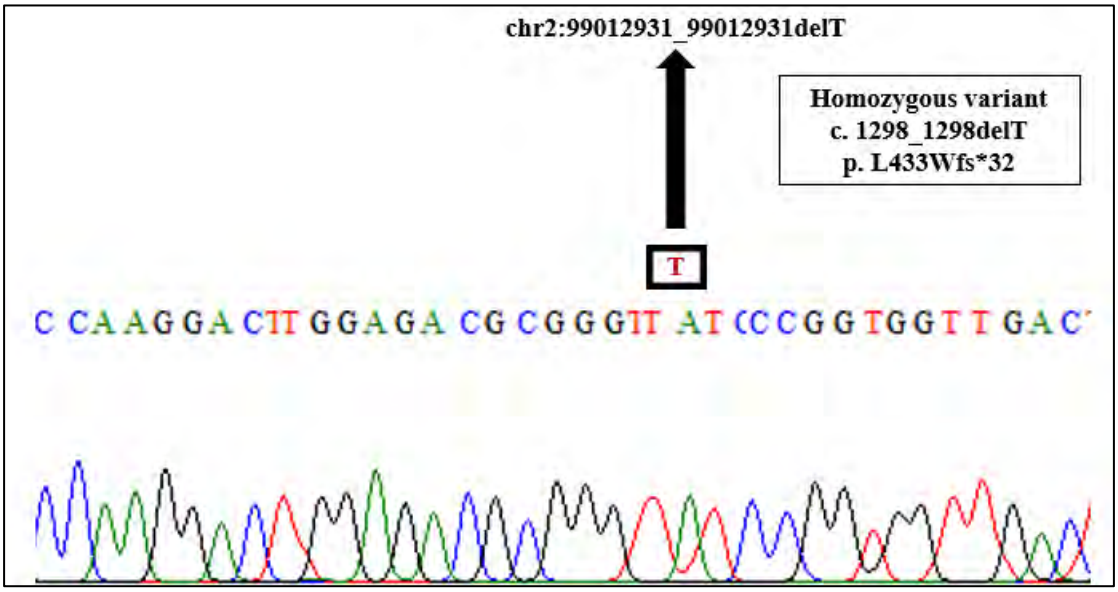

Figure 3.16: Sequencing chromatogram showing homozygous nucleotide variant c.1698_1698delT in the affected individual IV:2 of family B. Deletion of T results in frameshift of protein CNGA3 and is expected to cause nonsense mediated decay.

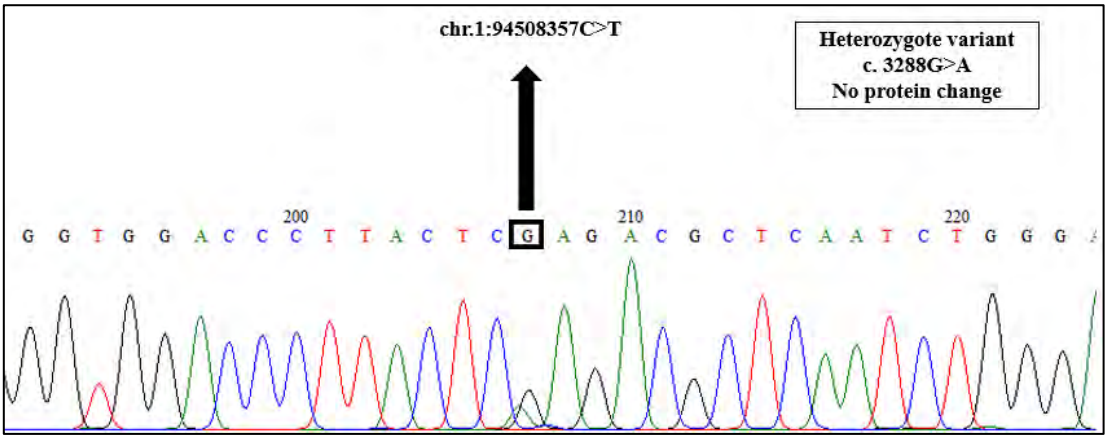

Figure 3.17: Sequencing chromatogram showing heterozygous nucleotide variant c.3288G>A in the affected individual IV:2 of family B. This is synonymous variant having no effect on protein.

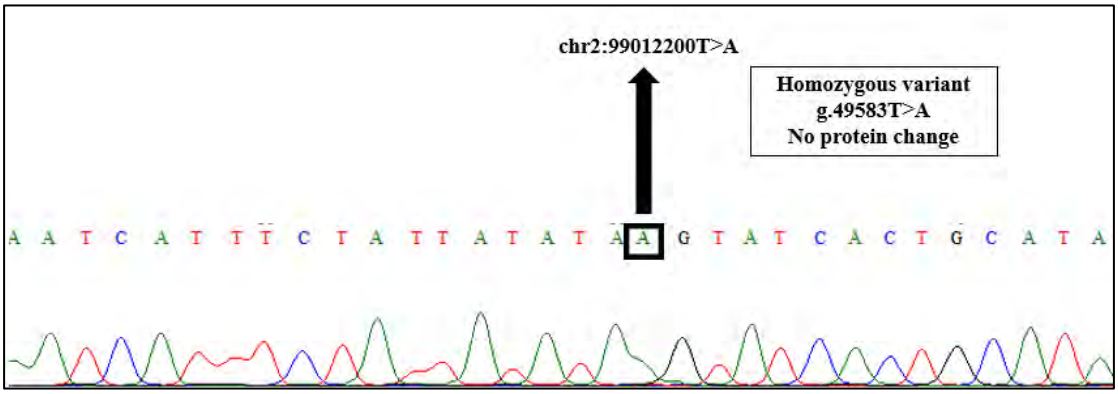

Figure 3.18: Sequencing chromatogram showing homozygous nucleotide variant g.49583T>A in the affected individual IV:2 of family B. This variant is present in *CNGA3* gene with no protein change.

(a)

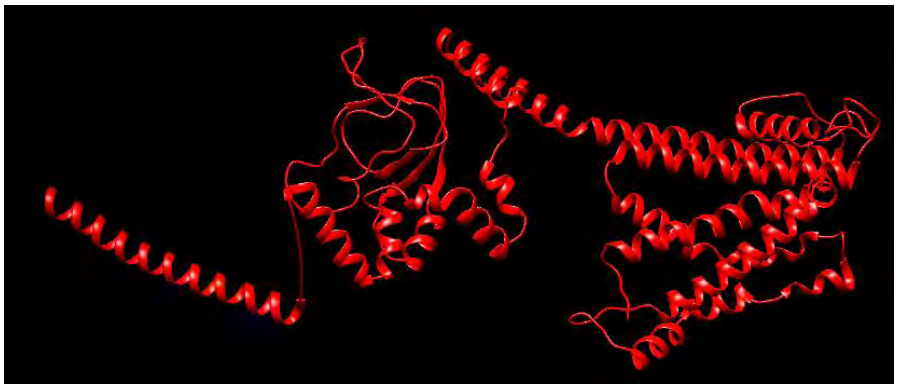

(b)

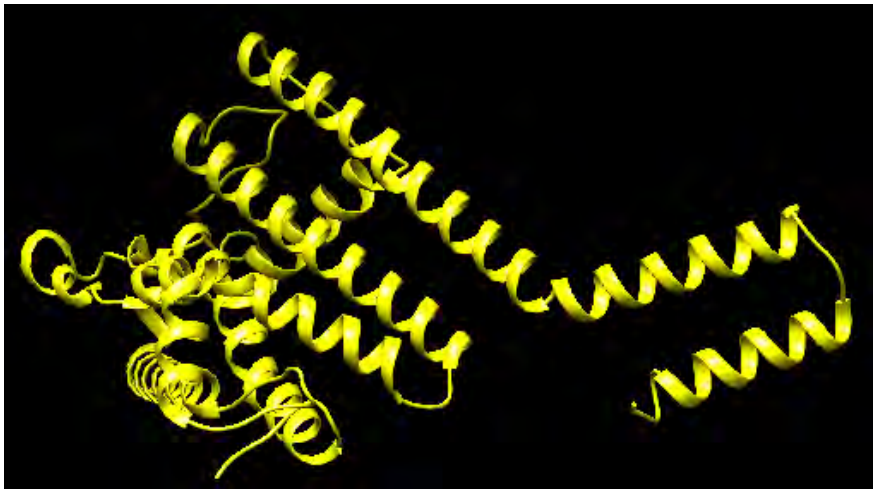

(c)

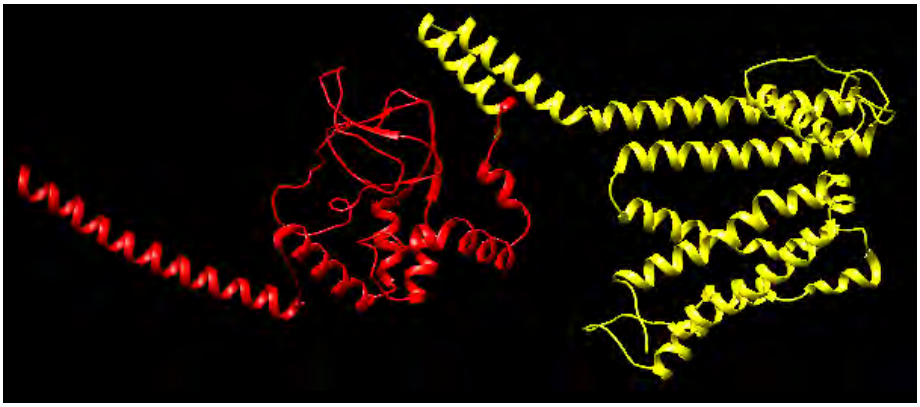

Figure 3.19: Structure comparison of normal *CNGA3* protein with truncated *CNGA3* having c.1698_1698delT variant **a**) Wild type of *CNGA3* **b)** Mutated *CNGA3* having c.1698_1698delT variant **c)** When both structures are superimposed in ChimeraX 1.4 version, we can observe the difference that protein is truncated.

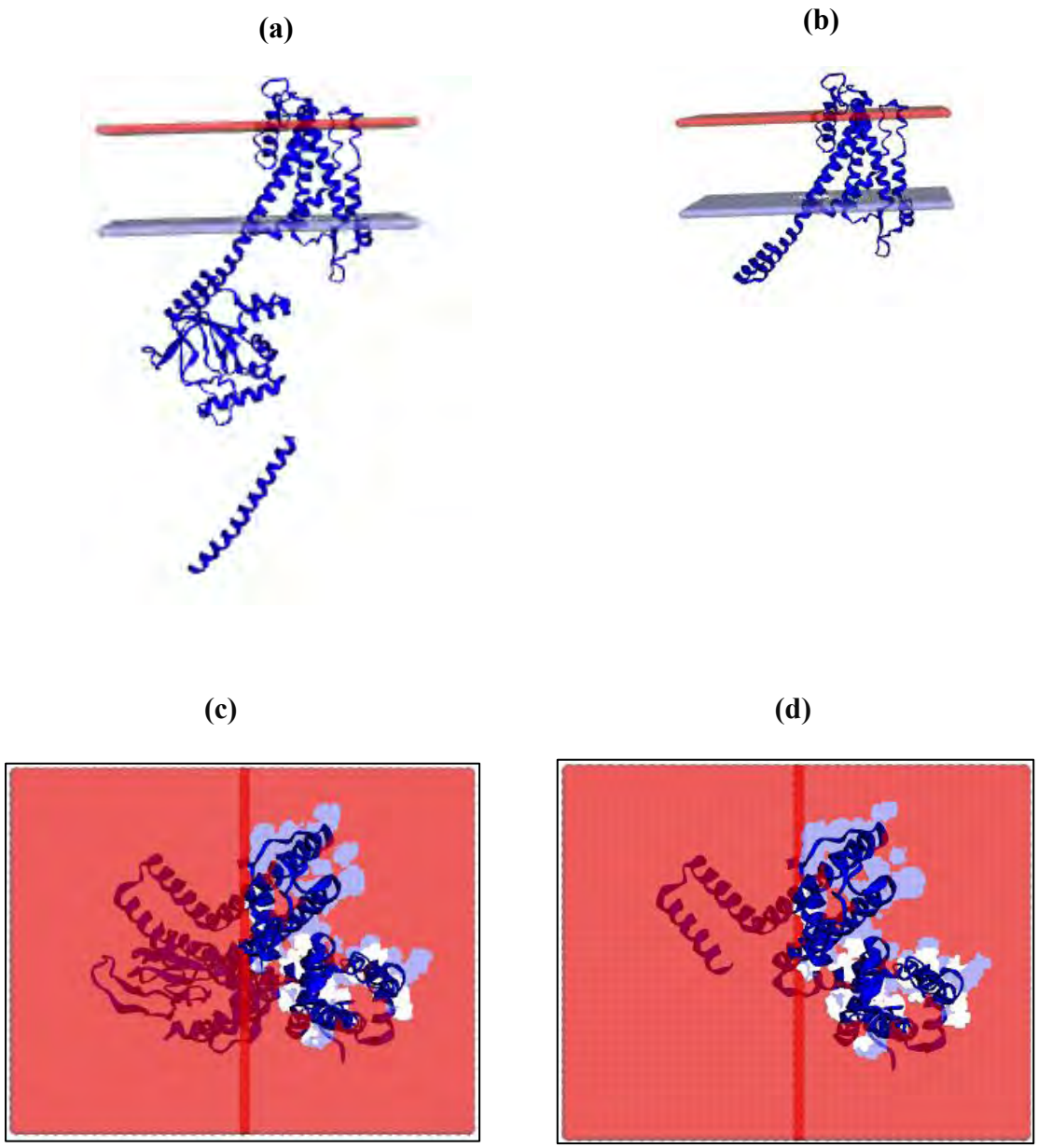

Figure 3.20: Membrane interaction of *CNGA3* protein (**a**) Longitudinal view of wild type of *CNGA3* (**b)** Longitudinal view of mutated *CNGA3* having c.1698_1698delT variant **(c)** Top view of wild type of *CNGA3* **(d)** Top view of mutated *CNGA3* having c.1698_1698delT variant. No difference in interaction is observed but due to truncated protein unable to form fully functional channel.

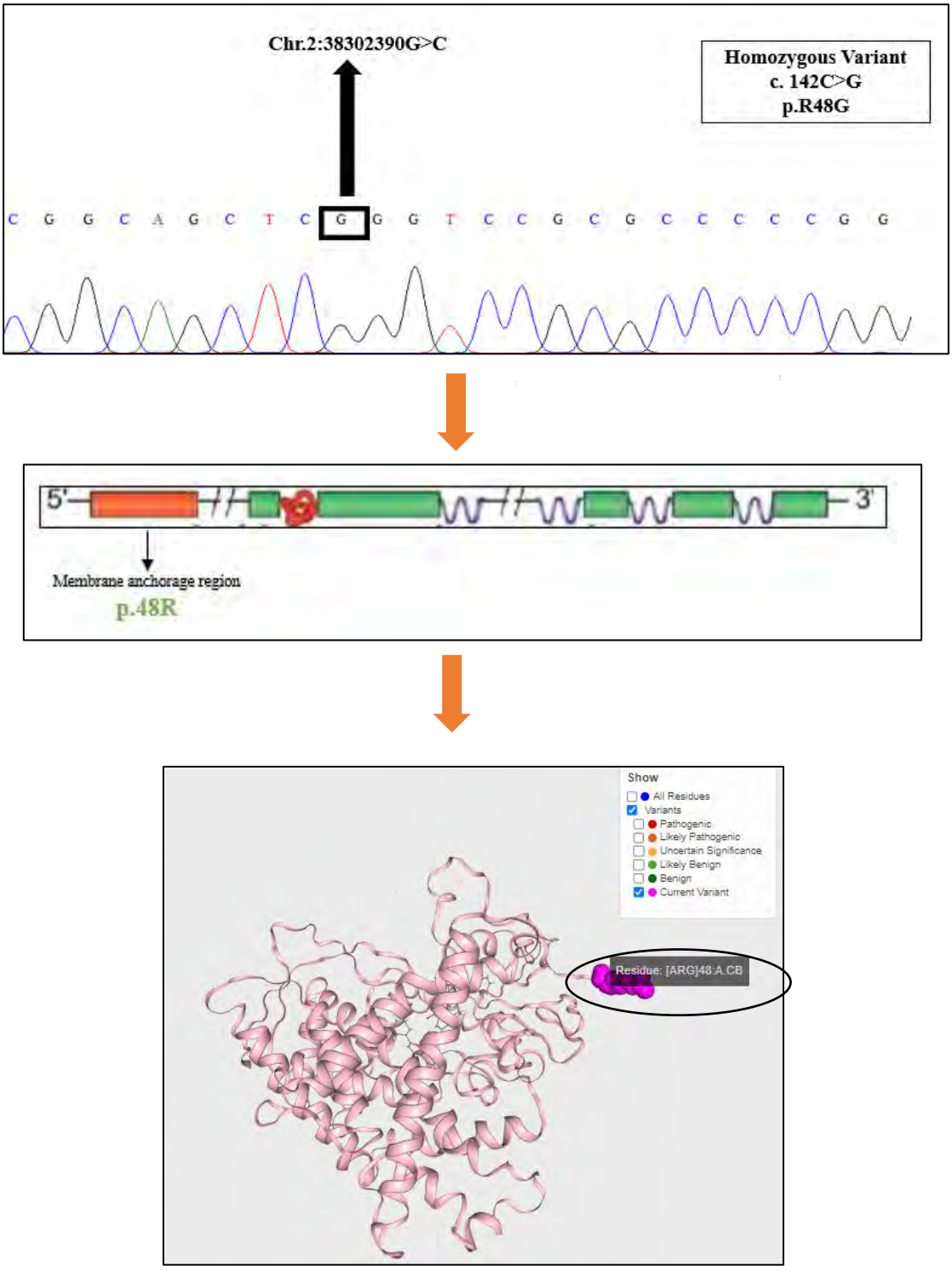

Figure 3.21: Sequencing chromatogram showing homozygous nucleotide variant c.142C>G in the affected individual IV:2 of family C. This variant results in substitution of arginine into glycine in the membrane anchorage region of *CYP1B1* at 48 position (p.R48G) .

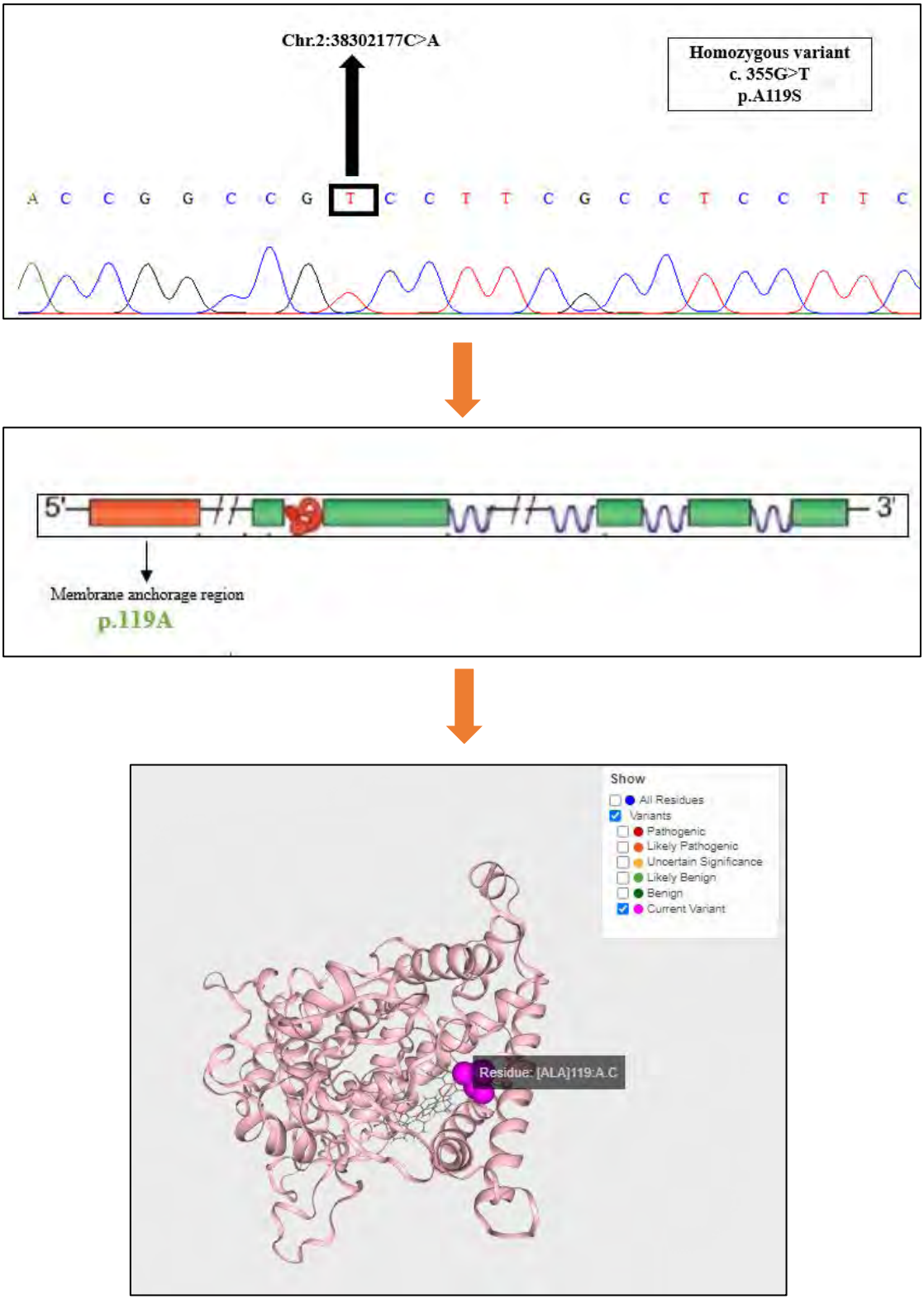

Figure 3.22: Sequencing chromatogram showing homozygous nucleotide variant c.355G>T in the affected individual of family C. This variant results in substitution of alanine into serine in the membrane anchorage region of *CYP1B1* at 119 position (p.A119S) .

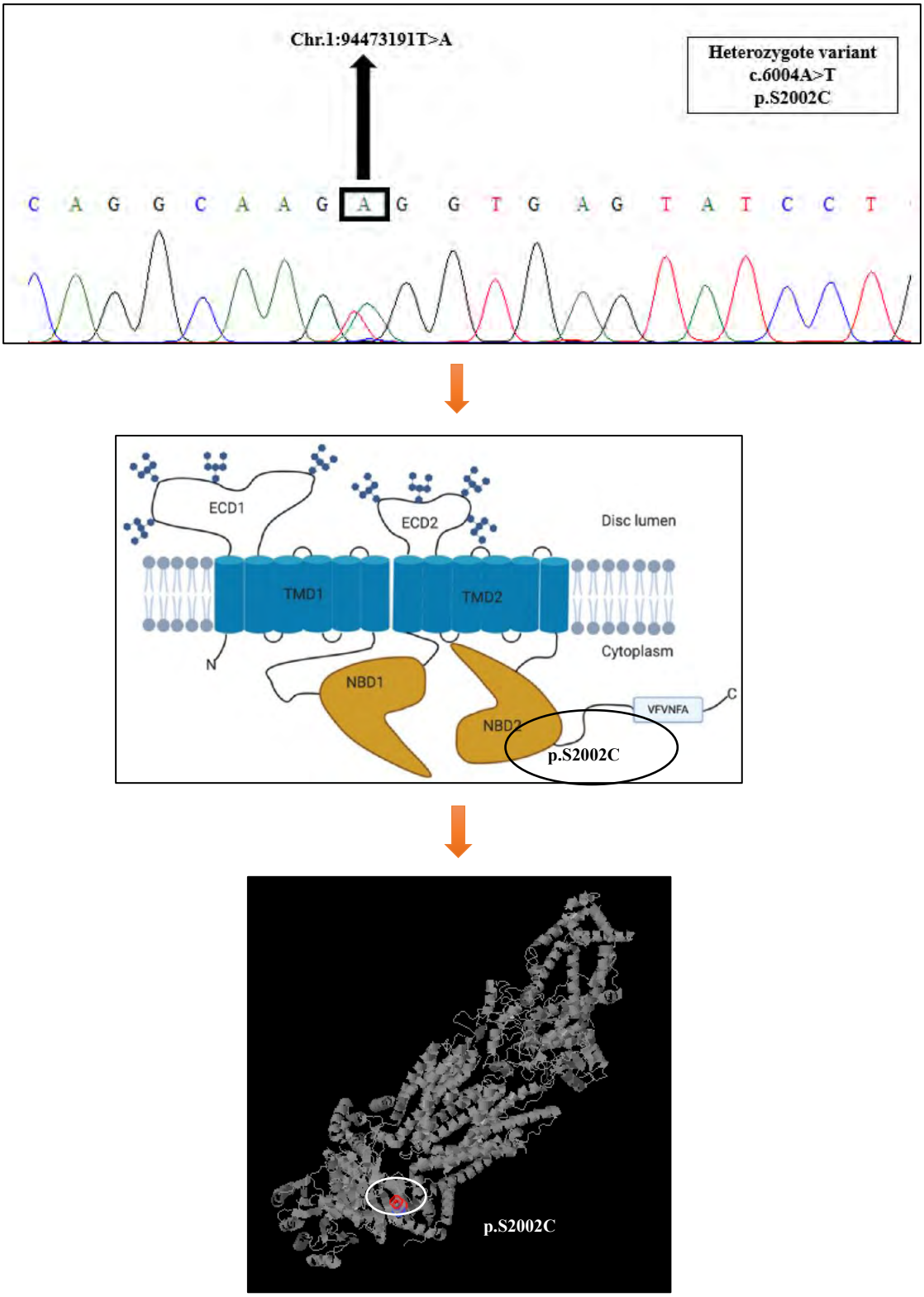

Figure 3.23: Sequencing chromatogram showing heterozygous nucleotide variant c.600A>T in the affected individual IV:4 of family D. This variation results in substituiton of serine into cysteine in the cGMP binding domain of ABCA4 at 2002 position (p.S2002C).

(a) (b)

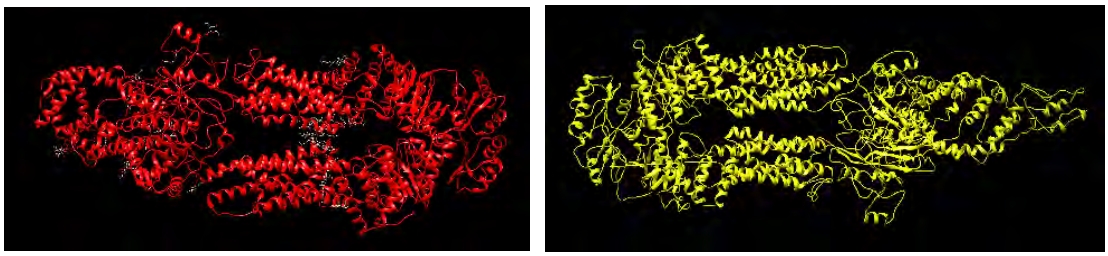

(c)

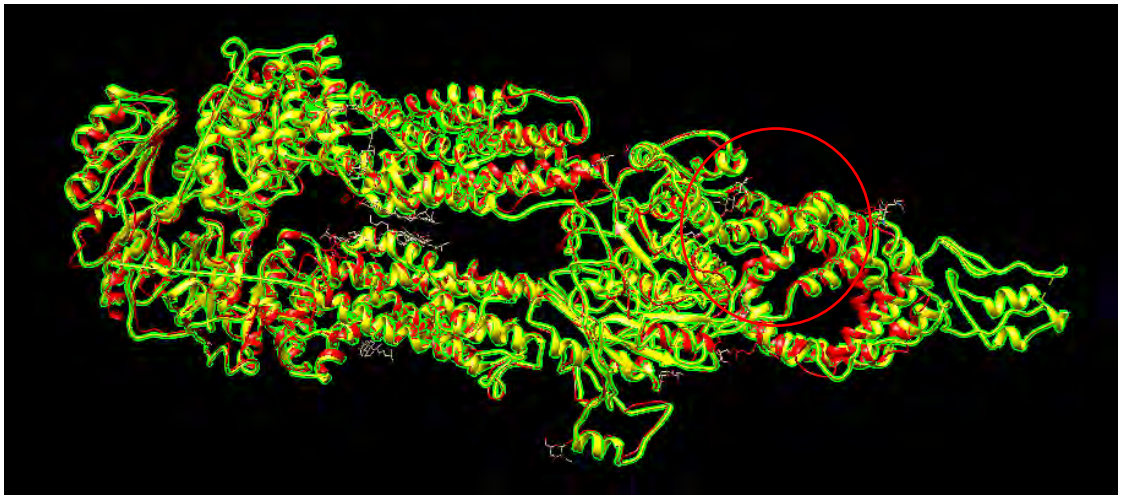

(d)

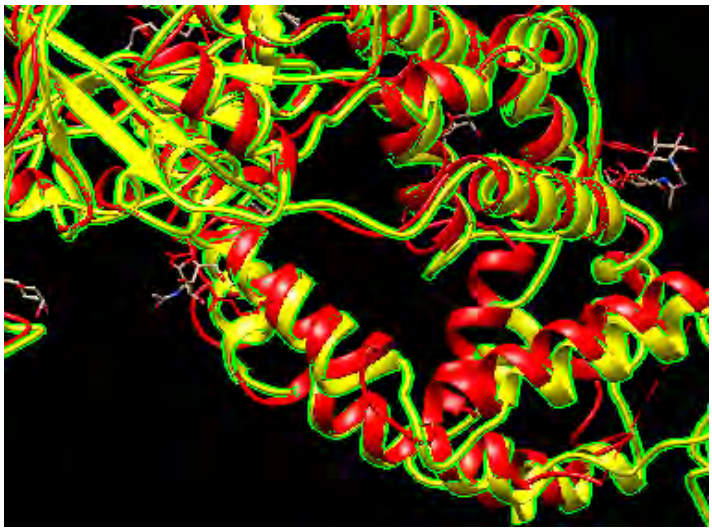

Figure 3.24: Structure comparison of normal ABCA4 protein with mutated ABCA4 having p.S2002C variant **(a)** Wild type of ABCA4 **(b)** Mutated ABCA4 having p.S2002C **(c & d)** When both structures are superimposed in ChimeraX 1.4 version, we can see the difference.

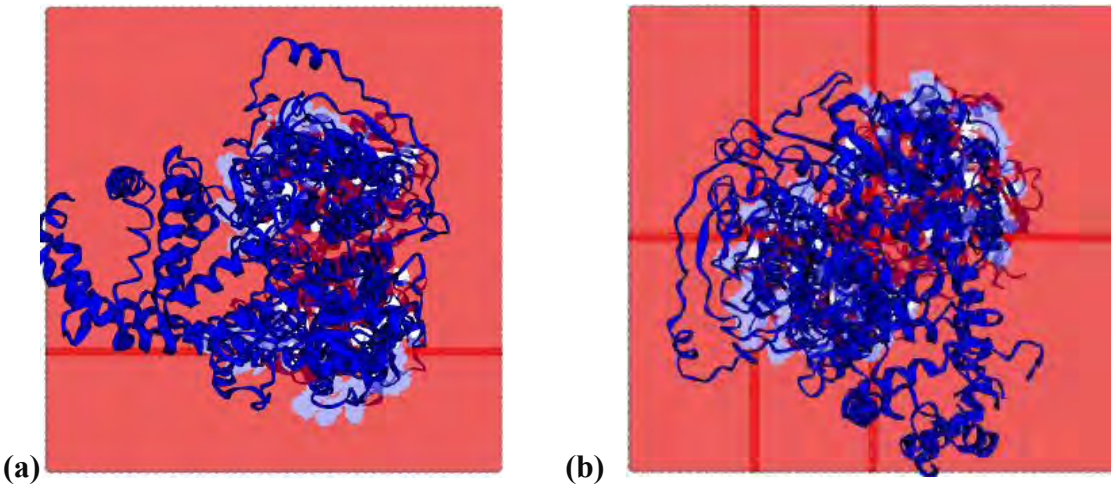

(a) **(b)**

Figure 3.25: Membrane interaction of *ABCA4* protein (**a**) Wild type of *ABCA4* (**b)** Mutated *ABCA43* having p.S2002C variant**.** Mutated protein is showing more interaction with membrane as compared to wild type because of misfolding of protein.

Table 3.5: In silico analysis of variants identified in family A, B, C and D.

Family Name	**A**		**B**			**C**		**D**
Individual ID	VI:1		IV:2			IV:2		IV:4
Gene Name	***CNGA3***	*RPGRIP1*	***CNGA3***		*ABCA4*	*CYP1B1*		***ABCA4***
Exon	8	13	8	8	22	2	2	43
DNA position	**c.1694C>T**	c.1678A>T	**c.1298_1298delT**	g.49583T>A	c. 3288G>A	c.142C>G	c. 355G>T	**c.6004A>T**
Protein Change	**p.T565M**	p.R560W	**p. L433Wfs*32**	No change	No change	p.R48G	p.A119S	**p.S2002C**
Zygosity	Heterozygous	Heterozygous	Homozygous	Homozygous	Heterozygous	Homozygous	Homozygous	Heterozygous
Effect of change	**Pathogenic**	Benign	**Pathogenic**	Benign	Benign	Benign	Benign	**Pathogenic**
Previously reported	Yes	No	Yes in HGMD	Novel	Novel	Yes	Yes	Novel
Reference ID	201747279	-	CM084799	-	-			-
Mutation Taster	Disease causing	Polymorphism	Disease causing			Polymorphism	Polymorphism	Disease causing
CADD	Deleterious	Non-Deleterious	-	Non deleterious	Non-Deleterious	Non deleterious	Non deleterious	Deleterious
Genomnis HSF	Yes splicing effect	No splicing effect	-	No splicing effect	No splicing effect	No splicing effect	No splicing effect	Yes splicing effect
VARSEAK	Yes splicing effect	No splicing effect	-	No splicing effect	No splicing effect	No splicing effect	No splicing effect	Pathogenic
PROVEAN	Pathogenic	Pathogenic	-	-	-	Benign	Benign	Uncertain
PolyPhen-2	Probably damaging	Probably damaging	-	-	-	Neutral	Neutral	Probably damaging
SNPs & GO	Disease	Neutral	-	-	-	Neutral	Neutral	Disease
PANTHER-PSEP	Possibly damaging	Neutral	-	-	-	Possibly damaging	Possibly damaging	Probably damaging
REVEL	Pathogenic	Benign	-	-		Benign	Benign	Pathogenic
SIFT	Not tolerated	Not tolerated	-	-	-	Bening	Bening	Not tolerated
ACMG	Pathogenic	Uncertain Significance	Likely pathogenic	-	Benign	Bening	Bening	Pathogenic

Note: The bold text is indicating the pathogenic variant in the respective family.

4. Discussion

Inherited eye disorders encompass different types of phenotypes that affect the structure and function of the eye due to abnormalities in the genes responsible for eye development and maintenance (García Bohórquez et al., 2021; Chawla & Vohra, 2022). These disorders can affect various parts of the eyes including the cornea, lens, retina, optic nerve, and other structures (Griffth et al.,2022; Murro et al., 2023). Like CORD that is characterized by the degenerations of cone and rod cells, ultimately leading towards blindness (Hamel et al., 2000) and STGD that mainly affects the macular region involving the cone cells (Lu et al., 2017). However, glaucoma that is accompanied by retinal ganglion damage with the significant changes in the anterior structure of eye and elevation of IOP (Schwartz and Yoles, 2000; Firasat et al., 2008; Faiq et al., 2013; Badawi et al., 2019).

In the present study four families with different phenotype presentations were recruited and genetic analysis was performed. Affected individual of family A, with the clinical symptoms like blurriness in the central vision, myopia, outer retinal layer deterioration as observed in SD OCT, pigment deposition and appearance of flecks on fundoscopic images, correlating it with STGD (Rotenstreich et al., 2003). Screening for various exons of selected genes in the affected individual VI:I identified one heterozygous variant c.1694C>T (p.T565M) in the exon 8 of *CNGA3* and one heterozygous variant c. 1678A>T (R560W) in the exon 13 of RPGRIP1.

c.1678A>T variant in *RPGRIP1* is novel and suggested it as benign by 9 tools out of 11. Mutations in *RPGRIP1* have been linked with macular atrophy and CORD with the severe phenotype and early onset of disease (Hameed et al., 2003),but mostly associated with LCA (Dryja et al., 2001; Gerber 2001), so ruling out this variant having no pathogenic role in the phenotype of this family after sequencing.

c.1694C>T variant in CNGA3 is the potential candidate in affected individual VI:I of family A. Insilico analysis of this variant by 11 different bioinformatic tools which include protein predictors and evolutionary conservation score, supports the pathogenic effect. In this variant (p.T565M), threonine, a polar amino acid that contains hydroxyl group (-OH), is substituted by methionine, non-polar amino acid containing thiol group (-SH), so it affects the functional properties of protein by disrupting the proper folding of proteins.

As the mutated amino acid is present in the cGMP binding site and advanced modeling of protein sequence indicates that it can affect the binding of cGMP with CNGA3 and is expected to disrupt the protein function (Wissinger et al., 2011). Wissinger and his colleagues also reported that mutation either in the pore region or cGMP binding site is the potent player for encoding the *CNGA3* channels with reduced functional activity and can affect activity of cone cells (Wissinger et al., 2011).

This variant has been reported both in homozygous as well as in heterozygous form in various studies (Vincet et al 2011; Yang et al., 2014; Solaki e al., 2022). Various functional and experimental studies support the pathogenic nature of this variant. In an experimental study, low response of mutated CNGA3-T565M channel was detected in a patch clamp technique as compared to the normal channel (Muraki-Oda et al., 2007). There is a need to screen the remaining *CNGB3* exons also, as this variant is reported in heterozygous form with *CNGB3 (*Yang et al., 2014).

Sanger sequencing in affected individual IV:2 of family B was performed on various exons of selected genes based on the phenotype. Affected individual presented with CORD like clinical indications such as decreased visual acuity, color issues, photophobia, and bull's eye maculopathy (Gill et al., 2019). A homozygous deletion c.1298_1298delT (p. L433Wfs*32)**,** a polymorphism g.49583T>A (no protein change) in exon 8 of *CNGA3* and one heterozygous variant c.3288G>A (no protein change) in exon 22 of ABCA4 was identified.

g.49583T>A is a polymorphism and is not expected to impart its effect even on splice site as indicated benign by several tools. Similarly variant in ABCA4 is synonymous, not affecting the protein as well as not going to affect splice site as suggested benign according to insilico analysis performed by various tools. Both these variants are suggested as non-pathogenic polymorphisms by mutation taster and not reported in 1000G nor ExAc.

c.1298_1298delT (p. L433Wfs*32) in CNGA3 is the potential variant in affected individual IV:2 of family B as 62.2% cases of autosomal recessive CORD are linked with CNGA3 mutations (Gill et al., 2019). This deletion leads to the frameshift and result in truncated protein. It is suggested as pathogenic by several bioinformatic tools. It imparts the deleterious effect as the truncated protein results in loss of function. The 3D structure analysis of *CNGA3* also confirms the formation of truncated protein

because of this deletion. However, functional studies are required to further validate the in silico analysis of this novel variant.

CYP1B1 gene was sequenced in family C with clinical presentation of PCG as 50% of autosomal recessive PCG cases are linked with *CYP1B1* (Waryah et al., 2019). Sanger sequencing of *CYP1B1* gene revealed two already reported homozygous variants c.142C>G and c.355G>T. The amino acids i.e p.R48G and p.A119S that are changed because of this variation, are present in membrane anchorage region, but their low evolutionary conservation score (Table 3.5) indicates that these variants are not expected to affect the function of protein. In silico analysis of these variants which include various protein predictors also proved their benign nature and ruled out that *CYP1B1* is not involved in causing the PCG in this family. So, there is a need to screen out the other genes involved in PCG.

Sanger sequencing of various exons of targeted genes in the affected individual IV:4 of family D suffering from maculopathy identified a heterozygous variant c.6004A>T (p.S2002C) in exon 43 of ABCA4. This variant is novel and predicted as pathogenic based on bioinformatic analysis performed by 11 tools which include protein predictors, ACMG classification and high evolutionary conservation score. The 3D structural analysis of mutated protein has shown the differences when compared with normal.

The functional properties of protein will be affected as this variant results in substitution of serine, a polar amino acid that contains hydroxyl group (-OH) by cysteine containing thiol group (-SH) that disrupts the proper folding of protein. The p.S2002C variant is present in NBD2 region of *ABCA4* through which it interacts with ATP, and it has been observed that mutations in NBD region lowers ability of *ABCA4* to interact with its substrate (Garces et al., 2018). The differences in folding of protein have been observed through the analysis of 3D structure of mutated protein with the normal one..

Only this heterozygous mutation is not enough to cause this phenotype in the affected individual IV:4 of family D. 95% cases of macular degeneration are linked with *ABCA4* mutations. So further screening is required as mutations in deep intronic regions, canonical and non-canonical splice sites are also correlated with macular degeneration, CORD and STGD (Abdollahi and Hirose 2011).

Further investigations in Family C and D using advanced molecular techniques such

as SNP microarray, panel sequencing, whole exome sequencing and whole genome sequencing would help to find the mutations in the disease-causing genes. Functional studies of the identified mutations would help to further validate the effect of the variants on the respective proteins.

5. References

Aboshiha, J., Dubis, A. M., Carroll, J., Hardcastle, A. J., & Michaelides, M. (2016).The cone dysfunction syndromes. *British Journal of Ophthalmology*, *100*(1), 115-121.

Abu-Amero, K. K., Edward, D. P. (2017). Primary Congenital Glaucoma. GeneReviews®.*University of Wasington.* https://www.ncbi.nlm.nih.gov/book/NBK1135/

Adzhubei, I. A., Schmidt, S., Peshkin, L., Ramensky, V. E., Gerasimova, A., Bork, P., Kondrashov, A. S., & Sunyaev, S. R. (2010). A method and server for predicting damaging missense mutations. *Nature Methods*, *7*(4), 248-249.

Maumenee A. E. (1958). The pathogenesis of congenital glaucoma: a new theory. *Transactions of the American Ophthalmological Society*, *56*, 507–570.

AE, M. (1958). The pathogenesis of congenital glaucoma: a new theory. *Transactions of the American Ophthalmological Society*, *56*, 507-570.

Afzal, R., Firasat, S., Kaul, H., Ahmed, B., Siddiqui, S. N., Zafar, S. N., Shahzadi, M., & Afshan, K. (2019). Mutational analysis of the CYP1B1 gene in Pakistani primary congenital glaucoma patients: Identification of four known and a novel causative variant at the 3′ splice acceptor site of intron 2. *Congenital Anomalies*, *59*(5), 152-161.

Agrawal, P., & Bradshaw, S. E. (2018). Systematic literature review of clinical and economic outcomes of micro-invasive glaucoma surgery (MIGS) in primary open-angle glaucoma. *Ophthalmology and Therapy*, *7*, 49-73.

Aklillu, E., Oscarson, M., Hidestrand, M., Leidvik, B., Otter, C., & Ingelman-Sundberg, M. (2002). Functional analysis of six different polymorphic CYP1B1 enzyme variants found in an Ethiopian population. *Molecular Pharmacology*, *61*(3), 586-594.

Ali, M., McKibbin, M., Booth, A., Parry, D. A., Jain, P., Riazuddin, S. A., Hejtmancik, J. F., Khan, S. N., Firasat, S., & Shires, M. (2009). Null mutations in LTBP2 cause primary congenital glaucoma. *The American Journal of Human Genetics*, *84*(5), 664-671.

Allikmets, R., Singh, N., Sun, H., Shroyer, N. F., Hutchinson, A., Chidambaram, A., Gerrard, B., Baird, L., Stauffer, D., & Peiffer, A. (1997). A photoreceptor cell-specific ATP-binding transporter gene (ABCR) is mutated in recessive Starqardt macular dystrophy. *Nature Genetics*, *15*(3), 236-246.

Allingham, R., Damji, K., Freeman, S., Moroi, S., & Shafranov, G. (2005). Congenital glaucomas and developmental glaucomas with associated anomalies. *Shields Textbook of Glaucoma*, *5*, 235-271.

Anderson, J. R., & Parsons, J. H. (2013). Hydrophthalmia or congenital glaucoma. *Cambridge University Press*.

Anderson, R. E., & Maude, M. B. (1970). Lipids of ocular tissues. 6. Phospholipids of bovine rod outer segments. *Biochemistry*, *9*(18), 3624-3628.

Aquino, M. C. D., Barton, K., Tan, A. M. W., Sng, C., Li, X., Loon, S. C., & Chew, P. T. (2015). Micropulse versus continuous wave transscleral diode cyclophotocoagulation in refractory glaucoma: a randomized exploratory study. *Clinical & Experimental Ophthalmology*, *43*(1), 40-46.

Arshad, M. W., Lee, Y., Malik, M. A., Khan, J., Khan, A., Kareem, A., Kang, C., & Shabbir, M. I. (2019). Identification of Novel Mutation in CNGA3 gene by Whole-Exome Sequencing and In-Silico Analyses for Genotype-Phenotype Assessment with Autosomal Recessive Achromatopsia in Pakistani families. *JPMA*.

Azam, M., Collin, R. W., Shah, S. T. A., Shah, A. A., Khan, M. I., Hussain, A., Sadeque, A., Strom, T. M., Thiadens, A. A., & Roosing, S. (2010). Novel CNGA3 and CNGB3 mutations in two Pakistani families with achromatopsia. *Molecular Vision*, *16*, 774.

Badawi, A. H., Al-Muhaylib, A. A., Al Owaifeer, A. M., Al-Essa, R. S., & Al-Shahwan, S. A. (2019). Primary congenital glaucoma: An updated review. *Saudi Journal of Ophthalmology*, *33*(4), 382-388.

Bashir, R., Tahir, H., Yousaf, K., Naz, S., & Naz, S. (2015). Homozygous p. G61E mutation in a consanguineous Pakistani family with co-existence of juvenile-onset open angle glaucoma and primary congenital glaucoma. *Gene*, *570*(2), 295-298.

Bennett, R. L., French, K. S., Resta, R. G., & Doyle, D. L. (2008). Standardized human pedigree nomenclature: update and assessment of the recommendations of the National Society of Genetic Counselors. *Journal of Genetic Counseling*, *17*, 424-433.

Bernstein, P. S., Tammur, J., Singh, N., Hutchinson, A., Dixon, M., Pappas, C. M., Zabriskie, N. A., Zhang, K., Petrukhin, K., & Leppert, M. (2001). Diverse macular dystrophy phenotype caused by a novel complex mutation in the ELOVL4 gene. *Investigative Ophthalmology & Visual Science*, *42*(13), 3331-3336.

Biel, M., Seeliger, M., Pfeifer, A., Kohler, K., Gerstner, A., Ludwig, A., Jaissle, G., Fauser, S., Zrenner, E., & Hofmann, F. (1999). Selective loss of cone function in mice lacking the cyclic nucleotide-gated channel CNG3. *Proceedings of the National Academy of Sciences*, *96*(13), 7553-7557.

Birnbach, C. D., Järveläinen, M., Possin, D. E., & Milam, A. H. (1994). Histopathology and immunocytochemistry of the neurosensory retina in fundus flavimaculatus. *Ophthalmology*, *101*(7), 1211-1219.

Capriotti, E., Calabrese, R., Fariselli, P., Martelli, P. L., Altman, R. B., & Casadio, R. (2013). WS-SNPs&GO: a web server for predicting the deleterious effect of human protein variants using functional annotation. *BMC Genomics*, *14 Suppl 3*(Suppl 3), S6.

Cascella, R., Strafella, C., Germani, C., Novelli, G., Ricci, F., Zampatti, S., & Giardina, E. (2015). The genetics and the genomics of primary congenital glaucoma. *BioMed Research International*, *2015*.

Chaumet-Riffaud, A. E., Chaumet-Riffaud, P., Cariou, A., Devisme, C., Audo, I., Sahel, J.-A., & Mohand-Said, S. (2017). Impact of retinitis pigmentosa on quality of life, mental health, and employment among young adults. *American Journal of Ophthalmology*, *177*, 169-174.

Chawla, H., & Vohra, V. (2022). Retinal dystrophies. https://www.ncbi.nlm.nih.gov/books/NBK564379/

Christian, P. H. (2007). Cone rod dystrophies. *Orphanet Journal of Rare Diseases*, *2*(1), 7.

Cideciyan, A. V., Aleman, T. S., Swider, M., Schwartz, S. B., Steinberg, J. D., Brucker, A. J., Maguire, A. M., Bennett, J., Stone, E. M., & Jacobson, S. G. (2004). Mutations in ABCA4 result in accumulation of lipofuscin before slowing of the retinoid cycle: a reappraisal of the human disease sequence. *Human molecular genetics*, *13*(5), 525-534.

Cremers, F. P., Boon, C. J., Bujakowska, K., & Zeitz, C. (2018). Special issue introduction: inherited retinal disease: novel candidate genes, genotype–phenotype correlations, and inheritance models. In (Vol. 9, pp. 215): *MDPI*.

Cvekl, A., & Wang, W.-L. (2009). Retinoic acid signaling in mammalian eye development. *Experimental Eye Research*, *89*(3), 280-291.

de Nava, A. S. L., Somani, A. N., & Salini, B. (2022). Physiology, Vision. In *StatPearls.* StatPearlsPublishing.https://www.ncbi.nlm.nih.gov/books/NBk538493/.

Desmet, F. O., Hamroun, D., Lalande, M., Collod-Béroud, G., Claustres, M., & Béroud, C. (2009). Human Splicing Finder: an online bioinformatics tool to predict splicing signals. *Nucleic acids research*, *37*(9), e67.

Dryja, T. P., Adams, S. M., Grimsby, J. L., McGee, T. L., Hong, D. H., Li, T., Andréasson, S., & Berson, E. L. (2001). Null RPGRIP1 alleles in patients with Leber congenital amaurosis. *American Journal of Human Genetics*, 68(5), 1295–1298.

Duester, G. (2009). Keeping an eye on retinoic acid signaling during eye development.*Chemico-Biological Interactions*, *178*(1-3), 178-181.

Eldred, G. E., & Lasky, M. R. (1993). Retinal age pigments generated by self-assembling lysosomotropic detergents. *Nature*, *361*(6414), 724-726.

Faiq, M., Sharma, R., Dada, R., Mohanty, K., Saluja, D., & Dada, T. (2013). Genetic, biochemical and clinical insights into primary congenital glaucoma. *Journal of Current Glaucoma Practice*, *7*(2), 66.

Faiq, M. A., Dada, R., Qadri, R., & Dada, T. (2015). CYP1B1-mediated pathobiology of primary congenital glaucoma. *Journal of Current Glaucoma Practice*, *9*(3), 77.

Fan, B. J., & Wiggs, J. L. (2010). Glaucoma: genes, phenotypes, and new directions fortherapy. *The Journal of Clinical Investigation*, *120*(9), 3064-3072.

Firasat, S., Kaul, H., Ashfaq, U. A., & Idrees, S. (2018). In silico analysis of five missense mutations in CYP1B1 gene in Pakistani families affected with primary congenital glaucoma. *International Ophthalmology*, *38*, 807-814.

Firasat, S., Riazuddin, S. A., Khan, S. N., & Riazuddin, S. (2008). Novel CYP1B1 mutations in consanguineous Pakistani families with primary congenital glaucoma. *Molecular Vision*, *14*, 2002.

Fishman, G. (2001). The electroretinogram. *Ophthalmology Monographs*, *2*, 1-156.

Francois, J. (1980). Congenital glaucoma and its inheritance. *Ophthalmologica*, *181*(2), 61-73.

Fujinami, K., Lois, N., Davidson, A. E., Mackay, D. S., Hogg, C. R., Stone, E. M., Tsunoda, K., Tsubota, K., Bunce, C., & Robson, A. G. (2013). A longitudinal study of Stargardt disease: clinical and electrophysiologic assessment, progression, and genotype correlations. *American Journal of Ophthalmology*, *155*(6), 1075-1088. e1013.

Fujinami, K., Lois, N., Mukherjee, R., McBain, V. A., Tsunoda, K., Tsubota, K., Stone, E. M., Fitzke, F. W., Bunce, C., & Moore, A. T. (2013). A longitudinal study of Stargardt disease: quantitative assessment of fundus autofluorescence, progression, and genotype correlations. *Investigative Ophthalmology & Visual Science*, *54*(13), 8181-8190.

Fujinami, K., Sergouniotis, P. I., Davidson, A. E., Wright, G., Chana, R. K., Tsunoda, K., Tsubota, K., Egan, C. A., Robson, A. G., & Moore, A. T. (2013). Clinical and molecular analysis of Stargardt disease with preserved foveal structure and function. *American Journal of Ophthalmology*, *156*(3), 487-501. e481.

Fujinami, K., Singh, R., Carroll, J., Zernant, J., Allikmets, R., Michaelides, M., & Moore, A. T. (2014). Fine central macular dots associated with childhood-onset Stargardt disease. *Acta Ophthalmologica*, *92*(2), e157-e159.

Fujinami, K., Zernant, J., Chana, R. K., Wright, G. A., Tsunoda, K., Ozawa, Y., Tsubota, K., Robson, A. G., Holder, G. E., & Allikmets, R. (2015). Clinical and

molecular characteristics of childhood-onset Stargardt disease. *Ophthalmology*, *122*(2), 326-334.

Garces, F. A., Scortecci, J. F., & Molday, R. S. (2020). Functional characterization of ABCA4 missense variants linked to Stargardt macular degeneration. *International Journal of Molecular Sciences*, *22*(1), 185.

García Bohórquez, B., Aller, E., Rodríguez Muñoz, A., Jaijo, T., García García, G., & Millán, J. M. (2021). Updating the genetic landscape of inherited retinal dystrophies. *Frontiers in Cell and Developmental Biology*, *9*, 645600.

Gasteiger, E., Hoogland, C., Gattiker, A., Duvaud, S. e., Wilkins, M. R., Appel, R. D., & Bairoch, A. (2005). Protein identification and analysis tools on the ExPASy server. *Springer*.

Gerber, S., Perrault, I., Hanein, S., Barbet, F., Ducroq, D., Ghazi, I., Martin-Coignard, D., Leowski, C., Homfray, T., Dufier, J. L., Munnich, A., Kaplan, J., & Rozet, J. M. (2001). Complete exon-intron structure of the RPGR-interacting protein (RPGRIP1) gene allows the identification of mutations underlying Leber congenital amaurosis. *European Journal of Human Genetics* : EJHG, 9(8), 561–571.

Gill, J. S., Georgiou, M., Kalitzeos, A., Moore, A. T., & Michaelides, M. (2019). Progressive cone and cone-rod dystrophies: clinical features, molecular genetics and prospects for therapy. *British Journal of Ophthalmology*, *103*(5), 711-720.

Gomes, N. L., Greenstein, V. C., Carlson, J. N., Tsang, S. H., Smith, R. T., Carr, R. E., Hood, D. C., & Chang, S. (2009). A comparison of fundus autofluorescence and retinal structure in patients with Stargardt disease. *Investigative Ophthalmology & Visual Science*, *50*(8), 3953-3959.

Gootwine, E., Abu-Siam, M., Obolensky, A., Rosov, A., Honig, H., Nitzan, T., & Seroussi, E. (2017). Gene augmentation therapy for a missense substitution in the cGMP-binding domain of ovine CNGA3 gene restores vision in day-blind sheep. *Investigative Ophthalmology and Visual Science*, 58(3), 1577–1584.

Garces, F., Jiang, K., Molday, L. L., Stöhr, H., Weber, B. H., Lyons, C. J., Maberley, D., & Molday, R. S. (2018). Correlating the Expression and Functional Activity

a of ABCA4 Disease Variants with the Phenotype of Patients With Stargardt Disease. Investigative ophthalmology & visual science, 59(6), 2305–2315.

Griesinger, I. B., Sieving, P. A., & Ayyagari, R. (2000). Autosomal dominant macular atrophy at 6q14 excludes CORD7 and MCDR1/PBCRA loci. *Investigative Ophthalmology & Visual Science*, *41*(1), 248-255.

Griffith, J., 3rd, Sioufi, K., Wilbanks, L., Magrath, G. N., Say, E. A. T., Lyons, M. J., Wilkes, M., Pai, G. S., & Peterseim, M. M. W. (2022). Inherited Retinal Dystrophy in Southeastern United States: Characterization of South Carolina Patients and Comparative Literature Review. *Genes*, *13*(8), 1490.

Grigoryan, E. N. (2022). Self-Organization of the Retina during Eye Development, Retinal Regeneration In Vivo, and in Retinal 3D Organoids In Vitro. *Biomedicines*, *10*(6), 1458.

Grossniklaus, H. E., Geisert, E. E., & Nickerson, J. M. (2015). Introduction to the Retina. *Progress in Molecular Biology and Translational Science*, *134*,383-396.

Gulati, V., Fan, S., Gardner, B. J., Havens, S. J., Schaaf, M. T., Neely, D. G., & Toris, C. B. (2017). Mechanism of action of selective laser trabeculoplasty and predictors of response. *Investigative Ophthalmology & Visual Science*, *58*(3), 1462-1468.

Hadden, O. B., & Gass, J. (1976). Fundus flavimaculatus and Stargardt's disease. *American Journal of Ophthalmology*, *82*(4), 527-539.

Haji Abdollahi, S., & Hirose, T. (2013). Stargardt-Fundus flavimaculatus: recent advancements and treatment. Seminars in ophthalmology, 28(5-6), 372–376.

Hall, T.A. (1999) BioEdit: A User-Friendly Biological Sequence Alignment Editor and Analysis Program for Windows 95/98/NT. Nucleic Acids Symposium Series, 41, 95-98

Hameed, A., Abid, A., Aziz, A., Ismail, M., Mehdi, S., & Khaliq, S. (2003). Evidence of RPGRIP1 gene mutations associated with recessive cone-rod dystrophy. *Journal of Medical Genetics*, *40*(8), 616-619.

Hamel C. (2006). Retinitis pigmentosa. *Orphanet Journal of Rare Diseases*, *1*, 40. https://doi.org/10.1186/1750-1172-1-40.

Hamel, C., Griffoin, J., Bazalgette, C., Lasquellec, L., Duval, P., Bareil, C., Beaufrere, L., Bonnet, S., Eliaou, C., & Marlhens, F. (2000). Molecular genetics of pigmentary retinopathies: identification of mutations in CHM, RDS, RHO, RPE65, USH2A and XLRS1 genes. *Journal Francais D'ophtalmologie*, *23*(10), 985-995.

Harrell, C. R., Fellabaum, C., Arsenijevic, A., Markovic, B. S., Djonov, V., & Volarevic, V. (2019). Therapeutic potential of mesenchymal stem cells and their secretome in the treatment of glaucoma. *Stem Cells International*, *2019*.

Ho, C. L., & Walton, D. S. (2004). Primary congenital glaucoma: 2004 update. *Journal of Pediatric Ophthalmology & Strabismus*, *41*(5), 271-288.

Iribarne, M., & Masai, I. (2017). Neurotoxicity of cGMP in the vertebrate retina: from the initial research on rd mutant mice to zebrafish genetic approaches. *Journal of Neurogenetics*, *31*(3), 88-101.

Irvine, A. R., & Wergeland Jr, F. L. (1972). Stargardt's hereditary progressive macular degeneration. *The British Journal of Ophthalmology*, *56*(11), 817.

Issa, P. C., Barnard, A. R., Singh, M. S., Carter, E., Jiang, Z., Radu, R. A., Schraermeyer, U., & MacLaren, R. E. (2013). Fundus autofluorescence in the Abca4−/− mouse model of Stargardt disease—correlation with accumulation of A2E, retinal function, and histology. *Investigative Ophthalmology & Visual Science*, *54*(8), 5602-5612.

Jonas, J. B. (2005). Clinical implications of peripapillary atrophy in glaucoma. *Current Opinion in Ophthalmology*, *16*(2), 84-88.

Kaur, K., & Gurnani, B. (2022). Primary congenital glaucoma. In *StatPearls*. StatPearls Publishing. https://www.ncbi.nlm.nih.gov/books/NBK574553/.

Kaur, K., Reddy, A., Mukhopadhyay, A., Mandal, A., Hasnain, S., Ray, K., Thomas, R., Balasubramanian, D., & Chakrabarti, S. (2005). Myocilin gene implicated in primary congenital glaucoma. *Clinical Genetics*, *67*(4), 335-340.

Kawamura, S., & Tachibanaki, S. (2008). Rod and cone photoreceptors: molecular basis of the difference in their physiology. *Comparative Biochemistry and Physiology Part A: Molecular & Integrative Physiology*, *150*(4), 369-377.

Kelley, L. A., Mezulis, S., Yates, C. M., Wass, M. N., & Sternberg, M. J. (2015). The Phyre2 web portal for protein modeling, prediction and analysis. *Nature Protocols*, *10*(6), 845-858.

Khan, A. O. (2011). Genetics of primary glaucoma. *Current Opinion in Ophthalmology*, *22*(5), 347-355.

Khan, K. N., Kasilian, M., Mahroo, O. A., Tanna, P., Kalitzeos, A., Robson, A. G., Tsunoda, K., Iwata, T., Moore, A. T., & Fujinami, K. (2018). Early patterns of macular degeneration in ABCA4-associated retinopathy. *Ophthalmology*, *125*(5), 735-746.

Khan, M. I., Azam, M., Ajmal, M., Collin, R. W., Den Hollander, A. I., Cremers, F. P., & Qamar, R. (2014). The molecular basis of retinal dystrophies in Pakistan. *Genes*, *5*(1), 176-195.

Khan, M. U., Rehman, R., Kaul, H., Mahmood, S., & Ammar, A. (2019). Mutational analysis of CYP1B1 gene in Pakistani pediatric patients affected with Primary Congenital Glaucoma. *Advancements in Life Sciences*, *7*(1), 32-37.

Khazaeni, B., & Khazaeni, L. (2017). Acute closed angle glaucoma. https://www.ncbi.nlm.nih.gov/books/NBK430857/

Kim, H. J., & Sparrow, J. R. (2021). Bisretinoid phospholipid and vitamin A aldehyde: shining a light. *Journal of Lipid Research*, *62*.

Kim, Y., & Chen, J. (2018). Molecular structure of human P-glycoprotein in the ATP-bound, outward-facing conformation. *Science*, *359*(6378), 915-919.

Koenekoop, R. K. (2003). The gene for Stargardt disease, ABCA4, is a major retinal gene: a mini-review. *Ophthalmic Genetics*, *24*(2), 75-80.

Kohl, S., Baumann, B., Broghammer, M., Jägle, H., Sieving, P., Kellner, U., Spegal, R., Anastasi, M., Zrenner, E., Sharpe, L. T., & Wissinger, B. (2000). Mutations in the CNGB3 gene encoding the beta-subunit of the cone photoreceptor cGMP-gated channel are responsible for achromatopsia (ACHM3) linked to chromosome 8q21. *Human Molecular Genetics*, *9*(14), 2107–2116.

Kolb, H., Fernandez, E., & Nelson, R. (Eds.). (1995). *Webvision: The Organization of the Retina and Visual System*. University of Utah Health Sciences Center.

Kong, J., Kim, S., Binley, K., Pata, I., Mannik, J., Zernant-Rajang, J., Kan, O., Iqball, S., Naylor, S., & Sparrow, J. (2008). Correction of the disease phenotype in the mouse model of Stargardt disease by lentiviral gene therapy. *Gene Therapy*, *15*(19), 1311-1320.

Kopanos, C., Tsiolkas, V., Kouris, A., Chapple, C. E., Aguilera, M. A., Meyer, R., & Massouras, A. (2019). VarSome: the human genomic variant search engine. *Bioinformatics*, *35*(11), 1978.

Koster, C., van den Hurk, K. T., Lewallen, C. F., Talib, M., Ten Brink, J. B., Boon, C. J., & Bergen, A. A. (2021). The Lrat−/− rat: CRISPR/Cas9 construction and phenotyping of a new animal model for retinitis pigmentosa. *International Journal of Molecular Sciences*, *22*(13), 7234.

Krill, A., & Deutman, A. (1972). The various categories of juvenile macular degeneration. *Transactions of the American Ophthalmological Society*, *70*, 220.

Kupfer, C., & Kaiser-Kupfer, M. I. (1979). Observations on the development of the anterior chamber angle with reference to the pathogenesis of congenital glaucomas. *American Journal of Ophthalmology*, *88*(3 Pt 1), 424-426.

Lamb, T. D. (2016). Why rods and cones? *Eye*, *30*(2), 179-185.

Lambertus, S., van Huet, R. A., Bax, N. M., Hoefsloot, L. H., Cremers, F. P., Boon, C. J., Klevering, B. J., & Hoyng, C. B. (2015). Early-onset stargardt disease: phenotypic and genotypic characteristics. *Ophthalmology*, *122*(2), 335-344.

Lee, W., Noupuu, K., Oll, M., Duncker, T., Burke, T., Zernant, J., Bearelly, S., Tsang, S. H., Sparrow, J. R., & Allikmets, R. (2014). The external limiting membrane in early-onset Stargardt disease. *Investigative Ophthalmology & Visual Science*, *55*(10), 6139-6149.

Lee, W., Schuerch, K., Zernant, J., Collison, F. T., Bearelly, S., Fishman, G. A., Tsang, S. H., Sparrow, J. R., & Allikmets, R. (2017). Genotypic spectrum and phenotype correlations of ABCA4-associated disease in patients of south Asian descent. *European Journal of Human Genetics*, *25*(6), 735-743.

Libby, R. T., Smith, R. S., Savinova, O. V., Zabaleta, A., Martin, J. E., Gonzalez, F. J., & John, S. W. (2003). Modification of ocular defects in mouse developmental

glaucoma models by tyrosinase. *Science*, *299*(5612), 1578-1581.

Liu, C., & Varnum, M. D. (2005). Functional consequences of progressive cone dystrophy-associated mutations in the human cone photoreceptor cyclic nucleotide-gated channel CNGA3 subunit. *American Journal of Physiology. Cell Physiology*, *289*(1), C187–C198.

Lois, N., Holder, G. E., Bunce, C., Fitzke, F. W., & Bird, A. C. (2001). Phenotypic subtypes of Stargardt macular dystrophy–fundus flavimaculatus. *Archives of Ophthalmology*, *119*(3), 359-369.

Long, S. B., Campbell, E. B., & MacKinnon, R. (2005). Crystal structure of a mammalian voltage-dependent Shaker family K+ channel. *Science*, *309*(5736), 897-903.

Lu, B., Malcuit, C., Wang, S., Girman, S., Francis, P., Lemieux, L., Lanza, R., & Lund, R. (2009). Long-term safety and function of RPE from human embryonic stem cells in preclinical models of macular degeneration. *Stem Cells*, *27*(9), 2126-2135.

Lu, L. J., Liu, J., & Adelman, R. A. (2017). Novel therapeutics for Stargardt disease. *Graefe's Archive for Clinical and Experimental Ophthalmology*, *255*, 1057-1062.

Ludwig, P. E., Jessu, R., & Czyz, C. N. (2022). Physiology, Eye. In *StatPearls* StatPearls Publishing. https://www.ncbi.nlm.nih.gov/books/NBK470322/

Mahabadi, N., & Al Khalili, Y. (2021). Neuroanatomy, retina. In *StatPearls*. StatPearls Publishing. https://www.ncbi.nlm.nih.gov/books/NBK545310/

Mahabadi, N., Foris, L. A., & Tripathy, K. (2017). Open angle glaucoma. In *StatPearls*. StatPearls Publishing. https://www.ncbi.nlm.nih.gov/books/NBK441887/

Malvankar-Mehta, M. S., Iordanous, Y., Chen, Y. N., Wang, W. W., Patel, S. S., Costella, J., & Hutnik, C. M. (2015). iStent with phacoemulsification versus phacoemulsification alone for patients with glaucoma and cataract: a meta-analysis. *Plos one*, *10*(7), e0131770.

Masland, R. H. (2012). The neuronal organization of the retina. *Neuron*, *76*(2), 266-280.

Mata, N. L., Weng, J., & Travis, G. H. (2000). Biosynthesis of a major lipofuscin fluorophore in mice and humans with ABCR-mediated retinal and macular degeneration. *Proceedings of the National Academy of Sciences*, *97*(13), 7154-7159.

McGuffin, L. J., Bryson, K., & Jones, D. T. (2000). The PSIPRED protein structure prediction server. *Bioinformatics*, *16*(4), 404-405.

Michaelides, M., Aligianis, I. A., Ainsworth, J. R., Good, P., Mollon, J. D., Maher, E. R., Moore, A. T., & Hunt, D. M. (2004). Progressive cone dystrophy associated with mutation in CNGB3. *Investigative Ophthalmology & Visual Science*, *45*(6), 1975-1982.

Michaelides, M., Hunt, D., & Moore, A. (2003). The genetics of inherited macular dystrophies. *Journal of Medical Genetics*, *40*(9), 641-650.

Michalakis, S., Geiger, H., Haverkamp, S., Hofmann, F., Gerstner, A., & Biel, M. (2005). Impaired opsin targeting and cone photoreceptor migration in the retina of mice lacking the cyclic nucleotide-gated channel CNGA3. *Investigative Ophthalmology & Visual Science*, *46*(4), 1516-1524.

Micheal, S., Ayub, H., Zafar, S. N., Bakker, B., Ali, M., Akhtar, F., Islam, F., Khan, M. I., Qamar, R., & den Hollander, A. I. (2015). Identification of novel CYP1B 1 gene mutations in patients with primary congenital and primary open-angle glaucoma. *Clinical & Experimental Ophthalmology*, *43*(1), 31-39.

Micheal, S., Siddiqui, S. N., Zafar, S. N., Iqbal, A., Khan, M. I., & den Hollander, A. I. (2016). Identification of novel variants in LTBP2 and PXDN using whole-exome sequencing in developmental and congenital glaucoma. *Plos one*, *11*(7), e0159259.

Moiseyev, G., Chen, Y., Takahashi, Y., Wu, B. X., & Ma, J.-x. (2005). RPE65 is the isomerohydrolase in the retinoid visual cycle. *Proceedings of the National Academy of Sciences*, *102*(35), 12413-12418.

Molday, R. S. (2015). Insights into the molecular properties of ABCA4 and its role in the visual cycle and Stargardt disease. *Progress in Molecular Biology and Translational Science*, *134*, 415-431.

Molday, R. S., Garces, F. A., Scortecci, J. F., & Molday, L. L. (2022). Structure and function of ABCA4 and its role in the visual cycle and Stargardt macular degeneration. *Progress in Retinal and Eye Research*, *89*, 101036.

Moore, A. (1992). Cone and cone-rod dystrophies. *Journal of Medical Genetics*, *29*(5), 289.

Muraki-Oda, S., Toyoda, F., Okada, A., Tanabe, S., Yamade, S., Ueyama, H., Matsuura, H., & Ohji, M. (2007). Functional analysis of rod monochromacy-associated missense mutations in the CNGA3 subunit of the cone photoreceptor cGMP-gated channel. Biochemical and biophysical research communications, 362(1), 88–93.

Murro, V., Banfi, S., Testa, F., Iarossi, G., Falsini, B., Sodi, A., Signorini, S., Iolascon, A., Russo, R., Mucciolo, D. P., Caputo, R., Bacci, G. M., Bargiacchi, S., Turco, S., Fortini, S., & Simonelli, F. (2023). A multidisciplinary approach to inherited retinal dystrophies from diagnosis to initial care: a narrative review with inputs from clinical practice. *Orphanet Journal of Rare Diseases*, *18*(1), 223.

Muniz, A., Villazana-Espinoza, E. T., Hatch, A. L., Trevino, S. G., Allen, D. M., & Tsin, A. T. (2007). A novel cone visual cycle in the cone-dominated retina. *Experimental Eye Research*, *85*(2), 175-184.

Mustafi, D., Engel, A. H., & Palczewski, K. (2009). Structure of cone photoreceptors. *Progress in Retinal and Eye Research*, *28*(4), 289-302.

Nishiguchi, K. M., Sandberg, M. A., Gorji, N., Berson, E. L., & Dryja, T. P. (2005). Cone cGMP-gated channel mutations and clinical findings in patients with achromatopsia, macular degeneration, and other hereditary cone diseases. *Human mutation*, *25*(3), 248-258.

Noble, K. G., & Carr, R. E. (1979). Stargardt's disease and fundus flavimaculatus. *Archives of Ophthalmology*, *97*(7), 1281-1285.

Okada, A., Ueyama, H., Toyoda, F., Oda, S., Ding, W. G., Tanabe, S., Yamade, S., Matsuura, H., Ohkubo, I., & Kani, K. (2004). Functional role of hCngb3 in regulation of human cone cng channel: effect of rod monochromacy-associated mutations in hCNGB3 on channel function. *Investigative Ophthalmology & Visual cience*, *45*(7), 2324–2332.

Organization, W. H. (2021). World report on vision. In: World Health Organization.

Papermaster, D. S., Reilly, P., & Schneider, B. G. (1982). Cone lamellae and red and green rod outer segment disks contain a large intrinsic membrane protein on their margins: an ultrastructural immunocytochemical study of frog retinas. *Vision Research*, *22*(12), 1417-1428.

Papermaster, D. S., Schneider, B. G., Zorn, M. A., & Kraehenbuhl, J. P. (1978). Immunocytochemical localization of a large intrinsic membrane protein to the incisures and margins of frog rod outer segment disks. *The Journal of Cell Biology*, *78*(2), 415-425.

Parish, C. A., Hashimoto, M., Nakanishi, K., Dillon, J., & Sparrow, J. (1998). Isolation and one-step preparation of A2E and iso-A2E, fluorophores from human retinal pigment epithelium. *Proceedings of the National Academy of Sciences*, *95*(25), 14609-14613.

Peng, C., Rich, E. D., & Varnum, M. D. (2004). Subunit configuration of heteromeric cone cyclic nucleotide-gated channels. *Neuron*, *42*(3), 401-410.

Peng, C., Rich, E. D., & Varnum, M. D. (2003). Achromatopsia-associated mutation in the human cone photoreceptor cyclic nucleotide-gated channel CNGB3 subunit alters the ligand sensitivity and pore properties of heteromeric channels. *The Journal of Biological Chemistry*, *278*(36), 34533–34540.

Pettersen, E. F., Goddard, T. D., Huang, C. C., Couch, G. S., Greenblatt, D. M., Meng, E. C., & Ferrin, T. E. (2004). UCSF Chimera—a visualization system for exploratory research and analysis. *Journal of Computational Chemistry*, *25*(13), 1605-1612.

Pillunat, L. E., Erb, C., Jünemann, A. G., & Kimmich, F. (2017). Micro-invasive glaucoma surgery (MIGS): a review of surgical procedures using stents. *Clinical Ophthalmology*, 1583-1600.

Podda, M. V., & Grassi, C. (2014). New perspectives in cyclic nucleotide-mediated functions in the CNS: the emerging role of cyclic nucleotide-gated (CNG) channels. *Pflügers Archiv-European Journal of Physiology*, *466*, 1241-1257.

Pradeep, T., Mehra, D., & Le, P. H. (2019). Histology, eye. In *StatPearls*. StatPearls

Publishing. https://www.ncbi.nlm.nih.gov/books/NBK544343/.

Qian, H., Zhao, X., Cao, P., Lei, J., Yan, N., & Gong, X. (2017). Structure of the human lipid exporter ABCA1. *Cell*, *169*(7), 1228-1239. e1210.

Quazi, F., Lenevich, S., & Molday, R. S. (2012). ABCA4 is an N-retinylidene-phosphatidylethanolamine and phosphatidylethanolamine importer. *Nature Communications*, *3*(1), 925.

Quazi, F., & Molday, R. S. (2014). ATP-binding cassette transporter ABCA4 and chemical isomerization protect photoreceptor cells from the toxic accumulation of excess 11-cis-retinal. *Proceedings of the National Academy of Sciences*, *111*(13), 5024-5029.

Rashid, M., Yousaf, S., Sheikh, S. A., Sajid, Z., Shabbir, A. S., Kausar, T., Tariq, N., Usman, M., Shaikh, R. S., & Ali, M. (2019). Identities and frequencies of variants in CYP1B1 causing primary congenital glaucoma in Pakistan. *Molecular Vision*, *25*, 144.

Rauf, B., Irum, B., Kabir, F., Firasat, S., Naeem, M. A., Khan, S. N., Husnain, T., Riazuddin, S., Akram, J., & Riazuddin, S. (2016). A spectrum of CYP1B1 mutations associated with primary congenital glaucoma in families of Pakistani descent. *Human Genome Variation*, *3*(1), 1-4.

Rauf, B., Irum, B., Khan, S. Y., Kabir, F., Naeem, M. A., Riazuddin, S., Ayyagari, R., & Riazuddin, S. A. (2020). Novel mutations in LTBP2 identified in familial cases of primary congenital glaucoma. *Molecular Vision*, *26*, 14.

Rees, D. C., Johnson, E., & Lewinson, O. (2009). ABC transporters: the power to change. *Nature Reviews Molecular cell biology*, *10*(3), 218-227.

Rentzsch, P., Witten, D., Cooper, G. M., Shendure, J., & Kircher, M. (2019). CADD: predicting the deleteriousness of variants throughout the human genome. *Nucleic Acids Research*, *47*(D1), D886-D894.

Rotenstreich, Y., Fishman, G. A., & Anderson, R. J. (2003). Visual acuity loss and clinical observations in a large series of patients with Stargardt disease. *Ophthalmology*, *110*(6), 1151-1158.

Saari, J. C. (2016). Vitamin A and vision. *The Biochemistry of Retinoid Signaling II:*

The Physiology of Vitamin A-Uptake, Transport, Metabolism and Signaling, 231-259.

Sakai, N., Decatur, J., Nakanishi, K., & Eldred, G. E. (1996). Ocular age pigment "A2-E": an unprecedented pyridinium bisretinoid. *Journal of the American Chemical Society*, *118*(6), 1559-1560.

Sambrook, J., & Russell, D. W. (2006). Purification of nucleic acids by extraction with phenol: chloroform. *Cold Spring Harbor Protocols*, *2006*(1), pdb. prot4455.

Saqib, M. A. N., Awan, B. M., Sarfraz, M., Khan, M. N., Rashid, S., & Ansar, M. (2011). Genetic analysis of four Pakistani families with achromatopsia and a novel S4 motif mutation of CNGA3. *Japanese Journal of Ophthalmology*, *55*, 676-680.

Saqib, M. A. N., Nikopoulos, K., Ullah, E., Sher Khan, F., Iqbal, J., Bibi, R., Jarral, A., Sajid, S., Nishiguchi, K. M., & Venturini, G. (2015). Homozygosity mapping reveals novel and known mutations in Pakistani families with inherited retinal dystrophies. *Scientific Reports*, *5*(1), 9965.

Sarfarazi, M., & Stoilov, I. (2000). Molecular genetics of primary congenital glaucoma. *Eye*, *14*(3), 422-428.

Sautter, H. (1963). Entwicklung und Fortschritt in der Augenheilkunde: Dritter Fortbildungskurs der Deutschen Ophthalmologischen Gesellschaft Hamburg 1962.

Schuster, A. K., Erb, C., Hoffmann, E. M., Dietlein, T., & Pfeiffer, N. (2020). The diagnosis and treatment of glaucoma. *Deutsches Ärzteblatt International*, *117*(13), 225.

Schwarz, J. M., Cooper, D. N., Schuelke, M., & Seelow, D. (2014). MutationTaster2: mutation prediction for the deep-sequencing age. *Nature Methods*, *11*(4), 361-362.

Schwartz, M., & Yoles, E. (2000). Neuroprotection: a new treatment modality for glaucoma?. *Current opinion in ophthalmology*, *11*(2), 107–111.

Siepel, A., Bejerano, G., Pedersen, J. S., Hinrichs, A. S., Hou, M., Rosenbloom, K., Clawson, H., Spieth, J., Hillier, L. W., Richards, S., Weinstock, G. M., Wilson,

R. K., Gibbs, R. A., Kent, W. J., Miller, W., & Haussler, D. (2005). Evolutionarily conserved elements in vertebrate, insect, worm, and yeast genomes. *Genome Research*, *15*(8), 1034–1050.

Senior, K. R. (2010). *The eye: the physiology of human perception*. The Rosen Publishing Group, Inc.

Shah, B. R., Xu, W., & Mraz, J. (2019). Cytochrome P450 1B1: role in health and disease and effect of nutrition on its expression. *RSC advances*, *9*(36), 21050-21062.

Sheikh, S. A., Waryah, A. M., Narsani, A. K., Shaikh, H., Gilal, I. A., Shah, K., Qasim, M., Memon, A. I., Kewalramani, P., & Shaikh, N. (2014). Mutational spectrum of the CYP1B1 gene in Pakistani patients with primary congenital glaucoma: novel variants and genotype-phenotype correlations. *Molecular Vision*, *20*, 991.

Shimada, T., Watanabe, J., Inoue, K., Guengerich, F., & Gillam, E. (2001). Specificity of 17 β-oestradiol and benzo [α] pyrene oxidation by polymorphic human cytochrome P4501B1 variants substituted at residues 48, 119 and 432. *Xenobiotica*, *31*(3), 163-176.

Silverman, S. M., & Wong, W. T. (2018). Microglia in the retina: roles in development, maturity, and disease. *Annual Review of Vision Science*, *4*, 45-77.

Simonelli, F., Testa, F., Zernant, J., Nesti, A., Rossi, S., Allikmets, R., & Rinaldi, E. (2005). Genotype-phenotype correlation in Italian families with Stargardt disease. *Ophthalmic Research*, *37*(3), 159-167.

Simpson, J. A., & Weiner, E. S. (1989). The Oxford english dictionary. *(No Title)*.

Souma, T., Tompson, S. W., Thomson, B. R., Siggs, O. M., Kizhatil, K., Yamaguchi, S., Feng, L., Limviphuvadh, V., Whisenhunt, K. N., & Maurer-Stroh, S. (2016). Angiopoietin receptor TEK mutations underlie primary congenital glaucoma with variable expressivity. *The Journal of Clinical Investigation*, *126*(7), 2575-2587.

Souzeau, E., Dubowsky, A., Ruddle, J. B., & Craig, J. E. (2019). Primary congenital glaucoma due to paternal uniparental isodisomy of chromosome 2 and CYP1B1 deletion. *Molecular Genetics & Genomic Medicine*, *7*(8), e774.

Sparrow, J. R., & Boulton, M. (2005). RPE lipofuscin and its role in retinal pathobiology. *Experimental Eye Research*, *80*(5), 595-606.

Sparrow, J. R., Gregory-Roberts, E., Yamamoto, K., Blonska, A., Ghosh, S. K., Ueda, K., & Zhou, J. (2012). The bisretinoids of retinal pigment epithelium. *Progress in Retinal and Eye Research*, *31*(2), 121-135.

Stargardt, K. (1909). Über familiäre, progressive Degeneration in der Maculagegend des Auges. *Albrecht von Graefes Archiv für Ophthalmologie*, *71*, 534-550.

Stoilov, I., Akarsu, A. N., & Sarfarazi, M. (1997). Identification of three different truncating mutations in cytochrome P4501B1 (CYP1B1) as the principal cause of primary congenital glaucoma (Buphthalmos) in families linked to the GLC3A locus on chromosome 2p21. *Human Molecular Genetics*, *6*(4), 641-647.

Strauss, R. W., Ho, A., Muñoz, B., Cideciyan, A. V., Sahel, J.-A., Sunness, J. S., Birch, D. G., Bernstein, P. S., Michaelides, M., & Traboulsi, E. I. (2016). The natural history of the progression of atrophy secondary to Stargardt disease (ProgStar) studies: design and baseline characteristics: ProgStar Report No. 1. *Ophthalmology*, *123*(4), 817-828.

Sundin, O. H., Yang, J. M., Li, Y., Zhu, D., Hurd, J. N., Mitchell, T. N., Silva, E. D., & Maumenee, I. H. (2000). Genetic basis of total colourblindness among the Pingelapese islanders. *Nature Genetics*, *25*(3), 289–293.

Tang, H., & Thomas, P. D. (2016). PANTHER-PSEP: predicting disease-causing genetic variants using position-specific evolutionary preservation. *Bioinformatics*, *32*(14), 2230-2232.

Tanna, P., Georgiou, M., Aboshiha, J., Strauss, R. W., Kumaran, N., Kalitzeos, A., Weleber, R. G., & Michaelides, M. (2018). Cross-sectional and longitudinal assessment of retinal sensitivity in patients with childhood-onset Stargardt disease. *Translational Vision Science & Technology*, *7*(6), 10-10.

Tanna, P., Georgiou, M., Strauss, R. W., Ali, N., Kumaran, N., Kalitzeos, A., Fujinami, K., & Michaelides, M. (2019). Cross-sectional and longitudinal assessment of the ellipsoid zone in childhood-onset Stargardt disease. *Translational Vision Science & Technology*, *8*(2), 1-1.

Tanna, P., Strauss, R. W., Fujinami, K., & Michaelides, M. (2017). Stargardt disease: clinical features, molecular genetics, animal models and therapeutic options. *British Journal of Ophthalmology*, *101*(1), 25-30.

Tanna, P., Strauss, R. W., Fujinami, K., & Michaelides, M. (2017). Stargardt disease: clinical features, molecular genetics, animal models and therapeutic options. *British Journal of Ophthalmology*, *101*(1), 25-30.

Tehreem, R., Arooj, A., Siddiqui, S. N., Naz, S., Afshan, K., & Firasat, S. (2022). Mutation screening of the CYP1B1 gene reveals thirteen novel disease-causing variants in consanguineous Pakistani families causing primary congenital glaucoma. *Plos one*, *17*(9), e0274335.

Tham, Y.-C., Li, X., Wong, T. Y., Quigley, H. A., Aung, T., & Cheng, C.-Y. (2014). Global prevalence of glaucoma and projections of glaucoma burden through 2040: a systematic review and meta-analysis. *Ophthalmology*, *121*(11), 2081-2090.

Thiadens, A. A., Phan, T. M. L., Zekveld-Vroon, R. C., Leroy, B. P., van Den Born, L. I., Hoyng, C. B., Klaver, C. C., Roosing, S., Pott, J.-W. R., & van Schooneveld, M. J. (2012). Clinical course, genetic etiology, and visual outcome in cone and cone–rod dystrophy. *Ophthalmology*, *119*(4), 819-826.

Tian, H., Li, L., & Song, F. (2017). Study on the deformations of the lamina cribrosa during glaucoma. *Acta biomaterialia*, *55*, 340-348.

Traboulsi, E. I. (2012). *Genetic Diseases of the Eye*. Oxford University Press, USA.

Tsin, A., Betts-Obregon, B., & Grigsby, J. (2018). Visual cycle proteins: structure, function, and roles in human retinal disease. *Journal of Biological Chemistry*, *293*(34), 13016-13021.

Tsybovsky, Y., Molday, R. S., & Palczewski, K. (2010). The ATP-binding cassette transporter ABCA4: structural and functional properties and role in retinal disease. *Inflammation and retinal disease: complement biology and pathology*, 105-125.

Ur Rehman, A., Peter, V. G., Quinodoz, M., Rashid, A., Khan, S. A., Superti-Furga, A., & Rivolta, C. (2019). Exploring the genetic landscape of retinal diseases in

North-Western Pakistan reveals a high degree of autozygosity and a prevalent founder mutation in ABCA4. *Genes*, *11*(1), 12.

Vaser, R., Adusumalli, S., Leng, S. N., Sikic, M., & Ng, P. C. (2016). SIFT missense predictions for genomes. *Nature Protocols*, *11*(1), 1-9.

Vasiliou, V., & Gonzalez, F. J. (2008). Role of *CYP1B1* in glaucoma. *Annu. Rev. Pharmacol. Toxicol.*, *48*, 333-358.

Vincent, A., Wright, T., Billingsley, G., Westall, C., & Héon, E. (2011). Oligocone trichromacy is part of the spectrum of CNGA3-related cone system disorders. *Ophthalmic Genetics*, 32(2), 107–113.

Walia, S., & Fishman, G. A. (2009). Natural history of phenotypic changes in Stargardt macular dystrophy. *Ophthalmic Genetics*, *30*(2), 63-68.

Wang, J.-S., & Kefalov, V. J. (2011). The cone-specific visual cycle. *Progress in Retinal and Eye Research*, *30*(2), 115-128.

Waryah, Y. M., Iqbal, M., Sheikh, S. A., Baig, M. A., Narsani, A. K., Atif, M., Bhinder, M. A., Rahman, A. U., Memon, A. I., & Pirzado, M. S. (2019). Two novel variants in CYP1B1 gene: a major contributor of autosomal recessive primary congenital glaucoma with allelic heterogeneity in Pakistani patients. *International Journal of Ophthalmology*, *12*(1), 8.

Weinreb, R. N., Aung, T., & Medeiros, F. A. (2014). The pathophysiology and treatment of glaucoma: a review. *Jama*, *311*(18), 1901-1911.

Westerlund, E. (1947). Clinical and genetic studies on the primary glaucoma diseases. NYT Nordic Forlag. *Copenhagen Arnold Busck*,3(12).

Willoughby, C. E., Ponzin, D., Ferrari, S., Lobo, A., Landau, K., & Omidi, Y. (2010). Anatomy and physiology of the human eye: effects of mucopolysaccharidoses disease on structure and function–a review. *Clinical & Experimental Ophthalmology*, *38*, 2-11.

Wirtz, M. K., Samples, J. R., Xu, H., Severson, T., & Acott, T. S. (2002). Expression profile and genome location of cDNA clones from an infant human trabecular meshwork cell library. *Investigative Ophthalmology & Visual Science*, *43*(12), 3698-3704.

Wissinger, B., Gamer, D., Jägle, H., Giorda, R., Marx, T., Mayer, S., Tippmann, S., Broghammer, M., Jurklies, B., Rosenberg, T., Jacobson, S. G., Sener, E. C., Tatlipinar, S., Hoyng, C. B., Castellan, C., Bitoun, P., Andreasson, S., Rudolph, G., Kellner, U., Lorenz, & Kohl, S. (2001). CNGA3 mutations in hereidtarycone photoreceptor disorders. *American Journal of Human Genetics*, 69(4), 722–737.

Witsch-Baumgartner, M., Schwaninger, G., Schnaiter, S., Kollmann, F., Burkhard, S., Gröbner, R., Mühlegger, B., Schamschula, E., Kirchmeier, P., & Zschocke, J. (2022). Array genotyping as diagnostic approach in medical genetics. *Molecular Genetics & Genomic Medicine*, *10*(9), e2016.

Yang, P., Michaels, K. V., Courtney, R. J., Wen, Y., Greninger, D. A., Reznick, L., Karr, D. J., Wilson, L. B., Weleber, R. G., & Pennesi, M. E. (2014). Retinal morphology of patients with achromatopsia during early childhood: implication for gene therapy. JAMA ophthalmology, 132(7), 823–831.

Yang, S., Zhou, J., & Li, D. (2021). Functions and diseases of the retinal pigment epithelium. *Frontiers in Pharmacology*, *12*, 727870.

Yang, Z., Chen, Y., Lillo, C., Chien, J., Yu, Z., Michaelides, M., Klein, M., Howes, K. A., Li, Y., & Kaminoh, Y. (2008). Mutant prominin 1 found in patients with macular degeneration disrupts photoreceptor disk morphogenesis in mice. *The Journal of Clinical Investigation*, *118*(8), 2908-2916.

Yousaf, K., Bashir, R., Balqees, K., Naz, S., Munir, N., & Aslam, F. (2022). High prevalence of glaucoma-associated *CYP1B1* mutation (p.G61E) in primary congenital and open angle glaucoma patients in Pakistan. *Journal of the National Science Foundation of Sri Lanka*, *50*(3).

Zahid, T., Khan, M. U., Zulfiqar, A., Jawad, F., Saleem, A., & Khan, A. R. (2023). Investigation of mutational spectrum in cytochrome P4501B1 (CYP1B1) as the principal cause of primary congenital glaucoma. *Pakistan Journal of Medical Sciences*, *39*(2), 409.

Zhang, K., Kniazeva, M., Han, M., Li, W., Yu, Z., Yang, Z., Li, Y., Metzker, M. L., Allikmets, R., & Zack, D. J. (2001). A 5-bp deletion in ELOVL4 is associated with two related forms of autosomal dominant macular dystrophy. *Nature*

Genetics, *27*(1), 89-93.

6. Electronic References

BioEdit Version 7.2

https://bioedit.software.informer.com/7.2/

BLAT

https://genome.ucsc.edu/cgi-bin/hgBlat

ChimeraX Version1.4

https://www.rbvi.ucsf.edu/chimerax/

Ensemble

https://asia.ensembl.org/index.html

Genomnis HSF

http://www.umd.be/hsf/

Haplopainter

http://haplopainter.sourceforge.net/

In-Silico PCR

https://genome.ucsc.edu/cgi-bin/hgPcr

Mutation Taster

https://www.mutationtaster.org/

Oligo Calc

http://biotools.nubic.northwestern.edu/OligoCalc.html

Panther-PSEP

http://www.pantherdb.org/tools/csnpScoreForm.jsp

Phyre2

http://www.sbg.bio.ic.ac.uk/~phyre2/html/page.cgi?id=index

Polyphen-2

http://genetics.bwh.harvard.edu/pph2/

Primer 3

https://primer3.ut.ee/

PROVEAN

http://provean.jcvi.org/provean_seq_report.php?jobid=083693854426988

PSIPRED

http://bioinf.cs.ucl.ac.uk/psipred/

SIFT

https://sift.bii.a-star.edu.sg/

Varsome

https://varsome.com/

SNPs & GO

https://snps.biofold.org/snps-and-go/snps-and-go.html

VARSEAK

https://varseak.bio/

CAAD

https://cadd.gs.washington.edu/